AN INVESTIGATION OF THE LANDING LOADS EXPERIENCED BY THE A4D-2 AIRPLANE DURING FLIGHT TESTS AND DROP TESTS AND A COMPARISON WITH THEORY

October 1962

Prepared under Navy, BuWeps
Contract NOa(s) 59-6226-c

FINAL REPORT NO. LB-31038

Copy No. 14

DOUGLAS AIRCRAFT DIVISION • LONG BEACH, CALIFORNIA

AN INVESTIGATION OF THE LANDING LOADS EXPERIENCED BY THE A4D-2 AIRPLANE DURING FLIGHT TESTS AND DROP TESTS AND A COMPARISON WITH THEORY

October 1962

Prepared under Navy, BuWeps
Contract NOa(s) 59-6226-c

FINAL REPORT NO. LB-31038

Douglas Aircraft Company, Inc.
Long Beach, California

ABSTRACT

This report presents the results of an investigation conducted for the purpose of evaluating the adequacy of simulating landing loads by airplane laboratory drop tests and for the purpose of determining the accuracy with which these loads may be calculated by means of a dynamic analysis. Curves are presented which compare ground loads obtained from airplane landings, airplane drops, and theoretical analyses. The computing program for the theoretical analysis and its required input data are described.

FOREWORD

The work described in this report was accomplished by Douglas Aircraft Company, Aircraft Division, Long Beach, California, for the Bureau of Naval Weapons, Washington, D. C., under Contract NOa(s) 59-6226c. It represents the summary of a comprehensive program for the examination of loads experienced by Naval Aircraft during landings and the determination of the accuracy with which these loads may be duplicated by drop tests and analysis.

The project was performed under the general direction of Mr. C. T. Newby of the Bureau of Naval Weapons with Mr. D. C. Lindquist acting as cognizant technical project head. It was conducted by Douglas Aircraft Company with Mr. F. C. Allen providing the technical direction and Mr. L. B. Mosby acting as Chief Technical Investigator.

CONTENTS

ILLUSTRATIONS

TABLES

LIST OF SYMBOLS

Note: Symbols used in the Appendix are listed therein.

a_i, b_i	Coefficients for determining metering pin diameter as a function of stroke
C_{D_S}	Function of stroke for obtaining a variable rebound chamber orifice discharge coefficient
C_{Q_i}	Coefficients of fifth degree polynomial for rebound chamber orifice discharge coefficient
f	Frequency
FRL	Fuselage Reference Line
F_{HG}	Force on the gear at the ground parallel to the ground
F_{VG}	Force on the gear at the ground normal to the ground
h_i	Vertical translation of the wing in the natural mode shapes
h_i'	Slope of the h_i curve versus wing station
α_i	Pitching rotation of the wing in the natural mode shapes
α_i'	Slope of the α_i curve versus wing station
K_{ii}	Intercept coefficients for variation of strut spring constant with stroke
M	Generalized mass matrix; airplane mass, W/g
μ	Instantaneous value of ground coefficient of friction
V_v	Sinking speed at touch-down
W	Airplane gross weight
WL	Wing Lift
WRP	Wing Reference Plane

SUMMARY

This report presents the results of an investigation conducted for the purpose of evaluating the adequacy of simulating landing loads by airplane laboratory drop test and for the purpose of determining the accuracy with which these loads may be calculated by means of a dynamic analysis. The program consisted of the measurement of landing gear loads on an A4D-2 airplane during flight tests and during laboratory drop tests, with consistent instrumentation, and the computation of loads by means of analytical methods. A comparison was also made of the loads developed during flight test with the results of drop tests previously conducted with the same landing gear on the moving drop test rig at the Landing Loads Facility of the National Aeronautics and Space Administration at Langley Field, Virginia. Details of the instrumentation, the flight tests and the laboratory drop tests are presented in other reports. This report describes the analytical methods, presents the results of the analysis and provides the comparison between test data and theory.

The major portion of the testing and analytical work was concerned with symmetrical landings on a smooth runway and with a relatively clean airplane configuration. Additional flight test landings were, however, made to determine (a) the effects of asymmetry (roll), (b) the accelerations experienced by wing external stores and (c) the load increments resulting from running over an arresting cable. The results of these tests and an analytical investigation of the accelerations experienced by the external stores are presented in a separate report.

The major results of the primary phase of the investigation reported herein are summarized as follows:

1. Substantial differences in loading between the nominally symmetrical landings and the drop tests were measured. These differences were created to a large extent by small differences in initial conditions, by unavoidable asymmetries and by instrumentation accuracy. The differences were large enough to obscure those which might have been introduced in the drop tests by the simulation of forward speed by wheel spin-up or the simulation of wing lift by concentrated loads.

2. General correlation between drop test loads and landing loads was obtained to the extent that the maximum vertical loads were, on the average, within ± 16%, and the shape of the load curves showed marked similarity.

3. Vertical gear loads from flight test tended to be higher than drop test loads during the last part of the stroke.

4. Fore and aft loads from drop test were higher than fore and aft loads from flight. This was largely the result of an inappropriate choice of landing surface for the drop tests rather than a fundamental difference created by other testing conditions.

5. General agreement between analytical loads and flight test loads was obtained with the theory providing results which tended to be an average between right and left gear flight test loads.

6. The effects of airplane flexibility as represented by the wing and fuselage modes on the ground loads obtained from theory were negligible. This conclusion should not be generalized, however, since the test airplane was small and rigid. Larger effects of flexibility can be expected with more flexible aircraft.

7. General agreement was noted between vertical loads measured in flight and vertical loads measured on the NASA moving drop test rig. The maximum drag loads developed on the moving rig were of the same general magnitude as those developed during flight, however fundamental differences in the shape of the drag curve were noted which could be of significance in a fatigue analysis and which require further investigation.

The investigation revealed certain deficiencies in mensuration and testing techniques. Recommendations for improvement thereof are included.

Recommendations are also included for the improvement of the analytical techniques, among the most important of which are the incorporation of an improved representation of aerodynamic forces and the inclusion of damping in the tire deflection curve.

Further investigations are recommended. These include the determination of the differences between drop tests and flight tests by purely analytical means, the application of the analysis to the computation of load increments resulting from landing on an arresting cable and the analysis of rolled landings.

INTRODUCTION

The aircraft industry has for many years relied upon drop tests to check the adequacy of design with respect to landing loads. Intuitively it is recognized that airplane drop tests do provide a reasonable representation of the actual landing conditions, however, at least two techniques used in the drop tests have been viewed with skepticism, namely, the methods of simulating wing lift and the use of wheel spin-up to duplicate airplane forward velocity. In the case of wing lift, it has been necessary to apply the lift load abruptly near the start of the stroke, a procedure which introduces an entirely different dynamic situation with respect to structural loads than exists during actual landings. In the case of wheel spin-up, the tire is in contact throughout the stroke with one surface area whereas in actual landings, the contact is spread over many feet of runway.

In order to produce a more realistic test insofar as the duplication of aircraft forward velocity is concerned, a moving drop test jig was constructed by the National Aeronautics and Space Administration at Langley Field, Virginia. Features of this facility are described in Reference 1. Although forward velocity is adequately simulated in this test rig, aircraft flexibility is not, and wing lift simulation is subject to somewhat the same limitations as in laboratory drop tests.

The investigation described herein is an attempt to evaluate the differences between drop tests and actual landings and to determine the extent to which the loads may be computed by analytical methods. Consequently, this report contains the results of an experimental and analytical ground loads investigation, the purpose of which was to obtain a consistent set of measurements of landing gear loads, and parameters contributing to the loads, for actual airplane landings and for static and moving drop tests and to compare these data with the results of a dynamic analysis.

The airplane used was the Douglas A4D-2, general characteristics of which are shown in Figure 1. A left hand gear was used in the NASA tests (Reference 1), and this gear, together with similar instrumentation, was later used in the flight and drop tests. In the flight and drop tests, a right hand gear with nearly identical instrumentation was also used. Although the airplane used in the static drop tests was not the same article as that used in flight tests, the configuration was the same with respect to weight distribution and rigidity.

The flight test program was conducted at Patuxent River, Maryland, during the months of September and October 1960. Oscillograph records were obtained from a series of landings on both clean concrete and on a concrete runway coated with Navy non-skid deck compounds.

Upon completion of the flight tests the instrumented gear were returned to the Douglas El Segundo facility and installed on an A4D-2 static test airplane. Drop tests were then carried out for initial conditions corresponding to several of the flight test conditions.

The analytical phase of the program for predicting impact loads treated the landing gear and flexible wing structure as mutually interacting elements of a coupled system moving in response to the initial conditions chosen for the flight and drop tests. The equations for landing gear force were combined with the motions of the wing which were described by their natural modes of vibration. The landing gear force considers such factors as metering orifice damping, polytropic air compression, tire deflection and bearing friction loads. The system is governed by a set of simultaneous differential equations which are highly non-linear requiring that the solution resort to numerical integration methods which can be adapted to the electronic digital computer.

The work described in this report is concerned with nominally symmetrical landing conditions, with landings on smooth surfaces and with an airplane configuration without external wing stores. The complete investigation is described in three reports in addition to the present volume. A detailed description of the instrumentation and the calibration techniques is contained in Reference 2. A description of the flight tests and the data resulting therefrom is contained in Reference 3, and the drop test program is reported in Reference 4.

Additional data were obtained in the flight test phase of the investigation which provided information on the effects of roll, the accelerations experienced by external wing-mounted stores and the load increments resulting from landing on an arresting gear cable. The results of these additional tests and an analytical investigation of the accelerations experienced by the stores are contained in Reference 5.

INSTRUMENTATION

The strain gauges, accelerometers and other instruments used in the investigation are described in detail in Reference 2. Lists of parameters measured, method of measurement and the estimated accuracy and response characteristics are presented in Tables 1, 2 and 3.

The strain gauges for measuring strut loads were attached to the main gear axles at the junction to the strut piston. After calibration, they provided the vertical and drag loads in the strut perpendicular and parallel to the strut. The accelerometers for vertical and fore-aft accelerations of the lower mass were mounted inside the hollow axle. Ground loads were computed from strut loads and lower mass acceleration by means of the following equations:

$$F_{VG} = (F_A + F_{AA}) \cos (\phi - 6) - (F_N + F_{AN}) \sin (\phi - 6)$$

$$F_{HG} = (F_N + F_{AN}) \cos (\phi - 6) + (F_A + F_{AA}) \sin (\phi - 6)$$

where:

F_A = Axial load in the strut at the axle, pounds. Positive up.

F_N = Normal load in the strut at the axle, pounds. Positive aft.

F_{AA} = Inertia force on the lower mass in the strut axial direction, pounds. Positive down.

= Acceleration of the lower mass in g's times its weight. (The lower mass weight, which includes the wheel, tire axle and instrumentation, is 120 pounds.)

F_{AN} = Inertia force on the lower mass in a fore-aft direction normal to the strut, pounds. Positive forward.

F_{HG} = Force on the gear at the ground parallel to the ground, pounds.

F_{VG} = Force on the gear at the ground normal to the ground, pounds.

ϕ = Angle of the fuselage reference line with respect to the horizontal, degrees. Positive airplane nose up.

Instrumentation was originally provided to obtain side loads. However, the strain gauges which were to obtain these data were damaged early in the flight test program and could not be replaced without recalibration of the entire strut; therefore, side load data were not recorded.

The strut strain gauges for measuring vertical and drag load were calibrated both statically and dynamically. The dynamic calibration was of necessity used in the final reduction of data for the following reason. At the end of the flight test phase of the program, it was found that the response of the vertical strain gauge to vertical landing gear load was affected by the position of the axle plug containing the lower mass accelerometers. Since this plug was not installed during the initial static calibration and was removed and replaced during the flight test program, it was necessary to rely on the dynamic calibrations which were based on drop tests made at intervals throughout the program.

The dynamic calibration procedure consisted of comparing the vertical ground load based on the strain gauge with the vertical ground load obtained from the drop test reaction platform. The comparison was made at .002 sec. intervals and the calibration constant chosen so as to reduce the average error to a minimum. The drag gauge was unaffected by the accelerometer mounting plug; hence, the static calibration could be checked against a dynamic calibration.

The stroke was obtained from a slide wire device installed between the axle and upper part of the barrel. Strut velocity was measured by means of a magnetic type transducer mounted on the landing gear barrel and actuated by a rod attached to the lower mass. Pressure gauges were mounted at the top of the air chamber and in the metering chamber below the orifice plate. The airplane pitch and roll angles were measured by gyroscopes mounted at the airplane center of gravity. A discussion of the available frequency responses and the calibration work done before the flight test and before and after the drop test program can also be found in the instrumentation report, Reference 2.

FLIGHT TESTS

The procedures followed during the flight test phase of the investigation were intended to produce oscillograph records of symmetrical landings. The pilot was instructed to touch-down on a predetermined section of runway at a given sink and horizontal speed.

Vertical speeds were measured by a device known as a Photoscope, by a standard touch-down rate of descent indicator (TRODI) installation and by means of a Mitchell camera. The photoscope is a 35mm movie camera running precisely at 200 frames per second. It has a 6 1/8 inch, f4.5 lens and a shutter speed of 1/284th second. A circular etched glass grid is located in close proximity to the film plate so that vertical and horizontal grid lines are superimposed on the photograph of the airplane. Sinking speeds were determined at the test site by TRODI and the Mitchell. Final values for sinking speed and horizontal speed were derived from the Photoscope data.

The gross weight of the airplane was measured after refueling and the gross weight for each landing determined by subtracting the calculated weight of fuel required for go-around.

A series of landings was begun by conducting a preflight calibration of the strain gauges while the airplane was on jacks. Strut internal air pressure, tire pressure, ambient temperature, and wind direction were also recorded prior to each landing. A survey was made to determine longitudinal and lateral slopes of the landing area.

Records were made of 96 landings on concrete and 106 on the runway coated with Navy non-skid deck compound. Of these, two satisfactory landings, at different horizontal speeds, were picked at each of the desired sink speeds between 12 and 16 feet per second. A preliminary inspection for symmetry was made of the records and a landing was deemed satisfactory if there was less than one degree of roll, if the main gear touched down within four feet of each other, and the sink speed was not more than ±1.0 foot per second from the intended.

After the basic series of landings had been concluded, the investigation was extended to gather additional data. Two external 150 gallon fuel tanks were installed on the wings and records made from all of the gear instruments plus accelerometers attached to the fuel tanks. Landings were also made under unsymmetrical loading conditions by landing with an initial roll angle, and another group was conducted by setting the airplane down just in front of an arresting cable so that the tire would hit the cable while the tire was bottomed. The unsymmetrical, external tank and arresting cable data are presented in Reference 5.

Reference 3 describes the details of the flight testing. It contains the time-history plots of the reduced oscillograph records and the ground loads derived from the data. The ground loads were read at .001 second intervals. A Fortran program was written so that the digital computing equipment could use the oscillograph data which was punched on cards as the records were read.

DROP TESTS

The drop test phase of the investigation used the same two main gears and instrumentation as the flight test phase. A series of airplane drops were made duplicating the initial conditions of five of the landings made on the concrete surface. The drop height was adjusted to give the proper sink speed at touchdown which was checked by a TRODI installation. The attitude of the airplane was adjusted by moving the hoist point relative to the center of gravity until the pitch angle was the same as that of the landing. The wheels were spun-up prior to drop to a speed matching that of the landing. Wing lift was simulated by pneumatic dampers which introduced concentrated forces on the wings just prior to contact of the tire with the ground. The links attaching the dampers to the airplane were instrumented so that an accurate record of the variation of lift with time was obtained.

The ground loads obtained were checked by a reaction platform which had variable sized grooves in the surface for changing the coefficient of friction.

The recording equipment used in flight test was also used in the drop tests. In flight tests, this equipment was assembled in the shell of a 150 gallon external fuel tank and was carried on the centerline racks. In the drop tests, the same external store was used but it was set on the ground, signals from the sensors being transmitted by a flexible electronic cable. This arrangement improved the quality of the data by eliminating high frequency oscillations created by the landing shock.

Additional oscillograph channels were included to measure pressure in the rebound chamber, the reaction platform loads and wing lift.

The total of 128 drops included some at various wing lift values and wheel spin-up speeds to augment the theoretical investigation. The time histories of the measured data reduced from the oscillograph records are presented in Reference 4 along with a comparison of the ground loads from the strut data and reaction platform data. A Fortran program was written so that the IBM 7090 computer could calculate ground loads, coefficient of friction, average coefficient, and wing lift from the data read from the records. Reference 4 also reports on the details of the drop test phase of investigation and evaluates the accuracy to be expected from the work.

THEORY

In order to determine analytically the variation in loads on the A4D-2 gear during landing, equations of motion were written which simulated the operating characteristics of the gear and the elastic properties of the gear and airplane structure. Structural dynamics techniques of the type required for this investigation have been developed over a period of years in connection with the DC-8 aircraft (Reference 6). Further development of the methods was made in connection with an Army contract (Reference 7). Additional modifications were introduced for this landing loads investigation to account for the peculiarities of the A4D-2 landing gear. The equations are listed in Appendix A.

STRUT DESCRIPTION

Except for the use of splines to carry strut torque the main gear is a conventional air-oil landing gear strut. A photograph of the gear is shown in Figure 2 and a drawing of the internal parts is shown in Figure 3. The maximum possible stroke is 16 inches, but the strut is filled with hydraulic fluid (MIL-0-5606) while less than fully compressed so that it cannot bottom metal-to-metal. The air chamber is pressurized to 25 psi while the strut is extended. The tire is a Goodyear 24 x 5.5 Type VII with the pressure kept at 320 psi. The strut is attached to the wing 40 inches from the airplane centerline and at an angle of six degrees, aft from a perpendicular to the FRL. Figure 4 is a schematic of the internal parts of the strut.

BASIC ASSUMPTIONS

Airplane motion is represented by six degrees of freedom; four flexible modes and two rigid body displacements. The flexible modes are assumed to be undeflected at touch-down. Strut motion is assumed to be governed by four additional degrees of freedom. They are the displacements in the three planes plus torque about the strut centerline. The aerodynamic forces occurring during a landing are omitted, except that the small differences between "1g" and measured airplane acceleration are included as an initial rigid body acceleration. The airplane is assumed to experience no loss of lift during the time interval considered. Only symmetrical loads and deflections are used so that only one-half the airplane is considered. The nose gear is assumed to have no effect on the main gear load since the flight test data indicated it touched down after the maximum main gear loads were reached. The strut angle and the forward velocity are held constant at their initicl values throughout the calculations. The calculations are performed at an integration interval of

.0001 second and iteration is done by the predict-correct method. Loads and accelerations are calculated from time zero, as touch-down, and answers printed every .001 second until time equals .23 second. Further details of the Theory are described by showing the input required by the Fortran Program.

INPUT DATA

The input to the computing program consists of the geometry and operating characteristics of the strut, the initial velocities, both vertical and horizontal, and the attitude of the airplane. The geometry was determined from production drawings and the constants for input are listed in Table 4.

Figure 5 is a schematic of the metering pin and shows the parameters required by the program to calculate pin cross sectional area. Gear deflections measured during static tests were used to obtain the spring constants in Figure 6. Dynamic tire force deflection characteristics (Figure 7) were obtained from Douglas test data and extrapolated by means of data from Goodyear reports. The assumed force-deflection input curve used in all the calculations is close to both curves and gives the best match with the experimental data. It is entered in the program as a series of straight lines. The cornering power curve, Figure 8, was derived from the formulas in Reference 8. Figure 8 also shows the rebound chamber orifice coefficient. This coefficient was originally assumed to be a constant. The flow of oil into the rebound chamber was assumed, from Bernoulli's equation, to be proportional to the square root of the pressure difference, but the calculated variation in strut internal air pressure could not be made to match the measured values of air pressure while using a constant coefficient. The quadratic curve of Figure 8 was developed after an examination of the rebound chamber pressures measured during the drop test phase of the investigation. Figure 9 shows that the rebound chamber filled with oil as the stroke neared 13 inches. Three of the spline teeth are removed from the upper bearing to provide an orifice for flow of oil into the rebound chamber. The orifice area used was .126 in^2. This value falls between the .0818 $in.^2$ caused by removing three splines and the .2136 $in.^2$ possible gap between bearing and barrel if all of their dimensions are nominal. See Figure 10 and Page 59.

Damping coefficients were estimated by plotting the fore-aft and side accelerations, measured during the flight test phase, and using the peak-to-peak decay ratios.

The constants required to introduce the natural modes of vibration were derived from ground vibration tests of the model A4D-2 airplane, Reference 9. Table 5 and Figure 11 were obtained from this report. Table 6 lists the constants calculated using Table 5, Figure 11, and the equations on Page 100.

It should be noted that the highest structural frequency introduced into the calculations was 33.6 cps. A tire-wheel frequency of 50 cps was also introduced. These were the highest frequencies obtainable from the input data. The theory will not duplicate load variations of higher frequency.

The conditions at touch-down for the five landings on concrete are listed in Table 7 along with the data for the corresponding airplane drops. The initial conditions for the landings on non-skid are in Table 8. Table 9 gives the values entered into the computing program for each landing, and Page 104 the formulas used to obtain them from the initial conditions. The ground coefficient of sliding friction, μ_s, was chosen, for each of the landings, from the data plotted in Figures 12 to 29. The value for any landing is an average of the instantaneous friction coefficients from time of touch-down to the time of wheel spin-up.

OUTPUT

The Fortran Program's output data consists of a print-out of all of the input data followed by the calculated items listed in Appendix A. Each of the items is calculated from touch-down to a time of .23 second at intervals of .0001 second with every tenth value printed. With this integration interval the IBM 7090 machine running time was 4.8 minutes. Intervals as low as .00001 second were tried without causing any appreciable change to the answers.

PRESENTATION OF DATA

COMPARISON OF FLIGHT TEST, DROP TEST AND THEORY

Figures 12 through 21b compare the ground loads obtained from the airplane landings, airplane drops and theoretical analysis. Initial conditions corresponding to these curves are given in Table 7. The curves will be found to be identical to those in References 3 and 4 except for the start times. The curves for which touch-down differed too much from time zero were shifted to the left so that the times for initial contact were identical. A list of the plots affected and the time changes follows:

Drop	84 - Left Gear	.005 Sec.
Drop	84 - Right Gear	.004 Sec.
Landing	123 - Right Gear	.018 Sec.
Landing	125 - Right Gear	.009 Sec.
Landing	126 - Right Gear	.004 Sec.

The notation for vertical ground load, F_{VG}, and horizontal ground load, F_{HG}, are the same as P_V and P_D shown in the notation for the dynamic analysis in Appendix A. The curves of the horizontal ground load from the theory were not plotted past spin-up for clarity. The ground coefficient of rolling friction used was .03, so that the curve for F_{HG} beyond spin-up is a line nearly parallel to, and slightly above, the time axis.

Figures 22 through 29 compare the landings on non-skid with vertical and horizontal ground load calculated by the analysis. The landing data was taken from Reference 3. The input to the Fortran Program assumed a zero yaw angle so that the theory curves could apply to either right or left hand gears. The theoretical ground sliding coefficient of friction is not shown as it was assumed to be a constant. The values used are listed in Table 9. A comparison of maximum vertical and drag ground loads is provided in Tables 10 and 11.

The data plotted in Figures 30 through 34 compare the rest of the parameters measured during the testing phases with the calculated values. This comparison is supplied only for Landing 125, Drop 68 and the corresponding Tneory. The time-histories compared include air pressure, strut stroke and velocity, axle acceleration in the vertical, lateral, and fore-aft directions, the upper mass accelerations, and the strut oil and bearing friction loads. All of the experimental curves were plotted directly from the measured data presented in the test reports except the oil load and bearing friction load.

The "strut oil pressure" (pressure drop across the orifice) was obtained by subtracting the pressure measured in the air chamber from the pressure measured in the metering chamber. The bearing friction load was obtained by subtracting loads derived from air and metering chamber pressures from the strain gauge load measured at the axle.

EFFECT OF AIRPLANE FLEXIBILITY

Figure 35 demonstrates the degree to which the structural mode shapes affect the calculated ground loads. The curve marked "Flexible" is a duplicate of Landing 125 Theory curve of Figures 16 and 17. The input to the program included the four natural modes of vibration plus rigid body bobbing and pitch. The bobbing and pitching modes plus the gear flexibility were the only ones used to calculate the curve marked "Rigid".

EFFECT OF SINKING SPEED ON MAXIMUM LOAD

A summary was made of the data from the flight and drop test phase of the investigation to compare maximum vertical ground loads and sink speed. The maximums occur at either of two different times, one near .04 second and another near .15 second after touchdown. Figure 36 is a plot of the maximum vertical load versus sink speed of the first peaks from the flight test data, the drop test strut data, and the drop test platform data. The second peak vertical loads are plotted as Figure 37. The diagonal lines were added only as a guide to show the general trend. Figure 37a is a plot of maximum vertical load (wherever it occurs) versus sinking speed.

WHEEL SPIN-UP

The flight test landings were made on both concrete and nonskid surfaces. Table 12 provides certain information regarding the fore and aft forces obtained on the two surfaces. The time for the wheel to spin up, the average coefficient of sliding friction up to the time of spin-up, the maximum drag load, and the wheel rotational velocity at the time of spin-up are listed for all of the landings. As a check, wheel speed was calculated by integrating the torque caused by the horizontal ground load. The speed of the wheel which was calculated by the Fortran program is also listed for comparison.

METERING ORIFICE COEFFICIENT

The measurements of strut compressing velocity and internal pressures made it possible to check the orifice coefficient used in the theoretical analysis to calculate orifice damping load. The formula shown on Page 36 is:

$$P_o = \frac{P_o(A_1 - A_p)^3(\dot{S})^2}{2\left[C_D(A_o - A_p)\right]^2}$$

The oil load, P_o, from the pressure in Figure 34, was calculated for Landing 125 and Drop 68, and used to solve the formula for C_D. Figure 38 is a plot of the orifice coefficient as a function of stroke.

COMPARISON WITH NASA LANDING TRACK DATA

Reference 1 reported a series of landing impact tests, conducted with an A4D-2 main gear, to obtain data on tire spin-up friction coefficients at touch-down. The Langley landing-loads track was used to simulate landing conditions. Four of the runs from the NASA report are compared to landing in this report. The initial conditions for those comparisons are given in Table 13, and the vertical and horizontal ground loads are plotted in Figures 39 and 40.

DISCUSSION OF RESULTS

GENERAL

In evaluating the results of the test program reported herein, consideration must be given to the accuracy of the measurements and the basic assumptions of the theory. It has been noted that the sinking speeds have been determined within ± .4 feet per second in flight test and ± .2 feet per second in drop test. Energy-wise this accuracy represents ± 5% and ± 2 1/2% on a 16 fps sinking speed. The accuracy with which ground loads were measured has been estimated at ± 5%. If it is assumed that ground loads vary directly with energy of impact, a possible total error of ± 10% exists. In other words, if a comparison is being made between a computed vertical load and a measured flight test load, a discrepancy of ± 10% is possible due to mensuration problems alone. If a comparison is to be made between a drop test and a landing load, the possible difference due to mensuration accuracy can be even greater, if the error in one test is positive and the other is negative. Thus, it cannot be expected that small differences in loading created by the difference in testing technique between flight and drop testing will be discovered by this investigation.

A significant result of the tests described herein is the lack of symmetry of ground loads developed in both the landings and the drop tests under initial conditions which appeared to be symmetrical. This result was disappointing in that the lack of symmetry also obscured minor differences between drop tests and flight tests leaving only gross differences for discussion.

The result was of significance since it can be presumed that similar differences between right and left will exist in other practical designs and must be considered as part of the design criteria. The asymmetry is only partially apparent in the comparison of maximum loads (Table 10), however, examination of Figures 12 through 29 shows substantial differences in shape of the left and right load curves for nearly all conditions.

The asymmetry is attributed to the following factors:

1. Differences between right and left hand gears:

   The two landing gears used in these tests were identical except in the following respects: (a) the right gear was new; the left gear had been used extensively in previous test work and (b) the right gear had a structural reinforcement at the juncture of the axle and strut. The reinforcement was of such a nature that it increased the ultimate strength appreciably but had little effect on the

deflection or frequency characteristics. It is believed that the significant factor here is the service experience of the gears. Subsequent discussion will show that bearing friction resists a substantial portion of the total ground load, and friction will depend to some extent upon a "wearing in" process.

2. Rolled Attitudes or Rolling Velocity

In flight tests it was noted that there was a definite tendency for the left gear to strike the ground sooner than the right. For the landings chosen, the amount of the rolled attitude was low being equal or less than one degree, or four feet on the runway. Although this is a small asymmetry, it may have caused asymmetric input to the airplane and excited asymmetric structural modes. In drop tests, the attitude was also level within one degree and usually was much closer than that. Asymmetric input was to some extent introduced by differences in the lift load supplied by the lift dampers. (See Reference 4)

3. Runway Roughness

The general slope of the runway, both longitudinally and laterally, was measured. Localized irregularities were not. The effect of landing with one wheel on a tar strip is shown in Figure 25 for Landing 114. Calculations reported in Reference 7 show that small irregularities produce abnormally large load increments when the tire is flat. This occurs at an F_{VG} of 30,000 lbs. and at approximately 16.0 fps sinking speed.

A basic assumption in the dynamic analysis was that of symmetry. It is to be expected, therefore, that the theoretical loads would tend to be an average between left and right measured loads.

COMPARISON OF FLIGHT TEST AND DROP TEST RESULTS

A study of the ground load comparison curves presented in Figures 12 to 21 shows substantial differences between flight test and drop tests. Only three features, however, appear with any consistancy. First, in examining Figures 12 to 21, it is evident that the drop test loads are lower near the end of the stroke than are the flight test loads, suggesting that the flying wing lift is released in a different manner than the drop test lift. Second, the drop test drag loads are much larger than the flight test drag loads. Part of this difference is due to the difference in roughness of the contact surface. The drop test surface was chosen

on the basis of reaction platform readings to give the same average friction coefficient as the runway, but it was determined that the reaction platform drag readings were not accurate, and consequently, a poor choice of surface was made. Third, it is noted that in drop tests the first peak of the drag curve is as high as, or higher than, the second, whereas in flight tests the second peak is always higher than the first. It is believed that this phenomenon is attributable to the difference created by simulating forward speed by wheel spin-up.

The data in some instances shows remarkable similarity between flight and drop data. At other times it shows disturbing discrepancies. The probable reasons for this situation have been discussed on Page 15. In order to determine the general correlation, Tables 10 and 11 were prepared. These tables show a comparison of maximum loads obtained from right and left gears, the average load and the ratio of average drop test load to average flight test load. With the exception of Landing 123 versus Drop 70, the agreement on vertical loads is within ± 16%. Further comment on Landing 123 is made in subsequent paragraphs.

COMPARISON OF THEORY WITH FLIGHT TEST AND DROP TEST DATA

A study of Figures 12 through 29 shows that the theory produces curves of the same general shape as the flight tests and drop tests. The first, second and third peaks of the vertical load curve are reproduced although the timing is not identical. The vertical load from theory tends to fall off earlier toward the end of the stroke than does the vertical load from flight test. In this regard, the theory resembles more the drop test data than the flight test data. Where there is a large difference between left and right gear loads, for example Figure 22, the theory tends to predict an average.

Drag loads predicted by theory are again generally similar to those obtained from flight test data. The theory fails to predict the dip in the middle of the drag curve. The magnitude of the analytically derived drags is usually closer to the flight test drags than to the drop test drags. This is to be expected since the average friction coefficient used in the theory was made equal to that of flight test instead of the drop test coefficient.

Tables 10 and 11 also summarize the data with respect to maximum loads obtained from theory. It is evident from this table that the theory gives better correlation with flight test data than does the drop test data both as to vertical loads and drag loads. It can be said that, on the average, theory tends to be conservative. Landing 123 again stands out as being exceptional, lending evidence to an assumption that data from that landing is erroneous.

ENERGY RELATIONSHIPS

A peculiar phenomenon was noted in a comparison of the energy in the load-stroke curves and the initial energy of vertical motion of the airplane (see Table 14). Included in Colume (2) is the pitching motion energy remaining at the end of the stroke and in Column (3) the energy absorbed by wing lift in excess of 1W. Residual rolling energy is not included but has been estimated at less than 1000 ft-lbs.

It has been noted in other airplane drop test work that the energy accountable for after completion of the stroke is less than the original kinetic energy. This has been attributed to the energy absorbed by the structure in deflections and vibrations. This phenomena is noted herein. There is, however, no explanation for the greater disparity in drop tests than in flight tests except for the possibility that wing lift in flight tests is not constant at the initial value as assumed in the calculations. Landing 123 is again conspicuous by its lack of conformity with other conditions and should be discounted.

STRUT INTERNAL PARAMETERS FOR LANDING 125, DROP 68, THEORY

The three air pressure curves for this case are plotted in Figure 30. The theoretical curves follow the other two when plotted against stroke, and reach the same maximum after dipping when the rebound chamber fills. Plotted against time, the calculated curve rises too fast in accordance with the greater stroke values shown in Figure 31. The bump in the air pressure from Landing 125, which can be seen at a time of .06 second or 6.5 inches of stroke, appeared in several of the records made at the higher sink speeds, but is not predicted by theory.

The calculated strut velocity in Figures 31 is a good average of the test curves until the oscillations appear. The axle vertical acceleration, shown in Figures 32 and 33, matches the test data closer than the other accelerations, but it also deviates after the oscillations from the tire start. The curves of Figure 34 compare the internal forces in the strut and the manner in which the calculated tire oscillation is reacted. The maximum peaks of oil pressure are 180 degrees out of phase with those of bearing friction. The measured parameters show some high frequency oscillation but none of a magnitude exhibited in the theory. A damping term in the equation for $\ddot{a}$ or a damping load in the tire load equation would be necessary to obtain a better comparison.

It will be noted that the friction load from Figure 34 is 9,000 to 11,000 lbs. at t = .03-.06 seconds. The total load during this period from Figure 17 is 20,000 lb. maximum. Friction, therefore, resists approximately half of the total gear load at this point in the stroke.

CONCLUSIONS

The primary objectives of this investigation were:

1. To evaluate the adequacy of simulating landing loads by airplane drop tests.

2. To determine the accuracy with which these loads may be predicted by advanced analytical methods.

3. To compare the loads measured on the moving drop test rig at the Landing Loads Facility of NASA with the loads obtained in flight tests.

Based on the comparison contained herein of five actual landings with five drop tests, the following conclusions are reached with respect to simulating landings by drop tests:

1. Exact duplication of a given landing by a drop test is not possible using the methods of control available for this series of tests.

   In flight test landings, runway irregularities, small asymmetries, such as rolling velocity or displacement, inaccuracy in measurement of sinking speeds and minor differences between right and left gears create substantial differences in loading which are not reproducible in detail by a drop test.

2. Although exact duplication of a given landing is not obtained by a drop test with similar initial conditions, a large number of drop tests will, as a whole, produce a series of loadings which will substantiate the gear strength for actual landings.

3. General correlation exists between the vertical loads developed in flight tests and drop tests to the extent that maximum loads were, on the average, within $\pm$ 16% and the shape of the load curves showed marked similarity.

4. Maximum drag loads developed in drop test were substantially higher than those obtained in flight test.

   This was caused primarily by the surface used on the drop test reaction platform. Better drag load correlation could easily be obtained by a better choice of surface.

5. Vertical loads obtained from actual landings near the end of the stroke were in most cases higher than those obtained in drop tests.

6. The drag load versus time curve exhibited two well-defined peaks both in actual landings and in drop tests. In actual landings, the second peak was always higher than the first while in drop tests the first was higher than the second.

7. Asymmetries in loadings of significant magnitude will occur in nominally symmetrical landings and drop tests. Normal methods of control are not sufficient to eliminate these asymmetries.

The following conclusions are reached with respect to predicting landing loads by advanced analytical methods.

1. The analytical methods on the average predicted the maximum ground loads better than the drop tests.

2. The shape of the vertical load versus time curve derived from theory showed marked similarity to those obtained from landings.

3. Where large asymmetries in vertical load were recorded in landings, the theory tended to predict an average between left and right gears.

4. The theoretical curve vertical load peaks had a tendency to be reached sooner than the flight test load peaks and the load fell off more rapidly toward the end of the stroke. In this regard, the theory resembled the drop test data.

5. The drag loads predicted by theory were of the right magnitude, however, the dip in the middle part of the drag load versus time curve was not duplicated by theory.

6. Insofar as the secondary parameters, such as internal pressures, accelerations and friction load, are concerned the correlation of theory with test varied from good to poor. Load variations with a frequency higher than 50 cps were not duplicated by the analysis. Better correlation was obtained in the early part of the stroke than in the latter part of the stroke.

7. In contrast to the conclusion reached in Reference 10, the value of the polytropic exponent for air-compression was of primary importance in the analysis defining in several cases the magnitude of the maximum vertical load.

8. The analytical work was to some extent influenced by the test results. Test experience combined with correlation of test and analysis is desirable before relying heavily on the results of a dynamic analysis.

A comparison of data obtained from the NASA moving drop test rig with data from flight test landings showed a correlation of vertical loads which was as good as could be expected considering the accuracy of duplication of initial conditions and the degree of asymmetry registered in the flight tests.

The NASA data failed to register the double peak in the drag curve and showed large load oscillations after spin-up which did not exist in flight test or in laboratory drop tests.

A secondary objective of this project was to develop simplified methods of analysis which could be used in design. To this end, calculations were made in which the aircraft flexible modes were eliminated. The results showed that the flexible modes had little effect on the calculated ground reactions. This conclusion cannot be generalized, however, inasmuch as the extent to which these modes affect the ground loads will depend upon the relationship of their frequencies to the power and frequency content of the input. A more flexible airplane could be expected to react differently in this respect than the relatively rigid A4D-2 airplane. It should be noted that the gear flexibility was not eliminated at the time the flexible modes were removed.

Time limitations did not permit further investigation into the subject of analysis simplification. Undoubtedly, there are certain simplifying assumptions that could be made without compromising accuracy, on the other hand, it is evident that certain additional features need to be included for better correlation. These are discussed under Recommendations.

RECOMMENDATIONS

The recommendations which follow are categorized into groups relating to (a) instrumentation or testing techniques, (b) analytical procedures and (c) additional investigations.

A. Instrumentation and Testing Techniques:

1. It is recommended that a method or device for measuring more accurately the vertical velocity of a landing airplane be developed.

2. It is recommended that a standard drop test reaction platform be developed which measures vertical, drag and side loads with satisfactory accuracy under the dynamic conditions experienced in drop tests.

3. The accuracy of the slide-wire device as a means of measuring stroke and the velocity generator as a means of measuring strut velocity should be re-examined in the light of discrepancies noted in Reference 4.

4. In future landing loads tests involving flight landings, greater consideration should be given to obtaining a smooth landing surface, and automatic methods of maintaining a level attitude should be incorporated if symmetry is desired.

5. A thermocouple should be included in the strut air chamber to provide experimental data on the polytropic exponent, n, in the equation relating pressure, volume and temperature.

B. Analytical Procedures:

1. The gyroscopic forces created by wheel rotation should be included in a landing load analysis unless it can be demonstrated that they are negligible.

2. It is recommended that a more precise representation of the aerodynamic forces than the one used in this analysis be included. This representation should include the changes in angle of attack caused by rigid body rotation and change in vertical velocity.

3. More accurate tire-load deflection curves and wheel-tire polar moment of inertia data should be obtained to provide better basic data for the analysis.

4. A variable polytropic exponent for air compression should be incorporated.

5. A damping term should be incorporated in the equation of axial motion of the axle or in tire deflection curve after testing has been done to determine the information required

C. Additional Investigations:

1. It is recommended that the following analytical investigation be pursued:

   a. Revise the computing program to include as many of the changes listed in "B" above as are economically feasible but including as a minimum the gyroscopic forces and the more precise representation of aerodynamic forces.

   b. Correlate the results of calculations from the revised analysis with data from three of the landings. The three landings used should be those resulting in the greatest symmetry of loading and should cover as wide a range of sinking speeds as possible.

   c. After obtaining improved correlation with test data, compute the loads resulting from drop tests. The initial conditions should be identical to those of the flight test conditions. Appropriate differences related to spin-up and the introduction of wing lift should be incorporated.

   d. By comparing the results of (b) and (c), determine the differences between the analytically determined loads for drop tests and the analytically determined flight landing loads. Since the initial conditions in both sets of analytical calculations will be identical, it is expected that differences in loadings resulting from inherent differences between actual landings and drop tests will become apparent.

2. It is recommended that the revised analytical program be applied to the computation of the load increments resulting from running over an arresting cable, that the results of these computations be correlated with the test data obtained during the flight test phase of this program and that the analysis be used to determine methods of alleviating the load pulse from the cables. It is expected that the accurate prediction of the load pulses will require an accurate knowledge of the tire load-deflection curve. A test program to retain such information should therefore be a part of this investigation.

3. Recent development in the computing program has produced the capability of analyzing rolled landings, and it is therefore recommended that an attempt be made to correlate the analysis with the data from the unsymmetrical landings obtained during the flight test phase of the program. If a reasonable correlation can be obtained, the analytical procedures should be used to investigate the effects on landing loads of asymmetry over a wide range of angles of roll but with special emphasis on small angles. Also, the effect of initial roll rate should be studied. The results should be used to derive simplified analytical or semi-empirical methods of accounting for the effects of roll.

4. The difference in energy noted in Table 14 between the pre-contact conditions and the final conditions requires further study. The assumption that the missing energy is in the structural deflections or motions does not agree with the analytical conclusion that structural deflections have little effect on the load-stroke curve. Since the phenomenon violates the fundamental theorem of conservation of energy, and since the discrepancy is substantial in the case of drop tests, it is important that an explanation be obtained. Further intensive investigation of this item is, therefore, recommended.

APPENDIX A

EQUATIONS OF MOTION

DYNAMIC LANDING LOADS ANALYSIS

NOTATION

Theory	Fortran	Definition	Units
$a, \dot{a}, \ddot{a}$	A	Motion at axle parallel with strut of unsprung mass of rolling assembly, positive down.	in.,sec.
$\bar{a}$		Distance from lower piston bearing to axle parallel to strut with strut fully extended.	in.
A_0		Gross orifice area w/o reduction for pin.	$in.^2$
A_1		Internal area of oleo piston	$in.^2$
A_2		Piston area based on i, d. of lower bearing	$in.^2$
A_p	AP	Metering pin area, function of strut stroke	$in.^2$
a_i		Slopes of line equation for pin diameter	-
$[A_{ij}]$		Aerodynamic damping coefficients	1/sec.
$\alpha \dot{\alpha} \ddot{\alpha}$	Alpha	Angular motion of rolling assembly	Rad.,Sec.
b_i		Intercepts of line equations for pin diameter	in.
$\bar{b}$		Distance from upper to lower piston bearing parallel to strut, strut fully extended	in.
$[B_{ij}]$		Coefficients of displacements in airplane equation of motion	$1/sec.^2$
C	C	Tire deflection	in.
$\bar{C}$		Damping coefficient perpendicular to strut	lb.-sec./in.

NOTATION (Cont'd)

Theory	Fortran	Definition	Units
C_D		Coefficient of discharge	-
C_C		Discharge coefficient for compression	-
C_E		Discharge coefficient for extension	-
C_N		Maximum allowable tire deflection	in.
$\lvert C_i \rvert$		Coefficient of force from gear	$1/lb.sec^2$
$\Delta, \dot{\Delta}, \ddot{\Delta}$	D	Motion at axle perpendicular to strut of unsprung mass of rolling assembly, positive aft	in.,sec.
$\bar{\Delta}, \dot{\bar{\Delta}}, \ddot{\bar{\Delta}}$	BD	Motion at axle in relative coordinates	in.,sec.
δ		Distance from axle to gear attach point with strut fully extended	in.
D_o	DO	Coefficient of oil damping force in oleo	$lb/sec^2/ft^2$
$\lvert D_i \rvert$		Coefficient of moment from gear	$1/ft.lb.sec^2$
$\tilde{e}$		Distance from axle to strut $\mathbb{Q}$ normal to strut, positive for axle forward	in.
$\lvert E_i \rvert$		Vector column of constants	$1/sec^2$
ϕ		Angle of strut with vertical, positive for strut forward of gear attach point	
F_A	FA	Load on axle parallel to strut, positive down	lb.
$F_\perp$	FP	Load on axle $\perp$ to strut, positive aft	lb.

NOTATION (Cont'd)

Theory	Fortran	Definition	Units
F_H	FH	Load on airplane from gear, $\perp$ to reference plane, positive down	lb.
F_1	F1	Normal force on upper piston bearing, positive aft	lb.
F_2	F2	Normal force on lower piston bearing, positive aft	lb.
g		Gravitational constant	in/sec^2
$\lvert G_1 \rvert$		Coefficient of moment from gear	
$\lvert H_1 \rvert$		Coefficient of force from gear	
I_R		Mass moment of inertia of rolling assembly	$lb.in.sec^2$
K_1		Strut influence coefficient, deflection fwd. due to force acting down parallel to strut	in/lb
K_{32}, K_{33}		$K_{32}+S\,K_{33}$ is deflection aft due to force acting aft perpendicular to strut	lb./in., $lb./in.^2$
k_1, k_2		Coefficients of gear force for horizontal accelerations	-
λ		Instantaneous skidding velocity	ft/sec.
λ/V_L	SR	Slip ratio	-
ℓ_1		Intercepts in lines for tire load	lb.
m_1		Slopes in lines for tire load vs. deflection	lb/in.
n		Polytropic exponent for strut air load	-
o		Subscript to denote initial conditions	-

NOTATION (Cont'd)

Theory	Fortran	Definition	Units
P_A	PA	Strut air load	lb.
P_D	PD	Drag load in horizontal plane	lb.
P_E	PE	Airload in oleo with strut extended	lb.
P_F	PF	Bearing friction force on strut	lb.
P_O	PO	Strut oil load	lb.
$P_\perp$	PP	Force at axle (relative coordinates) perpendicular to strut positive fwd.	lb.
P_T	PT	Tire load	lb.
P_V	PV	Vertical ground reaction load	lb.
$[P]$		Coefficients of generalized displacement	ft or in.
$Q, \dot{Q}, \ddot{Q}$	A	Airplane motion, generalized coordinates	-, 1/sec, $1/sec^2$
ρ_o		Mass density of hydraulic fluid	$lb.sec^2/in.^4$
R_o		Radius of undeflected tire	in.
R	R	Instantaneous rolling radius of tire	in.
$[R]$		Coefficients of generalized acceleration	-
$S, \dot{S}, \ddot{S}$	S	Strut motion measured from full extension	in.,sec.
S_c		Maximum strut stroke	in.
S_1		Values of S associated with pin constants	in.

NOTATION (cont'd)

Theory	Fortran	Definition	Units
$[S]$		Coefficients of $\ddot{Q}$ in equation for airplane loads	-
t		Time	sec.
Δt		Interval of numerical integration	sec.
t_F		End of integration	sec.
$\lvert T_{H1} \rvert$		Generalized airplane coefficients of force at gear attaching point	in./lb.sec^2
$\lvert T\alpha_1 \rvert$		Generalized coefficients of moments at gear attaching point	1 lb/sec.^{2}
μ		Coefficients of friction identified (numerically) by its subscript	-
μ_1		Bearing coefficients friction before strut moves - static friction	-
μ_2		Bearing coefficients after strut moves	-
μ_s	GRMU	Ground coefficient sliding friction	-
μ_R	GRMU	Ground coefficient rolling friction	-
$\lvert u \rvert$		Arbitrary constants in equation for loads on airplane	-
V_E		Air volume in oleo strut extended	in.^{3}
V_L		Forward velocity of airplane	in./sec.
$[V]$		Coefficients of generalized velocities	in. or ft.

NOTATION (Cont'd)

Theory	Fortran	Definition	Units
W_U		Unsprung weight of gear	lb.
W_N		Airplane net weight supported by gear	lb.
X	X	Horizontal coordinate of ground contact point for rough terrain function	in.
X_i		Arguments in table of terrain roughness, $0 \leq i \leq 700$	in.
X_A	XA	Axle coordinate, horizontal displacement along terrain roughness	in.
X_1, X_2, X_3, X_4		Coordinates used to define terrain	in.
X_o		Initial (starting value) of X	in.
$Y_B, \dot{Y}_B, \ddot{Y}_B$	YB	Motion at top of strut	in., sec.
Z	Z	Vertical coordinate of ground contact point for rough terrain function	in.
Z_A	ZA	Axle displacement from touchdown, positive down	in.
Z_o		Initial (starting value) of Z	in.
θ		Ground slope	Rad.
TAN)	TAN	Printed for instantaneous value of ground slope	-
A,B,C,D		Amplitudes of terrain roughness entered in X-table, positive down	in.
M_α	AM	Moment from gear, positive airplane nose up	ft.lb.

NOTATION (Cont'd)

Theory	Fortran	Definition	Units
p		Multiple of Δt at which printing of program output takes place	-
	VA	Vertical accelerations	
	PA	Pitching acceleration	
	SH	Shear	
	BM	Bending moment	
	TQ	Torque	
	AA	Airplane angle of attack	
	AV	Airplane pitching velocity	
	APA	Airplane pitching acceleration	
	VP	Airplane vertical position	
	VV	Airplane vertical velocity	
	AVA	Airplane vertical acceleration	
	HA	Airplane horizontal acceleration	

The following information pertains to the modifications of Report No. SM-23895 for use in the Landing Loads Investigation.

Theory	Fortran	Definition	Units
Y_2	Y2	Motion of unsprung mass rolling assembly at axle perpendicular to the strut, positive inboard, relative to the ground	in./sec.
$P_{\psi re}$	PPSIR	Instantaneous lateral force on tire, perpendicular to the tire, positive outboard, applied at the ground contact point	lb.
P_S	PS	Side force on gear perpendicular to the strut at the axle, positive outboard	lb.
B	B1	Relaxation constant for ground lateral force	1/Rad.
$F_{\psi re}$	FSRE	Steady state ground lateral force on tire due to yaw, perpendicular to the tire, positive outboard	lb.
ψ	PSIMU	Yawed rolling ground friction coefficient	lb./lb.
Φ	PHI	Yaw angle parameter	-
N	-	Tire cornering power	lb./Rad.
F_{PS}	FPSE	Spring force on gear at axle, positive outboard	lb.
C_S	CS	Sidewise strut damping coefficient	lb.-sec./in.
Y_1	Y1	Motion of gear attachment point, positive inboard, relative to the ground	in./sec.
$T_{G\theta}$	TGθ	Matric row of spanwise wing slope components at the main gear attachment point, positive left wing down	Rad.

Theory	Fortran	Definition	Units
K_4	VK4	Strut influence coefficient, side deflection due to unit upward force parallel to strut at wheel-axle intersection	in./lb.
K_{22}, K_{23}	VK23,VK23	Strut influence coefficients such that $K_{22} + S\ K_{23}$ = influence coefficient of sidewise deflection due to unit side force perpendicular to the strut applied at the bottom of the wheel	lb./in, lb./in.^{2}
β	BETA	Torsional motion of unsprung mass about strut centerline, positive counter-clockwise looking down, zero at zero torsional deflection	Rad./sec.
T_β	TB	Torque on upper bearing splines, positive clockwise looking down	in.-lb.
d	D	Perpendicular distance from center line of the strut to the center line of the wheel axle intersection, positive outboard	in.
I_v	VI	Rotational moment of inertia of unsprung weight about the strut center line	lb.-in.-sec.^{2}
K_β	VKB	Influence coefficient of strut in torsional rotation	in./lb./Rad.
C_β	CB	Damping coefficient of strut in torsion	in.-lb.-sec./Rad.
Ψ	PSI	Tire yaw angle with respect to ground, positive counter-clockwise looking down	Rad.
F_{1S}	F1S	Side force on upper piston bearing, positive outboard	lb.
F_{2S}	F2S	Side force on lower piston bearing, positive inboard	lb.

Theory	Fortran	Definition	Units
F_{1T}	F1T	Resultant upper bearing force	lb.
F_{2T}	F2T	Resultant lower bearing	lb.
F_T	FT	Bearing normal force due to torque at splines	lb.
r	SMR	Mean contact radius of splines at the upper piston bearing	in.
$\mu_{3'4'5'6}$	BMU3 BMU4 TMU5 TMU6	Coefficient of friction for lower bearing (3,4) and torque (5,6). Odd numbers before strut moves and even numbers after strut moves.	lb./lb.
Q_O	QZRO	Oil discharge coefficient through splines	$\frac{\text{in.}^3}{\text{sec.-lb.}^{1/2}}$
A_R	AR	Cross-sectional area of rebound chamber at the piston upper bearing	in.^2
n_2	EXP2	Air exponent after rebound chamber fills	-
A_{SPL}	ASPL	Cross-sectional piston area at the upper bearing including splines	in.^2
A_{POD}	APOD	Cross-sectional area of piston based on the outside diameter at the lower bearing	in.^2
EQ	SUMQ	Oil volume escaping to rebound chamber	in.^3
F_1	FI	Coefficient of M_θ, moment from gear	$\frac{1}{\text{ft.-lb.-sec.}^2}$
M_θ	MTHETA	Wing bending moment from gear attach point. Only symmetrical component is considered. Positive wing tip down.	ft.-lb.

EQUATIONS OF MOTION

GEAR EQUATIONS

$$\ddot{\Delta} = \left[-P_V \sin\phi + P_D \cos\phi - P + W_U \sin\phi\right] \div \frac{W_U}{g}$$

$$\ddot{a} = \left[- P_V \cos\phi - P_D \sin\phi + F_A + W_U \cos\phi\right] \div \frac{W_U}{g}$$

$$= \left[T_{H_1}\right] \left| \ddot{Q}_1 \right| \cos\phi \quad \text{Before the strut moves}$$

$$\ddot{\alpha} = \mu P_T \left(R_o - \frac{C}{2}\right) \div I_R$$

$$F_\perp = \left[-\bar{\Delta} - K_1 F_A\right] \div \left[K_{32} + S K_{33}\right]$$

$$P_\perp = - F_\perp + \bar{C} \dot{\Delta}$$

$$F_A = P_A + P_O + P_F$$

$$= \frac{W_U}{g} \ddot{a} + P_V \cos\phi + \mu P_V \sin\phi - W_U \cos\phi$$

Before the strut moves

$$F_1 = \frac{P_\perp (\bar{a} - S) - F_A (\bar{e} - \bar{\Delta})}{\bar{b} + S}$$

$$F_2 = F_1 + P_\perp$$

$$P_F = \left|\mu_1 F_1\right| + \left|\mu_1 F_2\right|$$

$\dot{S} \geq 0$, P_F positive

$\dot{S} < 0$, P_F negative

$\mu_i = \mu_1$ Before strut moves

$= \mu_2$ After strut moves

$$\ddot{Y}_B = \left[T_{H_1}\right] \left| \ddot{Q}_1 \right|$$

$$\ddot{\bar{\Delta}} = \ddot{\Delta} - \ddot{Y}_B \sin\phi + (\delta - S) \left[T_{\alpha_1}\right] \left| \ddot{Q}_1 \right|$$

$$\ddot{S} = \left[T_{H_1}\right] \left| \ddot{Q}_1 \right| \cos\phi - \ddot{a}$$

$$P_O = D_o \dot{S} |\dot{S}| \qquad D_o = \frac{\rho_o (A_1 - A_p)^3}{2[C_D (A_O - A_p)]^2}$$

$$A_p = \frac{\pi}{4} (a_1 S + b_1)^2$$

$$C = R_o - R$$

$$P_T = \ell_1 + m_1 C$$

$$\lambda/V_L = 1 - \frac{(R_o - \frac{C}{2}) \dot{\alpha} + \dot{\Delta} \cos \phi}{V_L}$$

$\mu = \mu_S$ Before spinup

$= \mu_R$ After spinup

$$P_V = P_T \cos \theta + \mu P_T \sin \theta$$

$$P_D = - P_T \sin \theta + \mu P_T \cos \theta$$

Criterion for strut motion $F_A \geq P_E + P_F$

$$X_A = X_o + V_L t - \Delta \cos \phi + a \sin \phi$$

$$Z_A = Z_o + \Delta \sin \phi + a \cos \phi$$

$$X = X_A - R \sin \theta$$

$$Z = A \left[1 - \cos 2\pi \frac{X - X_1}{X_2 - X_1}\right] + C$$

$$\text{TAN } \theta = \frac{2\pi A}{X_2 - X_1} \sin 2\pi \frac{X - X_1}{X_2 - X_1} + C$$

$$R = \left[(X - X_A)^2 + (Z - Z_A)^2\right]^{1/2}$$

$$\sin \theta = \frac{\text{TAN } \theta}{(1 + \text{TAN}^2 \theta)^{1/2}}$$

$$\cos \theta = \frac{1}{(1 + \text{TAN}^2 \theta)^{1/2}}$$

AIRPLANE EQUATIONS

$$\left|\ddot{Q}_i\right| = \left[A_{ij}\right]\left|\dot{Q}_i\right| + \left[B_{ij}\right]\left|Q_i\right| + F_{H_1}\left|C_i\right|_1 + F_{H_2}\left|C_i\right|_2 + M_{\alpha_1}\left|D_i\right|_1 + M_{\alpha_2}\left|D_i\right|_2 + \left|E_i\right|$$

$$F_H = -F_A \cos\phi - F_\perp \sin\phi$$

$$M_\alpha = (\delta - S) F_\perp$$

$$\left[A_{ij}\right] = -\left[T^*MT + T^*A_1T\right]^{-1}\left[T^*A_2T\right]$$

$$\left[B_{ij}\right] = -\left[T^*MT + T^*A_1T\right]^{-1}\left[T^*KT + T^*CT + T^*A_3T\right]$$

$$\left|C_i\right| = \left[T^*MT + T^*A_1T\right]^{-1}\left|T^*_{H_1}\right|$$

$$\left|D_i\right| = \left[T^*MT + T^*A_1T\right]^{-1}\left|T_{\alpha_1}\right|$$

$$\left|E_i\right| = -\left[T^*MT + T^*A_1T\right]^{-1}\left(W_{U_1}\left|T^*_{H_1}\right| + W_{U_2}\left|T^*_{H_2}\right| - \delta_1 W_{U_1} \sin\phi_1\left|T^*_{\alpha_1}\right| - \delta_2 W_{U_2} \sin\phi_2\left|T^*_{\alpha_2}\right| - \left[T^*A_2T\right]\left|\dot{Q}_i\right|_{t=0}\right) \quad \text{when } \left|\ddot{Q}_i\right|_{t=0} = 0$$

INTEGRATION EQUATIONS

Prediction

$$X_{N+1} = X_N + \Delta t\dot{X}_N + .5\,\Delta t^2\ddot{X}_N$$

$$\dot{X}_{N+1} = \dot{X}_N + 1.5\,\Delta t\ddot{X}_N - .5\,\Delta t\ddot{X}_{N-1}$$

Correction

$$X_{N+1} = X_N + \Delta t\dot{X}_N + .5\,\Delta t^2\ddot{X}_{N+1}$$

$$\dot{X}_{N+1} = \dot{X}_N + .5\,\Delta t\ddot{X}_{N+1} + .5\,\Delta t\ddot{X}_N$$

where $X = a, \Delta, \alpha, Q$

EQUATIONS FOR LOADS

Accelerations $= \left[R_{ij}\right] \left| \ddot{Q}_i \right|$

Shear, Bending Moment,

Torque $= \left[S_{ij}\right] \left| \dot{Q}_i \right| + F_{H_1} \left|H_i\right|_1 + F_{H_2} \left|H_i\right|_2 + M_{\alpha_1} \left|G_i\right|_1 + M_{\alpha_2} \left|G_i\right|_2 + \left|u_i\right|$

Displacement $= \left[P_{ij}\right] \left| Q_i \right|$

Velocities $= \left[V_{ij}\right] \left| \dot{Q}_i \right|$

Horizontal Acceleration $= (k_1 P_{D_1} + k_2 P_{D_2}) \div W_N$

EQUATIONS

The additional equations for the Fortran program include a new sub-routine for computing the air load and modifications to existing sub-routines. Changes are related to their respective sub-routines.

I. The sub-routine AIR is replaced by the following:

1. $Q_0 = \sum_{i=0}^{5} C_{Q_i} S^i$

2. $Y_1 = \dot{Y}_1 Et$

3. $\Psi = \frac{\dot{Y}_2}{V_L - \cos I} + \beta$

4. $N = \sum_{i=0}^{5} C_{N_i} C_S^i$

5. a. If $\mu_\psi P_T \leq 0$

$\Phi = 0$

b. If $\mu_\psi P_T > 0$

$\Phi = \frac{N\Psi}{\mu_\psi P_T}$

6. a. If $\Phi \leq 1.5$

$F_{\psi re} = \mu_\psi P_T (\Phi - 4/27\ \Phi^3)$

b. If $\Phi > 1.5$

$F_{\psi re} = \mu_\psi P_T (\sin \Phi)$

7. a. If $\mu_\psi P_T = 0$

$P_{\psi re} = 0$

b. If $\mu_\psi P_T \pm 0$

$P_{\psi re} = F_{\psi re} (1 - e^{-B\alpha})$

EQUATIONS (Cont'd)

8. After each time increment the following sum is formed.

$$EQ = \sum_{i=t_o}^{tF} \left\{ Q_o \sqrt{PA} \quad \Delta t \right\}_i$$

9. a. If $EQ > A_R S$

$$n = n_2$$

$$K = 1$$

$$X = \frac{(A_{SPL} - A_R) S}{V_E}$$

b. If $EQ \leq A_R S$

$$n = n_1$$

$$K = \frac{A_{SPL}}{A_{POD}}$$

$$X = \frac{A_{SPL} S - EQ}{V_E}$$

10. $$P_A = \frac{P_E + 14.7 A_{POD} - 14.7 A_{POD} (1 - X)^n}{(1 - X)^n} \qquad (K)$$

II. Additions and revisions to sub-routine ETC3.

These changes follow the calculation for F_2 and replace the calculation for P_F.

1. $F_{PS} = (Y_1 - Y_2 - K_4 F_A - (\delta - S) T_{G\theta} Q_1) (K_{22} + S K_{23})$

2. $P_S = F_{PS} + C_S (\dot{Y}_1 - \dot{Y}_2 - (\delta - S) T_{G\theta} \dot{Q}_1)$

3. $$F_{1S} = \frac{P_S(\bar{a} - S) + F_A (d + Y_1 - Y_2) + P_{\psi re} (R) \cos (I + \theta)}{(\bar{b} + S)}$$

EQUATIONS (Cont'd)

4. $F_{1T} = \sqrt{F_1^2 + F_{1S}^2}$

5. $F_{2S} = F_{1S} + P_S$

6. $F_{2T} = \sqrt{F_2^2 + F_{2S}^2}$

7. $T_\beta = K_\beta \beta + C_\beta \beta$

8. $F_T = T_\beta / r$

9. $P_F = \mu_{1(2)} |F_{1T}| + \mu_{3(4)} |F_{2T}| + \mu_{5(6)} |F_T|$

III. Addition to sub-routine ETC4

$$M_\theta = -F_A (d + Y_1 - Y_2) / 12$$

IV. Modifications to sub-routine COMQ.

$$Q = [A_{ij}] |Q_i| + [B_{ij}] |Q_i| + |C_i|_1 F_{H1} + |C_1|_2 F_{H2} + |D_i|_1 M_{\alpha 1} + |D_i|_2 M_{\alpha 2} + |E_i| + |F_i|_1 M_{\theta_1} + |F_i|_2 M_{\theta_2}$$

V. Modification to the sub-routine ETC5

1. $\ddot{Y}_2 = (-P_{\psi re} + P_S) \frac{g}{W_u}$

2. $\ddot{\beta} = \frac{T_\beta + P_\perp d}{I_V}$

VI. The main program has been modified so that C_D is computed from a polynomial for the sub-routine $D_0 P_0$.

$$C_D = \sum_{i=0}^{5} C_{CD_i} S^i$$

VII. Additions to the sub-routines PRE and COR

The value of Y_2 and β are to be included in the predict-correct computations.

EQUATIONS (Cont'd)

VIII. Additions to the sub-routine OUTPUT

The following additional quantities are to be included in the output list.

P_S, F_T, F_{1T}, F_{2T}, Ψ, F_{PS}, $P_{\Psi re}$, T_β , M_θ, C_S $(\dot{Y}_1 - \dot{Y}_2 - (\delta\text{-}S)$ $T_{G\theta}\ \dot{Q}_1)$, Y_2, $\dot{Y}_2$, $\ddot{Y}_2$, β , $\dot{\beta}$, $\ddot{\beta}$

IX. Additions to the sub-routine INOUT

All new input values and starting conditions are to be included in the print list.

AERODYNAMIC LIFT AND MOMENT

The following formulas for lift, "P", and moment, "M", take into account the change in aerodynamic forces during landing and taxi. It is assumed that the air stream velocity is constant, and that the contribution to lift of circulation lag is negligible.

$$P = -\rho b^2 \Delta X \left[v\pi\dot{\alpha} + \pi\ddot{h} - \pi b a\ddot{\alpha} \right] - 2\pi\rho\Delta X v^2 b\alpha$$
$$- 2\pi\rho\Delta X v b\dot{h} - 2\pi\rho\Delta X v b^2 (.5 - a)\,\dot{\alpha}$$
$$= -\pi\rho \left[b^2\Delta X\ddot{h} - b^3 a\Delta X\ddot{\alpha} \right] - \pi\rho v \left[b^2\Delta x\dot{\alpha} \right]$$
$$-\pi\rho v2 \left[b\Delta X\dot{h} + b^2 (.5 - a)\,\Delta X\dot{\alpha} \right] - \pi\rho v^2 2 \left[b\Delta X\alpha \right]$$

$$M = -\rho b^2 \Delta X \left[\pi (.5 - a)\, vb\dot{\alpha} + \pi b^2 (1/8 + a^2)\,\ddot{\alpha} - a\pi b\ddot{h} \right]$$
$$+ 2\rho\Delta X v b^2 \pi (a + .5) \left[v\alpha + \dot{h} + b (.5 - a)\,\dot{\alpha} \right]$$

$$= -\pi\rho \left[-ab^3\Delta x\ddot{h} + b^4 (.125 + a^2)\,\Delta Z\ddot{\alpha} \right]$$
$$-\pi\rho v \left[b^3 (.5 - a)\,\Delta X\dot{\alpha} \right]$$
$$-\pi\rho v2 \left[-b^2 (a + .5)\,\Delta X\dot{h} + b^3 (a^2 - .25)\,\Delta X\dot{\alpha} \right]$$
$$-\pi\rho v^2 2 \left[-b^2 (a + .5)\,\Delta X\alpha \right]$$

The aerodynamic coefficients occurring in the equations of motion are A_1, A_2, A_3. In the form given below, these coefficients are equivalent to those shown above.

Coefficient of $\ddot{h}$, $\ddot{\alpha}$

$$-\left[A_1\right] = -\pi\rho \left[F_3\right]$$

Coefficient of $\dot{h}$, $\dot{\alpha}$

$$-\left[A_2\right] = -\pi\rho v \left[F_2\right] - \pi\rho v d_1 \left[H_1\right]$$

Coefficient of α

$$-\left[A_3\right] = -\pi\rho v^2 d_1 \left[H_2\right]$$

Where

$$\left[H_1\right] = \begin{bmatrix} \Delta Xb & \Delta Xb^2\ (.5 - a) \\ -\Delta Xb^2\ (.5 + a) & \Delta Xb^3\ (-.25 + a^2) \end{bmatrix}$$

$$\left[H_2\right] = \begin{bmatrix} 0 & \Delta Xb \\ 0 & \Delta Xb^2\ (.5 + a) \end{bmatrix}$$

$$\left[F_2\right] = \begin{bmatrix} 0 & \Delta Xb^2 \\ 0 & \Delta Xb^3\ (.5 - a) \end{bmatrix}$$

$$\left[F_3\right] = \begin{bmatrix} \Delta Xb^2 & -\Delta Xb^3 a \\ -\Delta Xb^3 a & \Delta Xb^4\ (.125 + a^2) \end{bmatrix}$$

d_1 is the slope of the lift curve over π. In Theodorsen's expressions $d_1 = 2\pi/\pi = 2$, which is infinte aspect ratio. For the general case in which $dC_L/d\alpha$ is experimentally determined, $d_1 = dC_L/d\alpha/\pi$. The generalized coefficients are $\left[T^*A_1T\right]$, $\left[T^*A_2T\right]$, $\left[T^*A_3T\right]$.

LOADS ON THE AIRPLANE STRUCTURE

The airplane may be fully represented in the generalized coordinate system. A maximum of eighteen generalized coordinates, Q, may be used. In the sectional coordinate system, X, the airplane is divided into as many mass bays as desired. Each bay may have six degrees of freedom: translation along or rotation about three axes. The transformation from generalized to sectional coordinates is given by $x = [T]\,Q$ where $[T]$ is a modal transform matrix. In the landing impact analysis the generalized vectors, Q, $\dot{Q}$, $\ddot{Q}$, are available at all times.

Through the use of the modal transform matrix, the sectional displacements, velocities, and accelerations at all points on the airplane structure are available for computing loads.

DATA OUTPUT

The following were printed at time intervals of .001 sec.:

P_A	Strut air load	lb.
P_o	Strut oil load	lb.
P_F	Strut friction force	lb.
F_A	Axle load ∥ strut	lb.
$F_\perp$ = FP	Axle load ⊥ strut	lb.
$P_\perp$ = PP	Axle load ⊥ strut in relative coordinates	lb.
F_1	Aft normal force on upper bearing	lb.
F_2	Forward normal force on lower bearing	lb.
P_T	Tire load	lb.
P_V	Vertical ground load	lb.
P_D	Horizontal drag load	lb.
F_H	Gear face on airplane	lb.
M_α = AM	Gear pitching moment on airplane	lb.
A_P	Area of metering pin	$in.^2$
D_O	Oil force damping coefficient	$lb\ sec^2/in.^2$
λ/V_L=SR	Slip ratio	-
X_A, Z_A	Coordinates of axle	in.
X, Z	Coordinates of ground contact point	in.
TAN θ	Slope of terrain at ground contact point	-
C	Tire deflection	in.
R	Rolling radius of ground contact point	in.

$\mu_{R,S}$ =	GRMU, ground coefficients of friction	
F_T	Normal force on splines due to torque	lb.
F_{1T}	Resultant upper bearing force	lb.
F_{2T}	Resultant lower bearing force	lb.
P_S	Side load at axle	lb.
F_{PS}	Side spring force at axle	lb.
T_β	Torque on upper bearing splines	in.-lb.
M_θ	Wing bending moment	ft.-lb.
$P_{\psi re}$	Side load at ground	lb.
C_S	Side damping force	lb.
ψ	Tire yaw angle	Rad.
$S, \dot{S}, \ddot{S}$	Strut motion in strut direction	in.,sec.
$a, \dot{a}, \ddot{a}$	Axle motion in strut direction	in.,sec.
$\Delta, \dot{\Delta}, \ddot{\Delta}$	Axle motion $\perp$ strut	in.,sec.
$\bar{\Delta}, \dot{\bar{\Delta}}, \ddot{\bar{\Delta}}$	Axle motion $\perp$ strut in relative coordinates	in.,sec.
$Y_B, \dot{Y}_B, \ddot{Y}_B$	Motion at top of strut	in.,sec.
$\alpha, \dot{\alpha}, \ddot{\alpha}$	Angular motion of rolling assembly	Rad.,sec.
$Y_2, \dot{Y}_2, \ddot{Y}_2$	Lateral motion of unsprung mass	in.,sec.
$\beta, \dot{\beta}, \ddot{\beta}$	Torsional motion of unsprung mass	in.,sec.

DATA OUTPUT (Cont'd)

The following data are general:

t	Time	sec.
Q, $\dot{Q}$, $\ddot{Q}$	Airplane response vectors	-

REFERENCES

1. Horne, Walter B.: Experimental Investigation of Spin-Up Friction Coefficients on Concrete and Non-Skid Carrier Deck Surfaces. NASA TN D-214, April 1960.

2. Harris, I. E. and Meriwether, H. D.: Landing Loads Investigation Instrumentation. Douglas Aircraft Co. Report ES 40636, October 1962.

3. Harris, I. E. and Tydeman, S. F.: Flight Test Measurement of Landing Loads on the A4D-2 Airplane. Douglas Aircraft Co. Report DEV 3616, November 1962.

4. Allen, F. C., Meriwether, H. D. and Mosby, L. B.: Landing Loads Investigation Laboratory Drop Tests. Douglas Aircraft Co. Report ES 40641, September 1962.

5. Mosby, L. B.: Loads Experienced by the A4D-2 Airplane During Landings with External Stores, During Landings on An Arresting Cable and During Unsymmetrical Landings. Douglas Aircraft Co. Report LB 31074, November 1962.

6. Barndollar, E. J.: Dynamic Landing Loads Analysis. Douglas Aircraft Co. Report SM 23895, in five volumes dated Feb., 1960; Feb., 1961; April, 1961; Sept., 1961; Jan., 1962.

7. Rehder, D. M. and Allen, F. C.: A Rough Terrain Induced Structural Landing Loads Study. Phase I, Analytical Determination of the Effect of Rough Terrain on the Loads, Weight, and Performance of the AO-1 Airplane. Prepared by the Douglas Aircraft Co. for U. S. Army Transportation Research Command, Fort Eustis, Virginia. Task 9R38-01-019-02 Contract DA44-177-TC-735, May, 1962. To be published.

8. Smiley, R. F. and Horne, W. B.: Mechanical Properties of Pneumatic Tires with Special Reference to Modern Aircraft Tires. NACA TN 4110, January 1958.

9. Chun, R. T. and Lenk, E. J.: Ground Vibration Tests on the Model A4D-2 Airplane, BuNo. 142088 for Landing Loads Analysis. Douglas Aircraft Co. Report ES 29972, April 1961.

10. Milwitzky, B. and Cook, F. E.: Analysis of Landing-Gear Behavior. NACA TN 2755, August 1952.

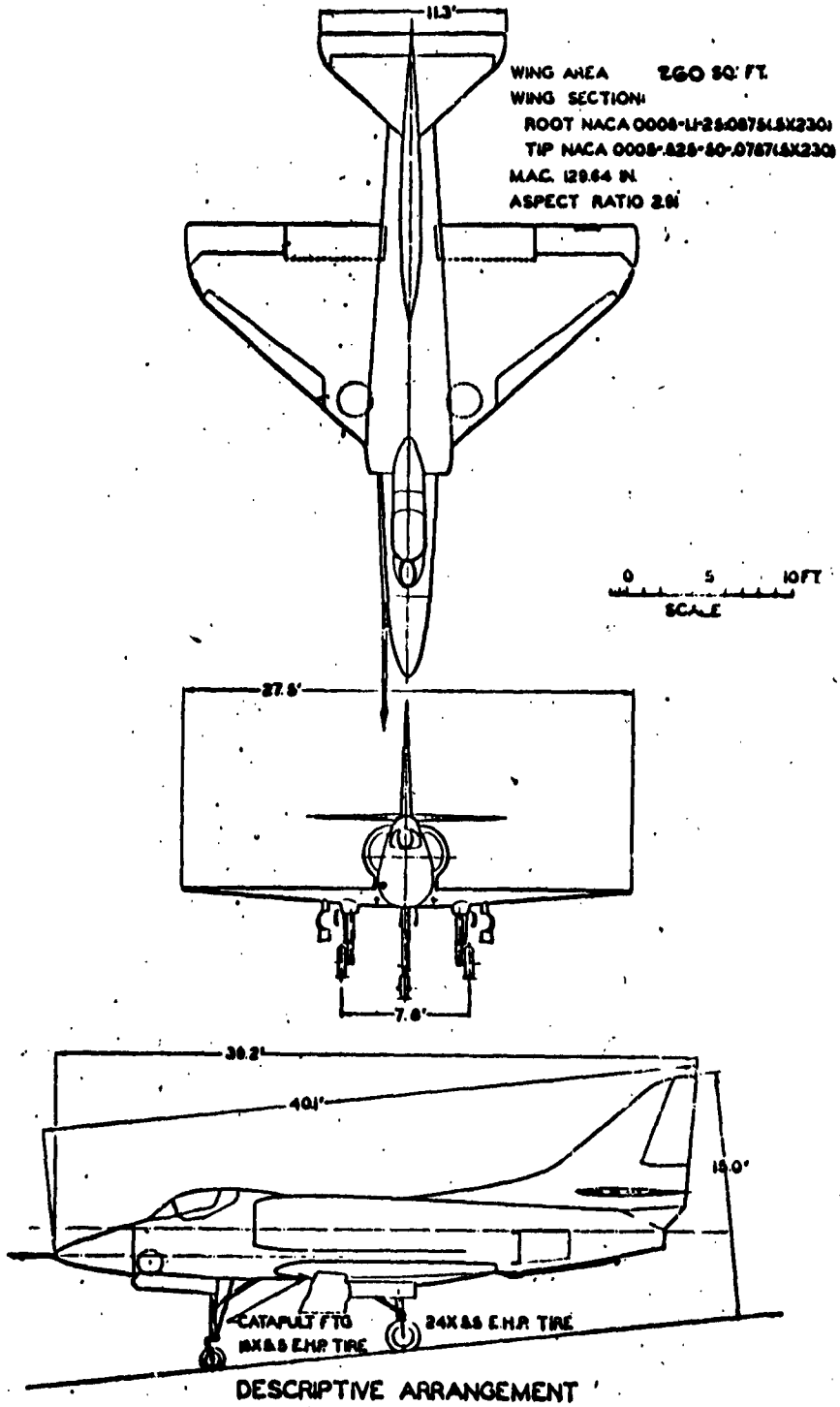

DESCRIPTIVE ARRANGEMENT

MODEL A4D-2

Figure 1.

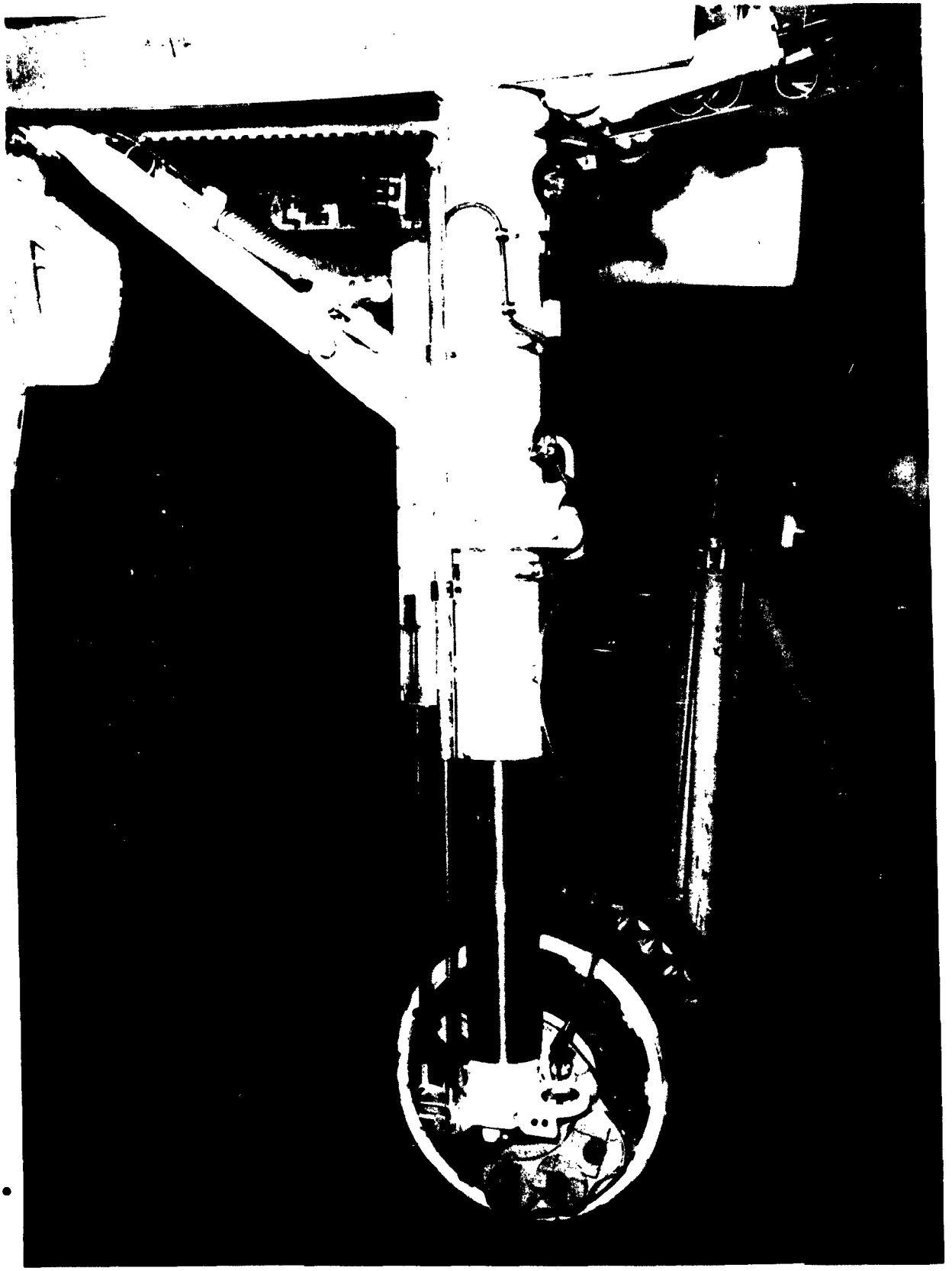

Figure 2. A4D-2 Main Gear.

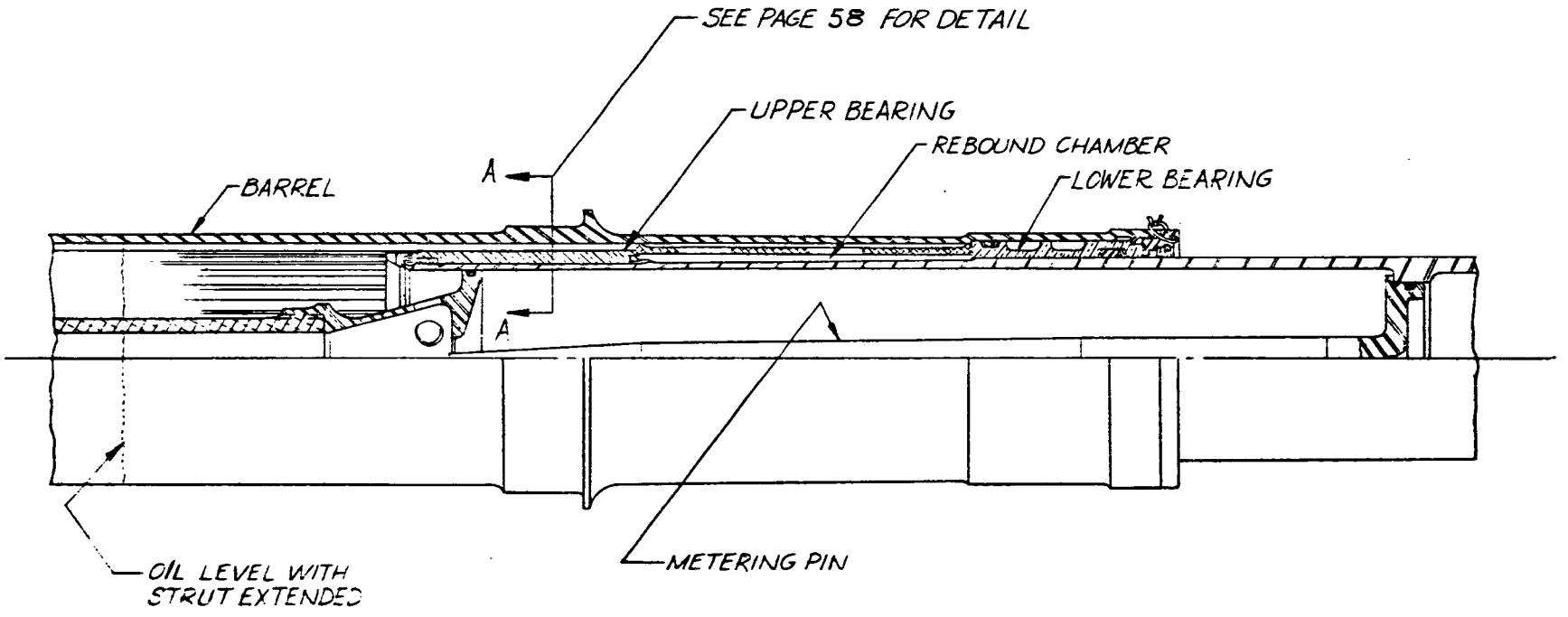

Figure 3. A4D-2 Main Gear Strut in Extended Position.

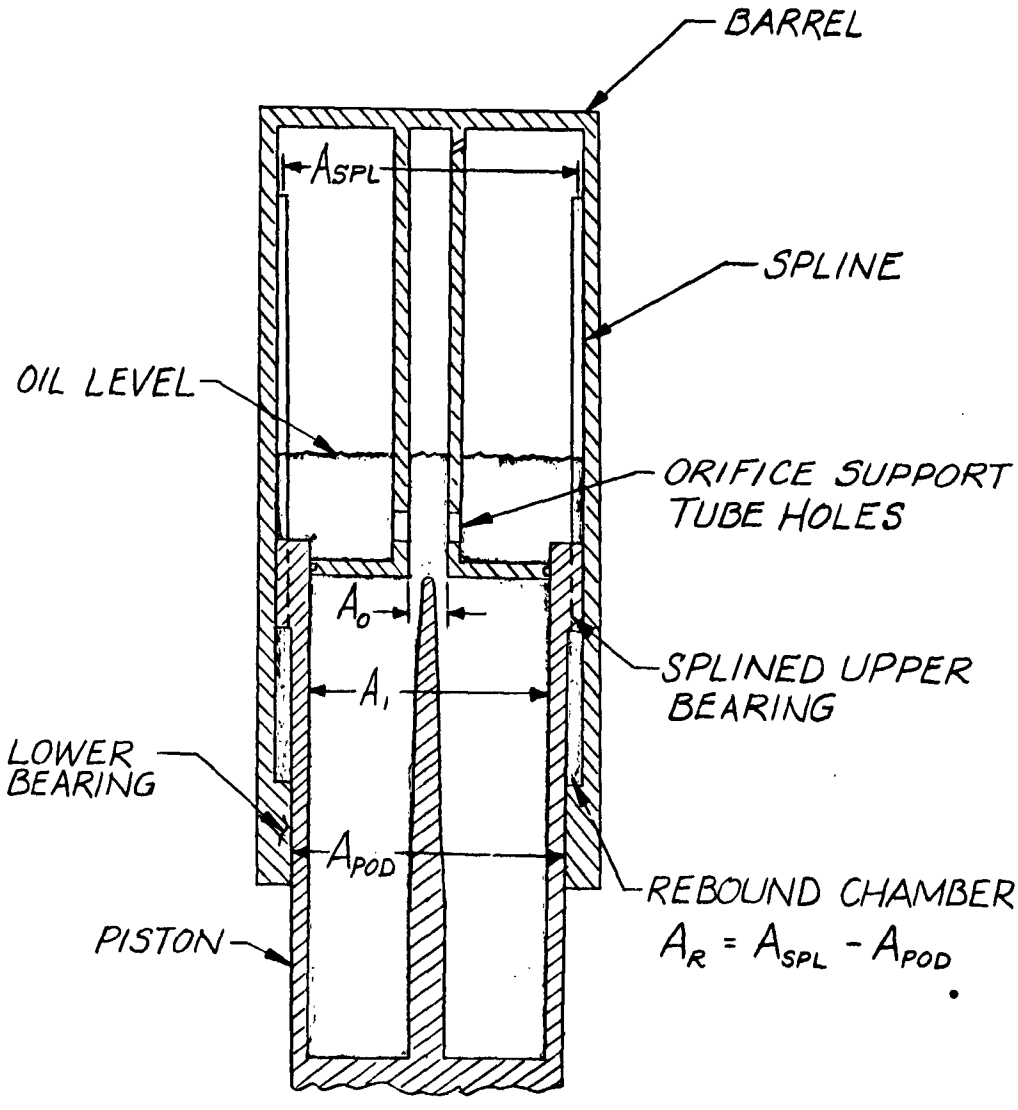

Figure 4. A4D Internal Main Gear Strut Schematic with Strut Extended.

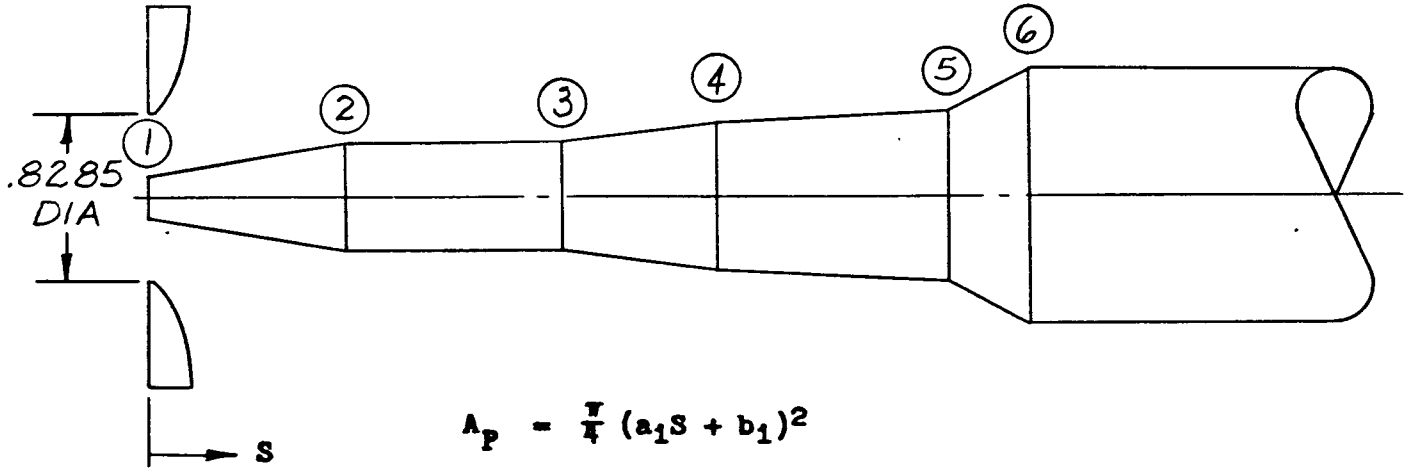

$$A_p = \frac{\pi}{4}(a_1 S + b_1)^2$$

SECTION	DIAMETER, INCHES	S, INCHES	a_1	b_1
(1)	.217	0	.1105	.217
(2)	.6105	3.5625	0	.6105
(3)	.6105	8.0625	.034833	.32966
(4)	.715	11.0625	.008889	.61667
(5)	.750	15.0	.1920	-2.13
(6)	.810	15.3125	0	.810

Figure 5. Coefficients for Metering Pin Cross Sectional Area, A_p.

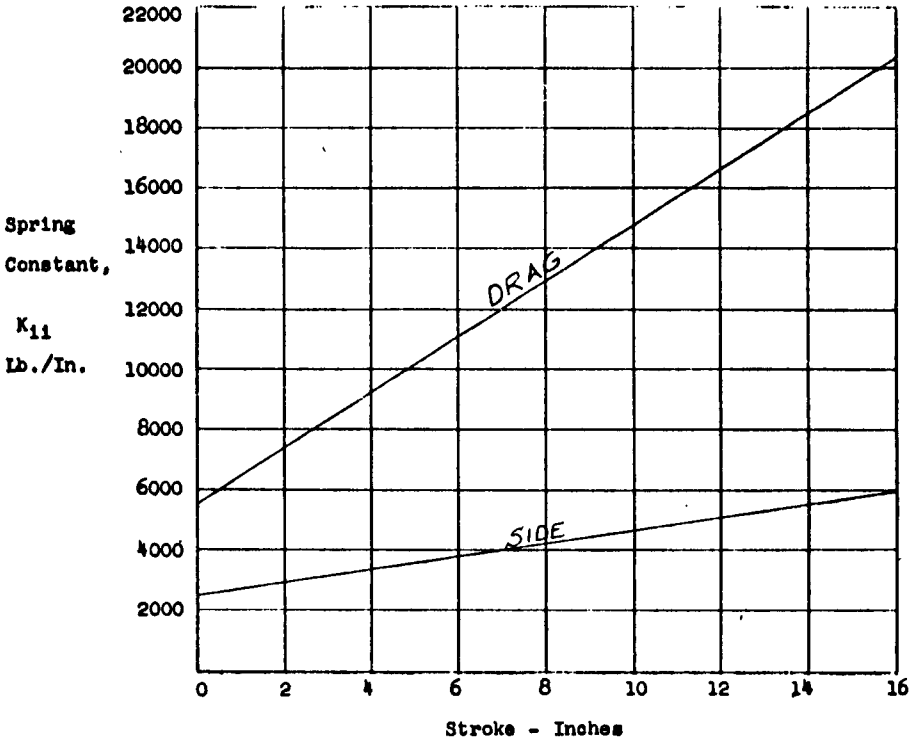

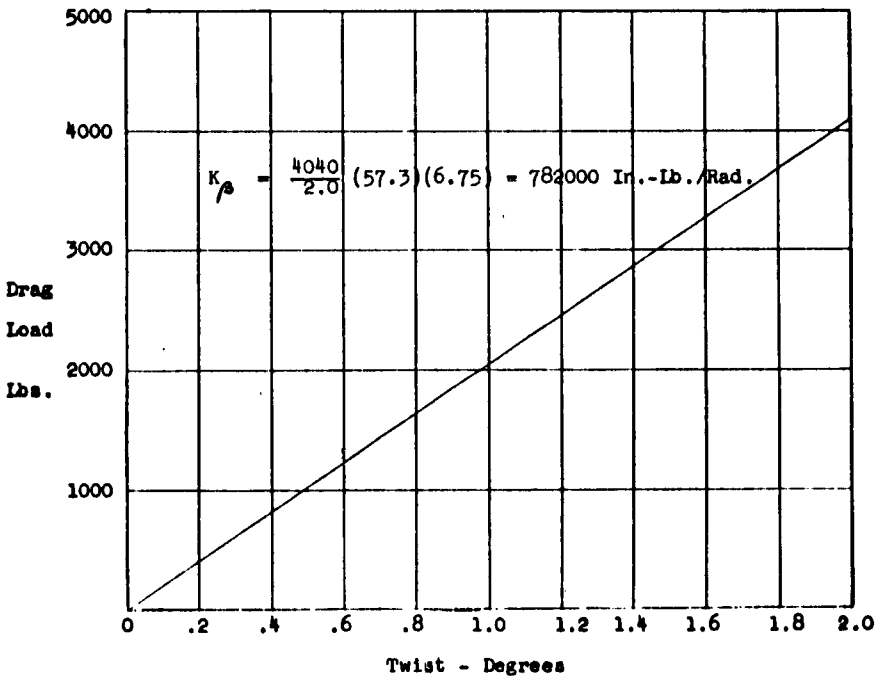

Figure 6. Spring Constants in the Fore-Aft and Side Direction Versus Stroke, and the Strut Angle of Twist for a Drag Load Applied at the Axle.

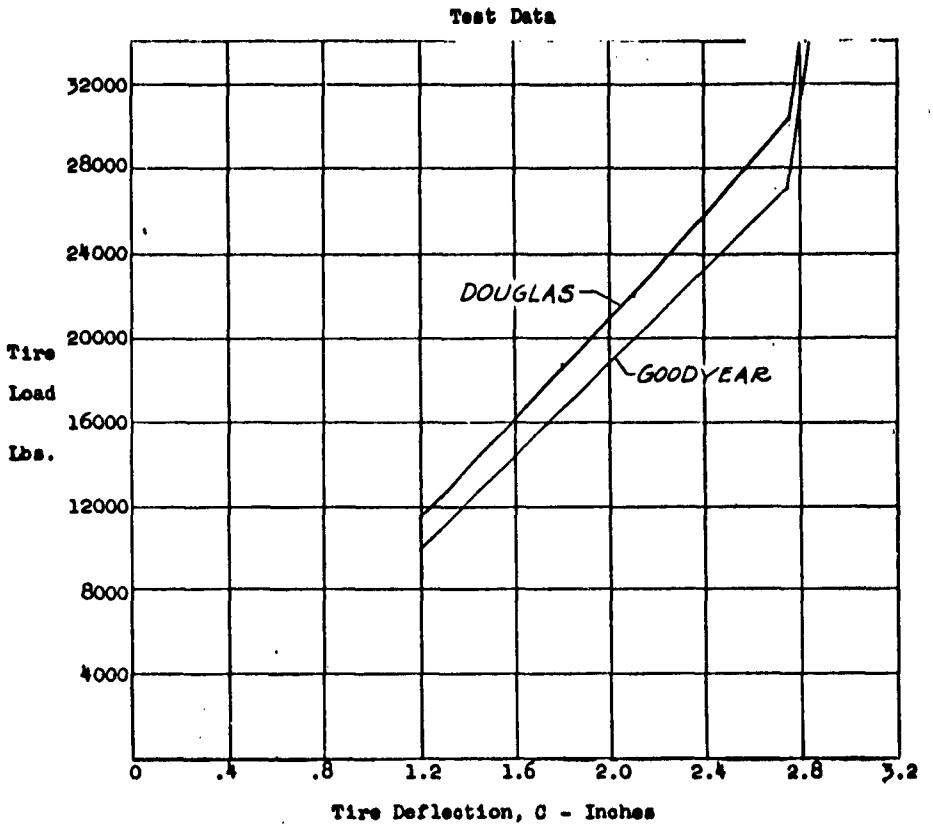

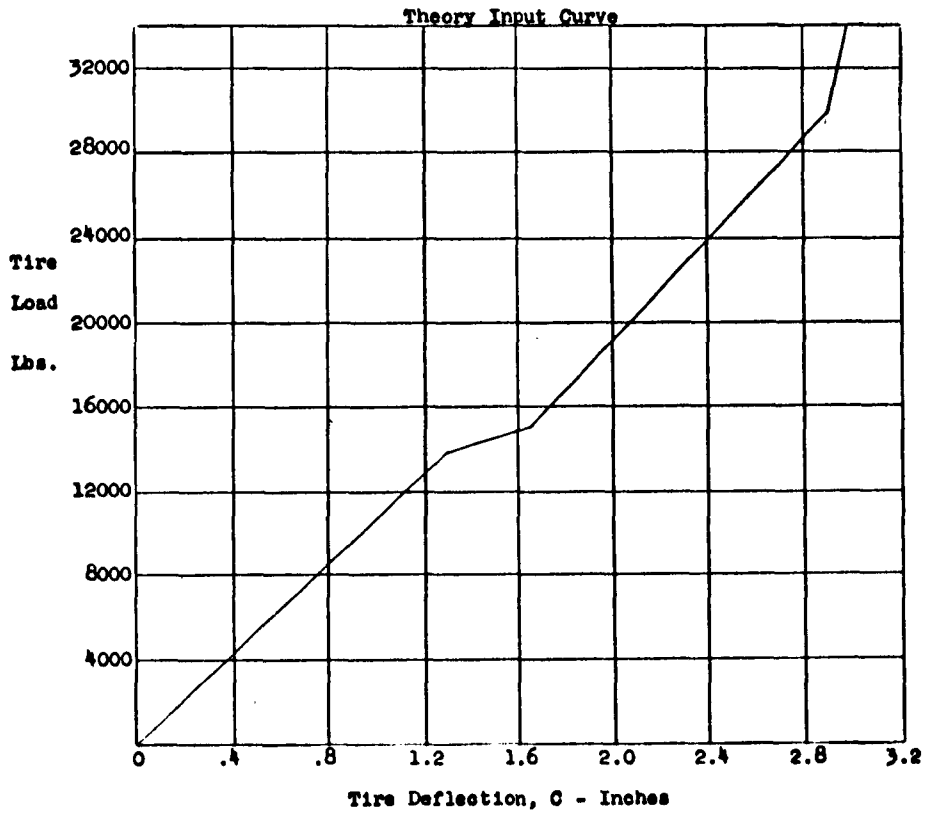

Figure 7. Impact Load-Deflection Curves for a Goodyear Tire, Size 24 x 5.5 Type VII, at 320 psi.

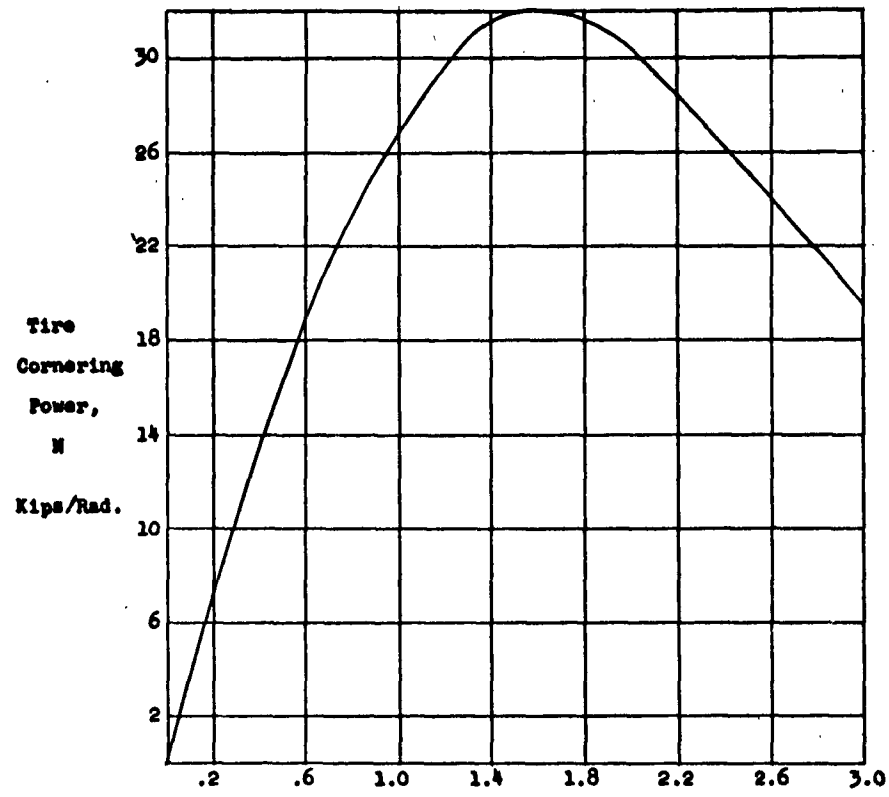

$N = -127.69C^5 + 1852.5C^4 - 6215.2C^3 - 4562.5C^2 + 36306C$

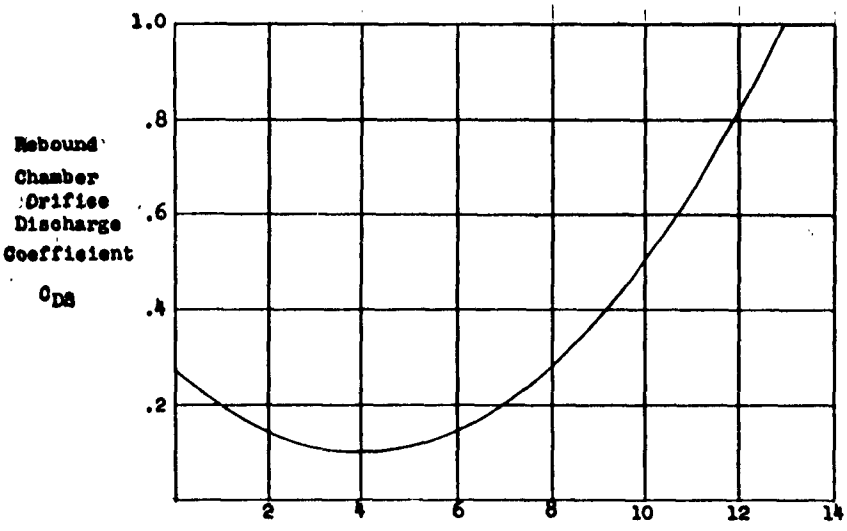

$C_{DS} = .0111S^2 - .0888S + .2777$

(See Page 59)

Figure 8. Input Data Coefficients for the Tire Cornering Power and Rebound Chamber Orifice Discharge Coefficient.

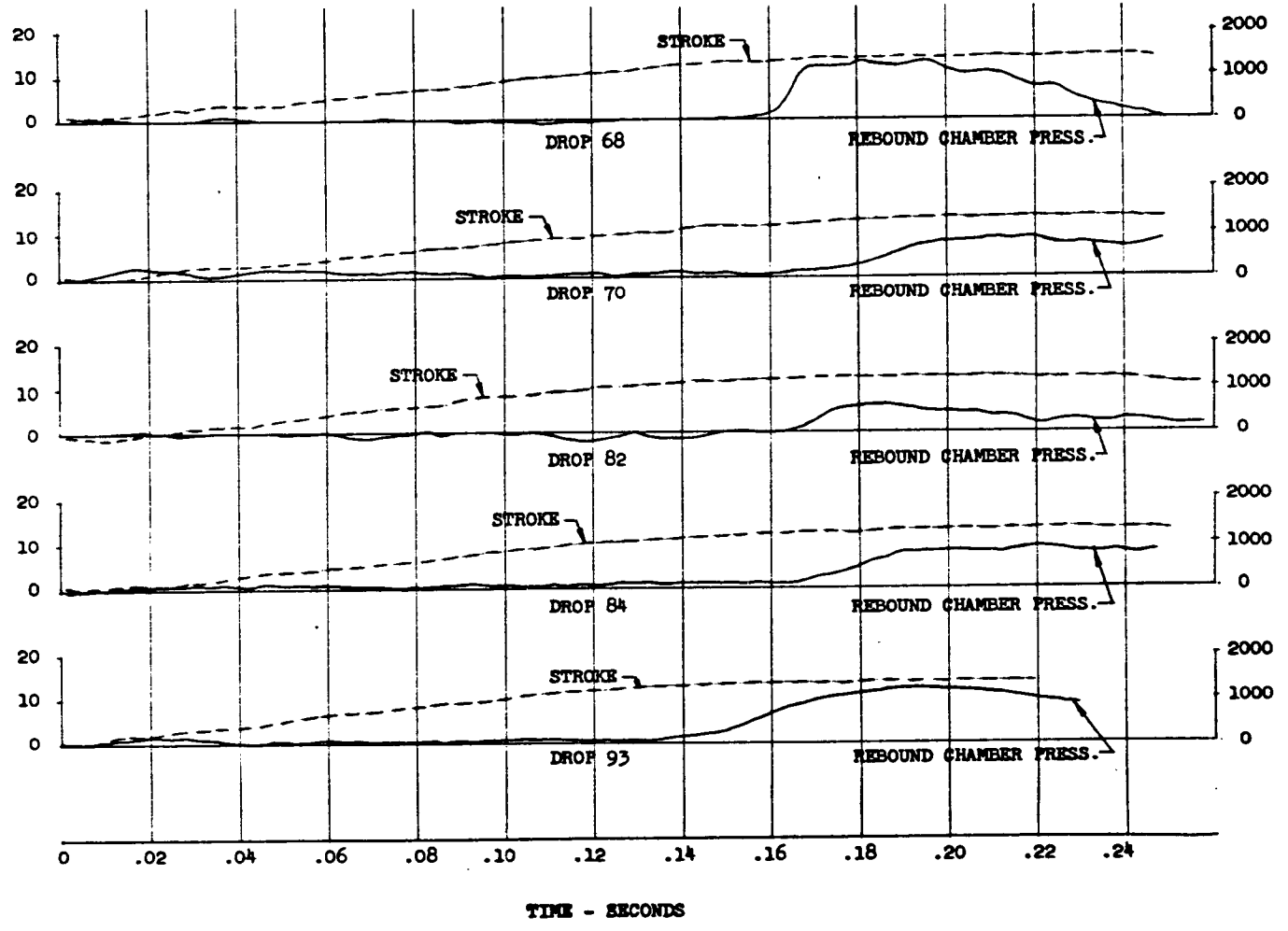

FIGURE 9. REBOUND CHAMBER PRESSURE AND STRUT STROKE

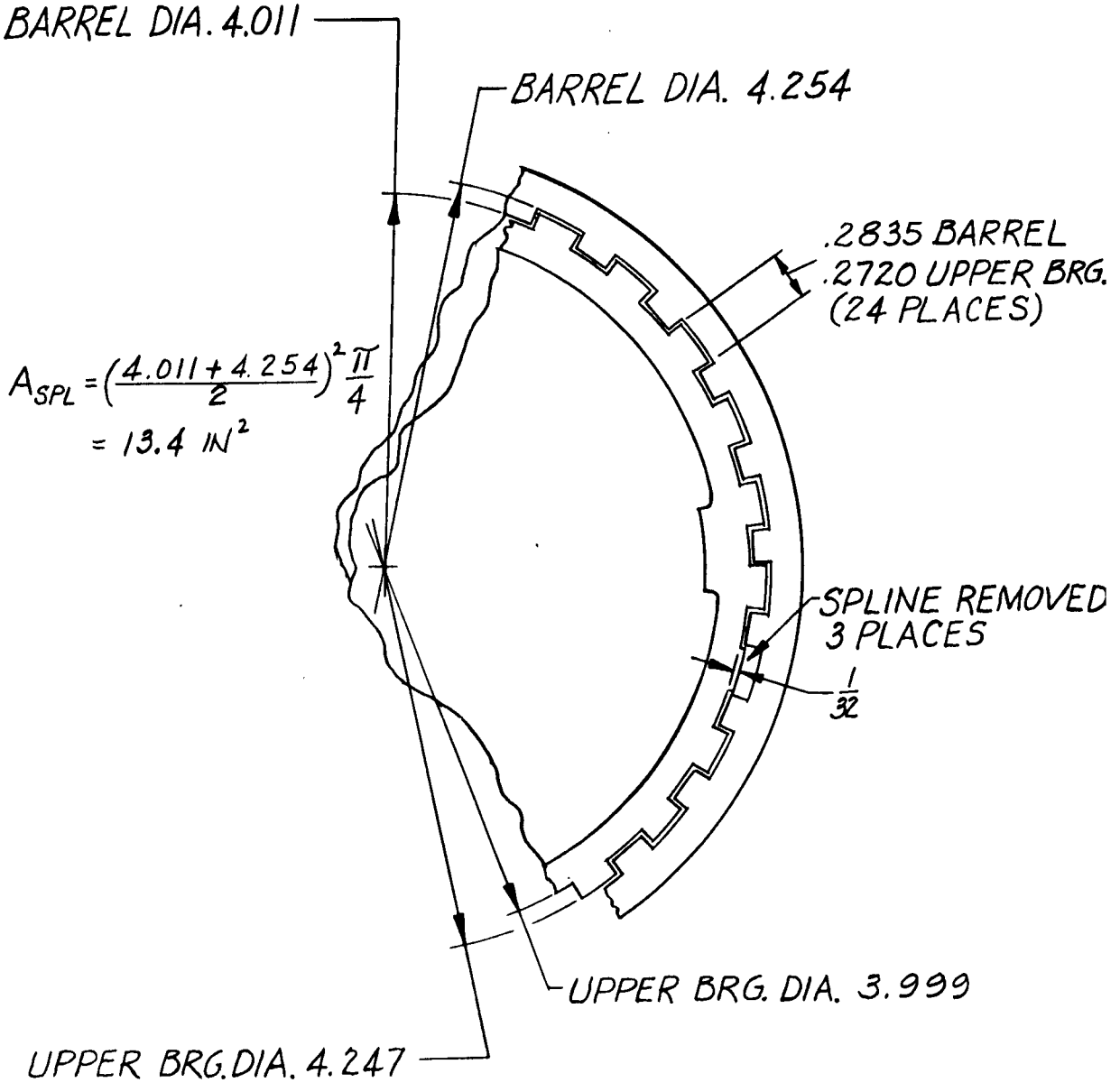

Section A-A

(See Page 5)

Figure 10. Section Showing Upper Bearing and Barrel Spline Details.

Figure 10 (Cont'd.)

INPUT DATA

ORIFICE REBOUND CHAMBER COEFFICIENT

$$EQ = \Sigma Q_o \sqrt{P_A}\ \Delta t$$

$$Q_o = \sum_{1}^{5} C_{Q_i} S$$

$$C_{Q_i} = C_{DS} A_S \sqrt{\frac{2}{A_{SPL}}} = A_S \sqrt{\frac{2}{A_{SPL}}}\ (.0111S^2 - .0888S + .2777)$$

A_S = Orifice area, in.^{2}

Assume A_S is caused by 3 missing splines.

$$A_S = .0818 \text{ in.}^2$$

Assume A_S is caused by the gap between bearing and barrel, at nominal dimensions, plus 3 missing splines.

$$A_S = .138 + .0756 = .2136 \text{ in.}^2$$

A_S was assumed to be .126 in.^{2}

$$A_S \sqrt{\frac{2}{A_{SPL}}} = 5.5$$

$$C_{Q_i} = 5.5\ (.0111S^2 - .0888S + .2777)$$

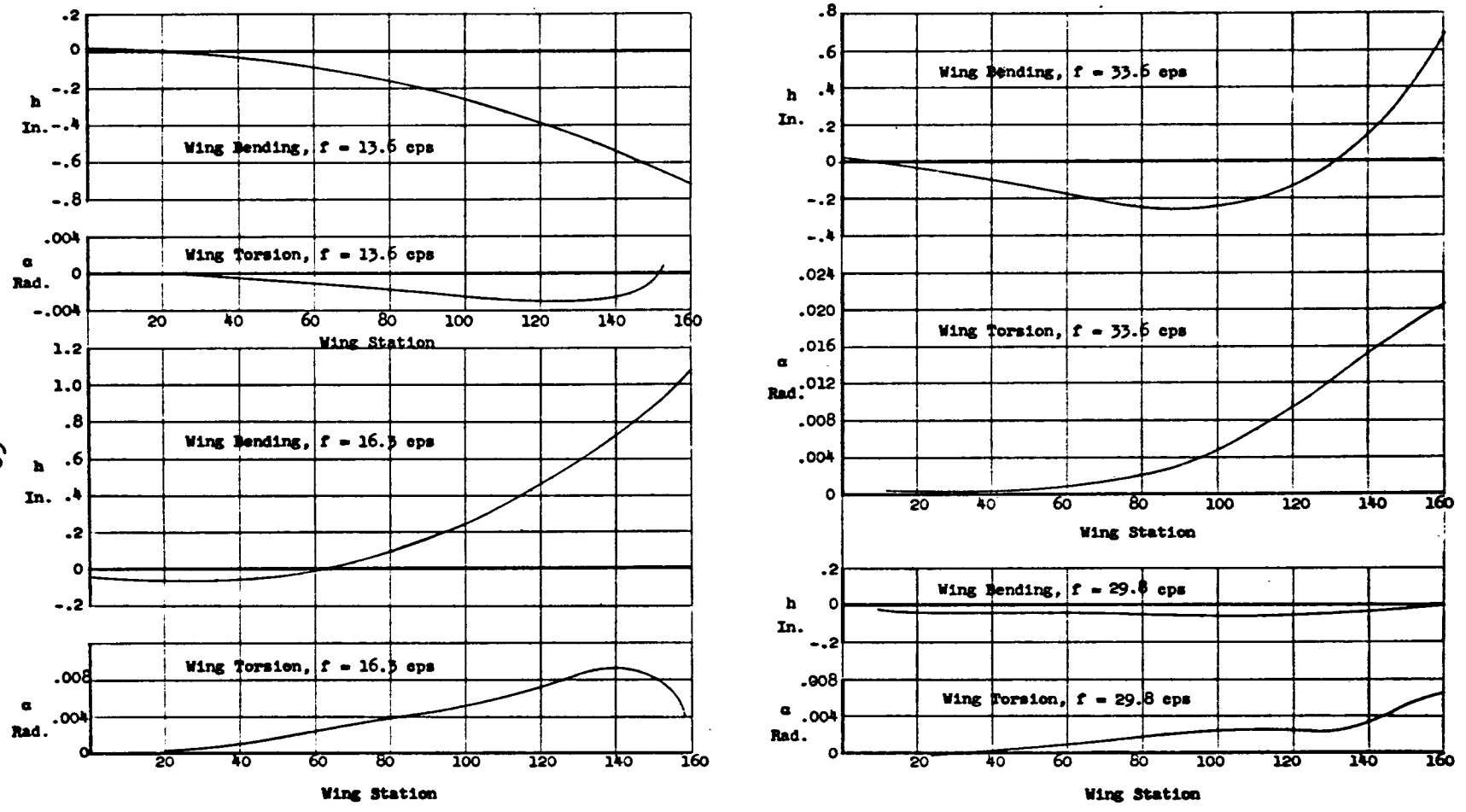

Figure 11. Vertical Translation, h, and Pitching Rotation, α, for the A4D-2 Symmetrical Modes from Ground Vibration Tests.

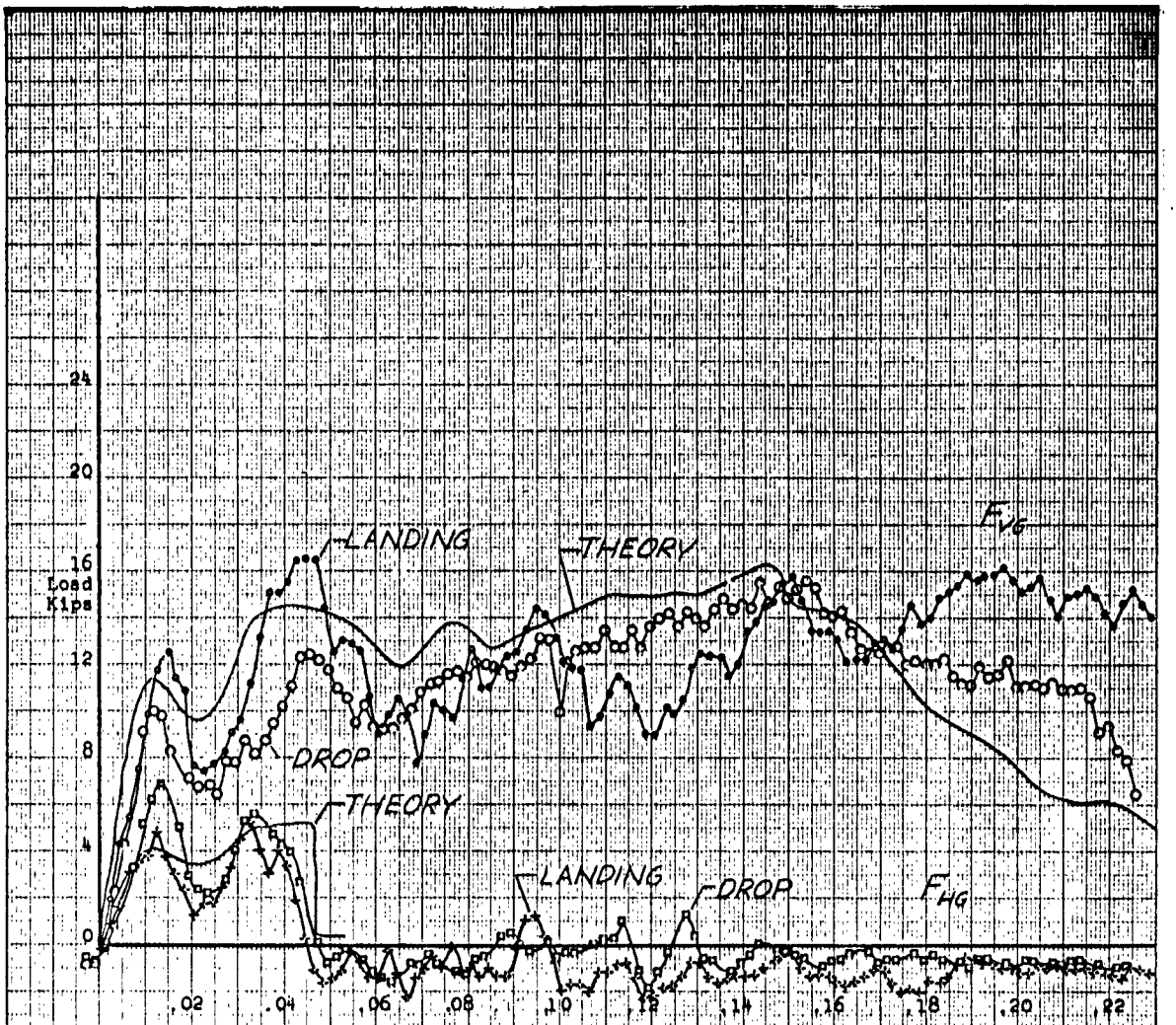

INITIAL CONDITIONS	UNITS	LDG, 121	DROP 84	THEORY
SINK SPEED	Ft./Sec.	13.2	13.9	13.2
HORIZ. SPEED	Knots	106.1	-	106.1
GROSS WEIGHT	Lbs.	12,876	12,876	12,876
PITCH ATTITUDE	Deg.	13.0	13.4	13.0
WING LIFT	g's	1.10	1.055	1.10
WHEEL SPEED	R.P.M.	1,793	1,794	-

Figure 12 . Vertical and Horizontal Ground Load Comparison

Landing 121 - Right Hand Gear

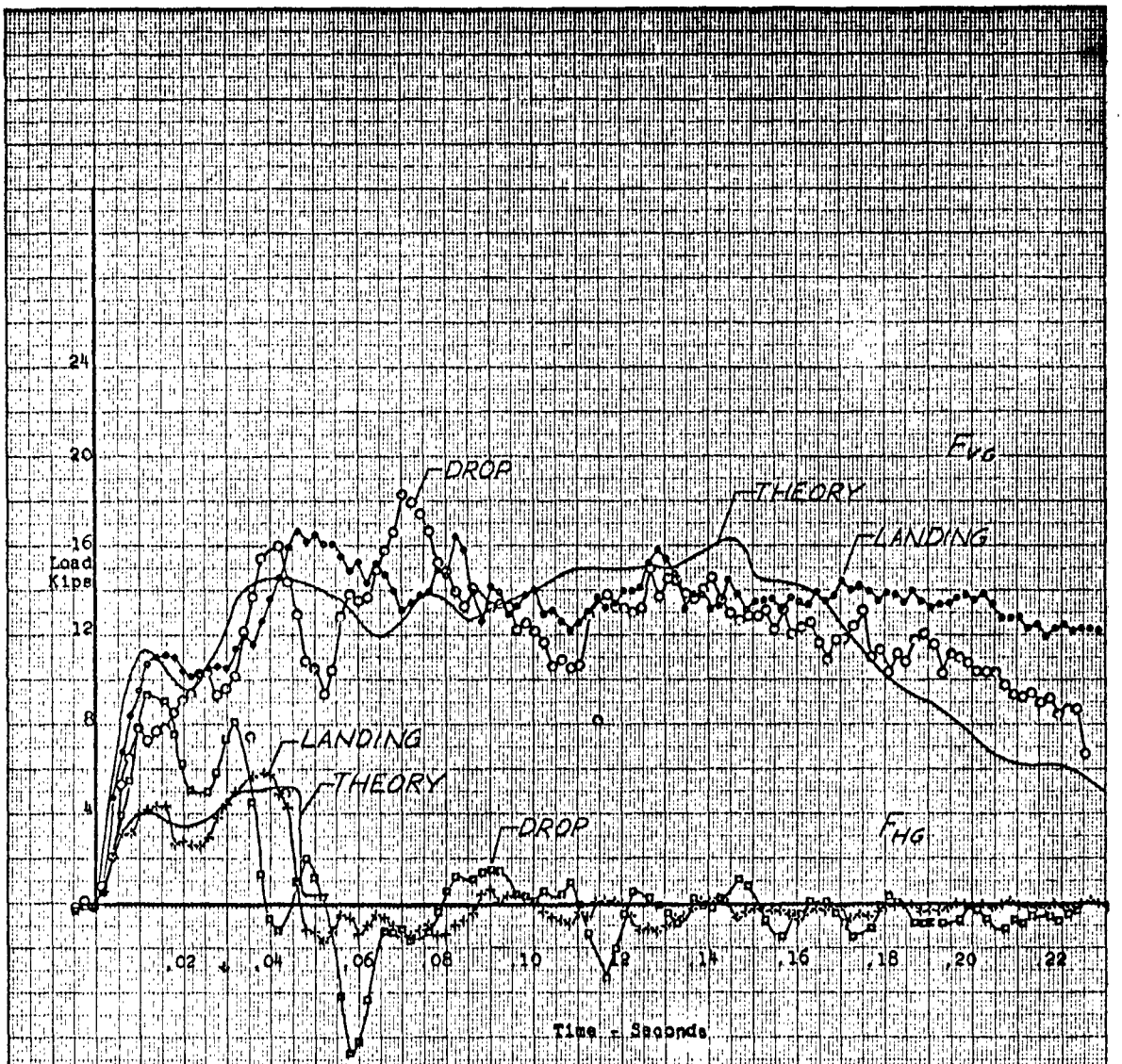

INITIAL CONDITIONS	UNITS	LDG. 121	DROP 84	THEORY
SINK SPEED	Ft./Sec.	13.2	13.9	13.2
HORIZ. SPEED	Knots	106.1	-	106.1
GROSS WEIGHT	Lbs.	12,876	12,876	12,876
PITCH ATTITUDE	Deg.	13.0	13.4	13.0
WING LIFT	g's	1.10	1.055	1.10
WHEEL SPEED	R.P.M.	1,793	1,811	-

Figure 13 . Vertical and Horizontal Ground Load Comparison
Landing 121 - Left Hand Gear

INITIAL CONDITIONS	UNITS	LDG. 123	DROP 70	THEORY
SINK SPEED	Ft./Sec.	12.0	12.8	12.0
HORIZ. SPEED	Knots	113.9	-	113.9
GROSS WEIGHT	Lbs.	13,735	13,516	13,516
PITCH ATTITUDE	Deg.	8.5	9.5	8.5
WING LIFT	g's	1.10	1.03	1.10
WHEEL SPEED	R.P.M.	1,930	2,069	

Figure 44 Vertical and Horizontal Ground Load Comparison

Landing 123 - Right Hand Gear

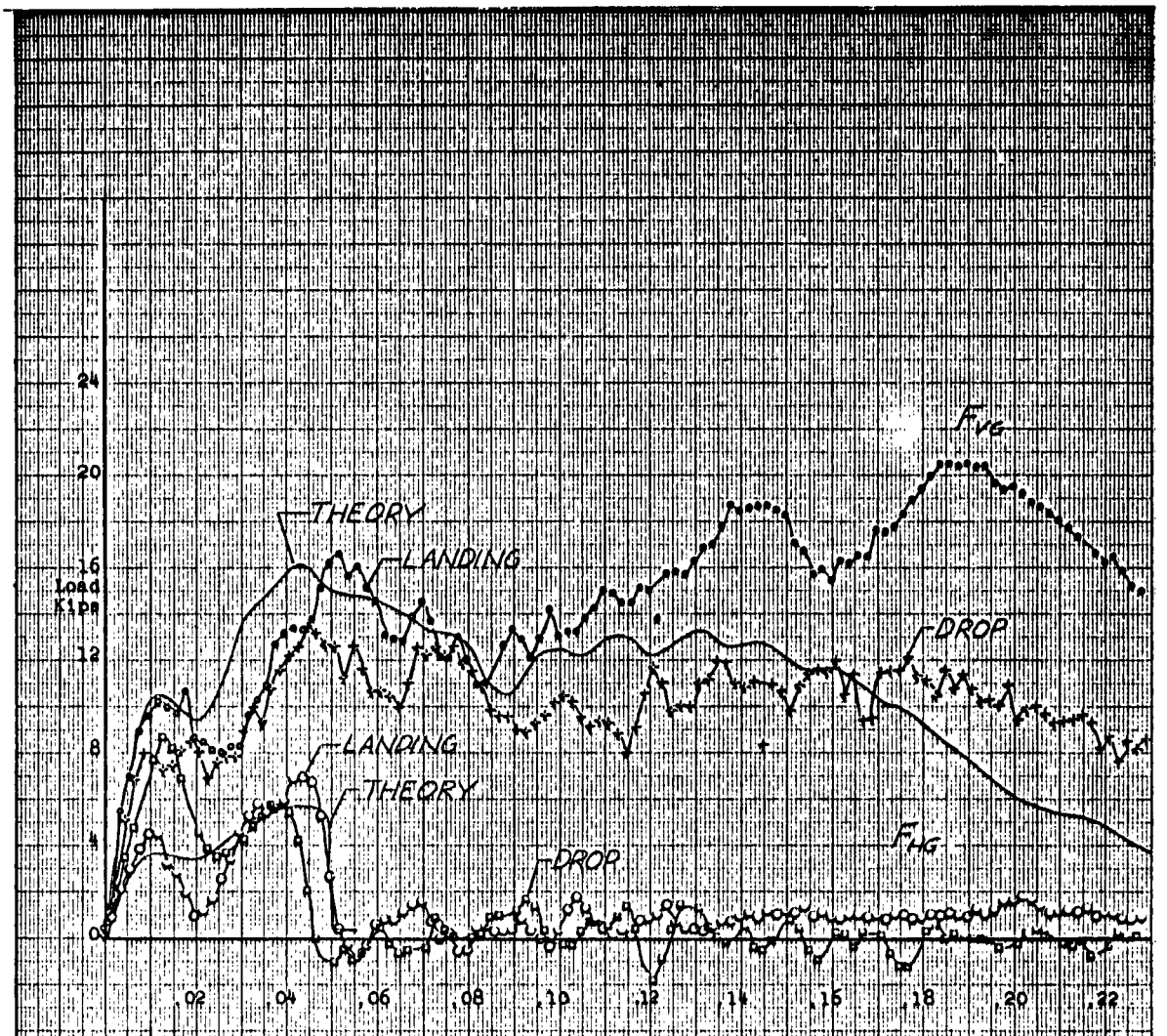

INITIAL CONDITIONS	UNITS	LDG. 123	DROP 70	THEORY
SINK SPEED	Ft./Sec.	12.0	12.2	12.0
HORIZ. SPEED	Knots	113.9	-	113.9
GROSS WEIGHT	Lbs.	13,735	13,516	13,516
PITCH ATTITUDE	Deg.	8.5	9.5	8.5
WING LIFT	g's	1.10	1.03	1.10
WHEEL SPEED	R.P.M.	1,930	2,097	

Figure 15. Vertical and Horizontal Ground Load Comparison

Landing 123 - Left Hand Gear

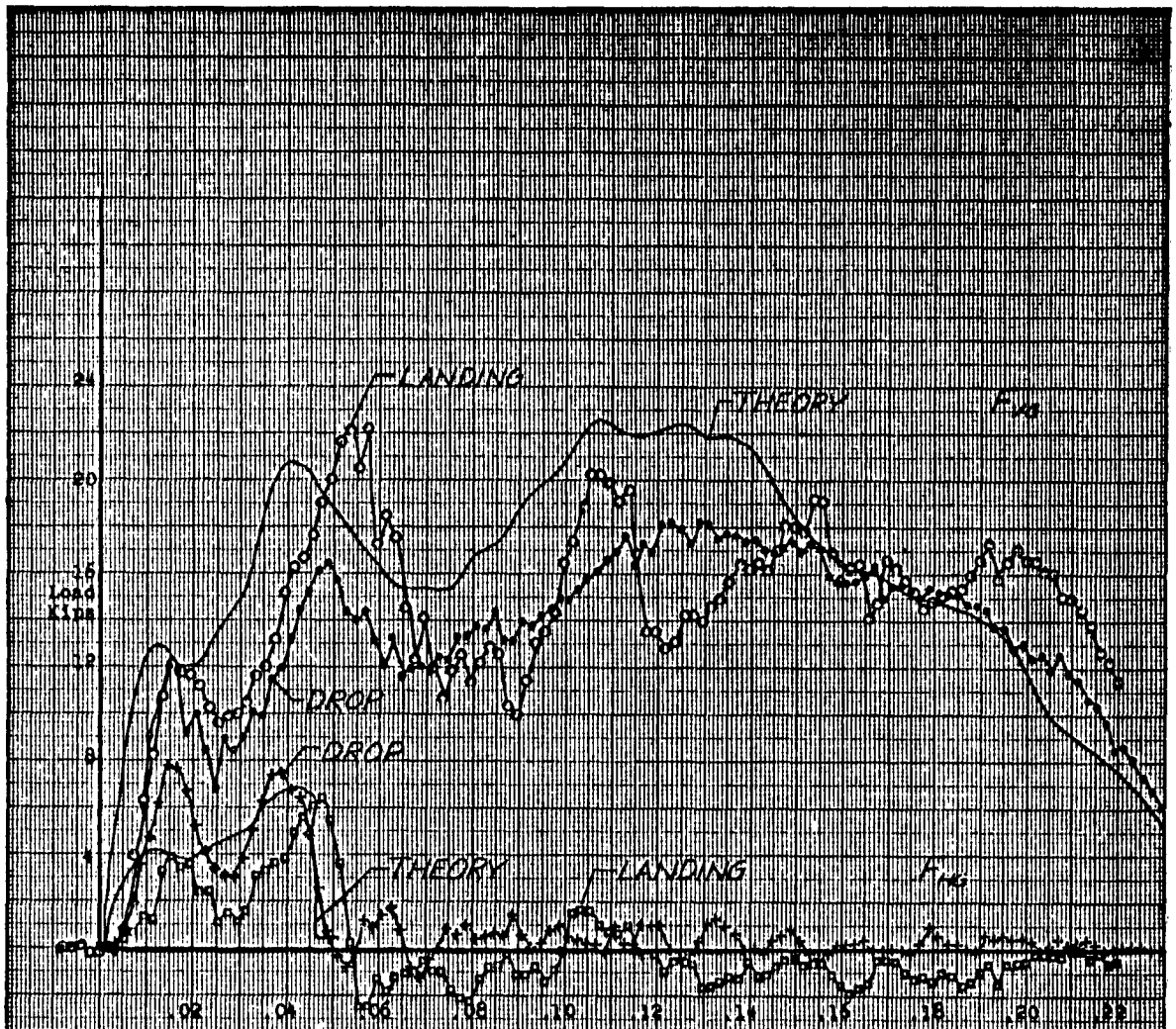

INITIAL CONDITIONS	UNITS	LDG. 126	DROP 68	THEORY
SINK SPEED	Ft./Sec.	15.0	15.0	15.0
HORIZ. SPEED	Knots	112.9	-	112.9
GROSS WEIGHT	Lbs.	13,446	13,446	13,446
PITCH ATTITUDE	Deg.	9.5	8.8	9.5
WING LIFT	g's	1.07	1.07	1.07
WHEEL SPEED	R.P.M.	1,931	1,918	-

Figure 16 Vertical and Horizontal Ground Load Comparison

Landing 126 - Right Hand Gear

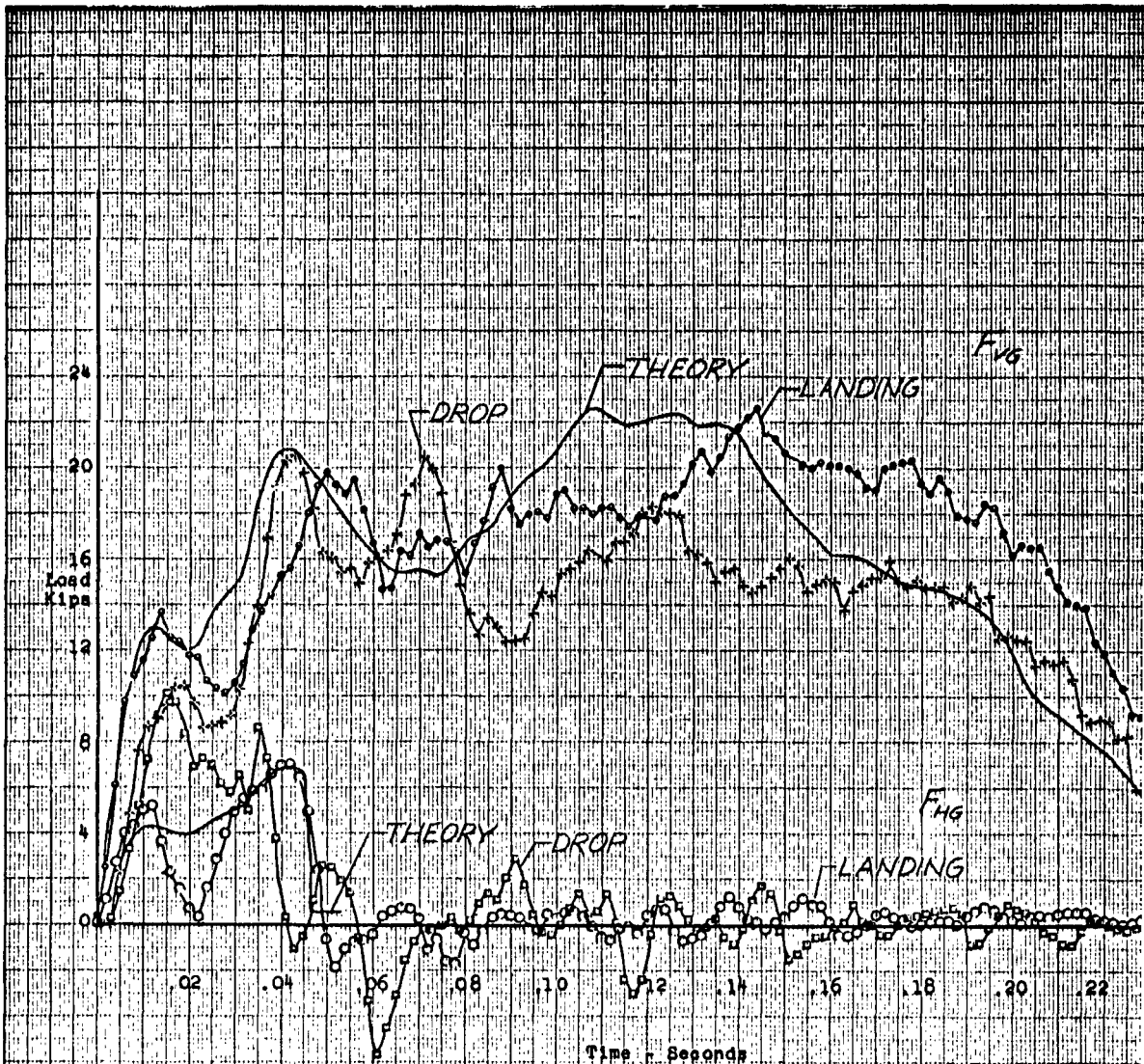

INITIAL CONDITIONS	UNITS	LDG. 125	DROP 68	THEORY
SINK SPEED	Ft./Sec.	15.0	15.0	15.0
HORIZ. SPEED	Knots	112.9	-	112.9
GROSS WEIGHT	Lbs.	13,446	13,446	13,446
PITCH ATTITUDE	Deg.	9.5	8.8	9.5
WING LIFT	g's	1.07	1.07	1.07
WHEEL SPEED	R.P.M.	1,933	1,925	-

Figure 17. Vertical and Horizontal Ground Load Comparison

Landing 125 - Left Hand Gear

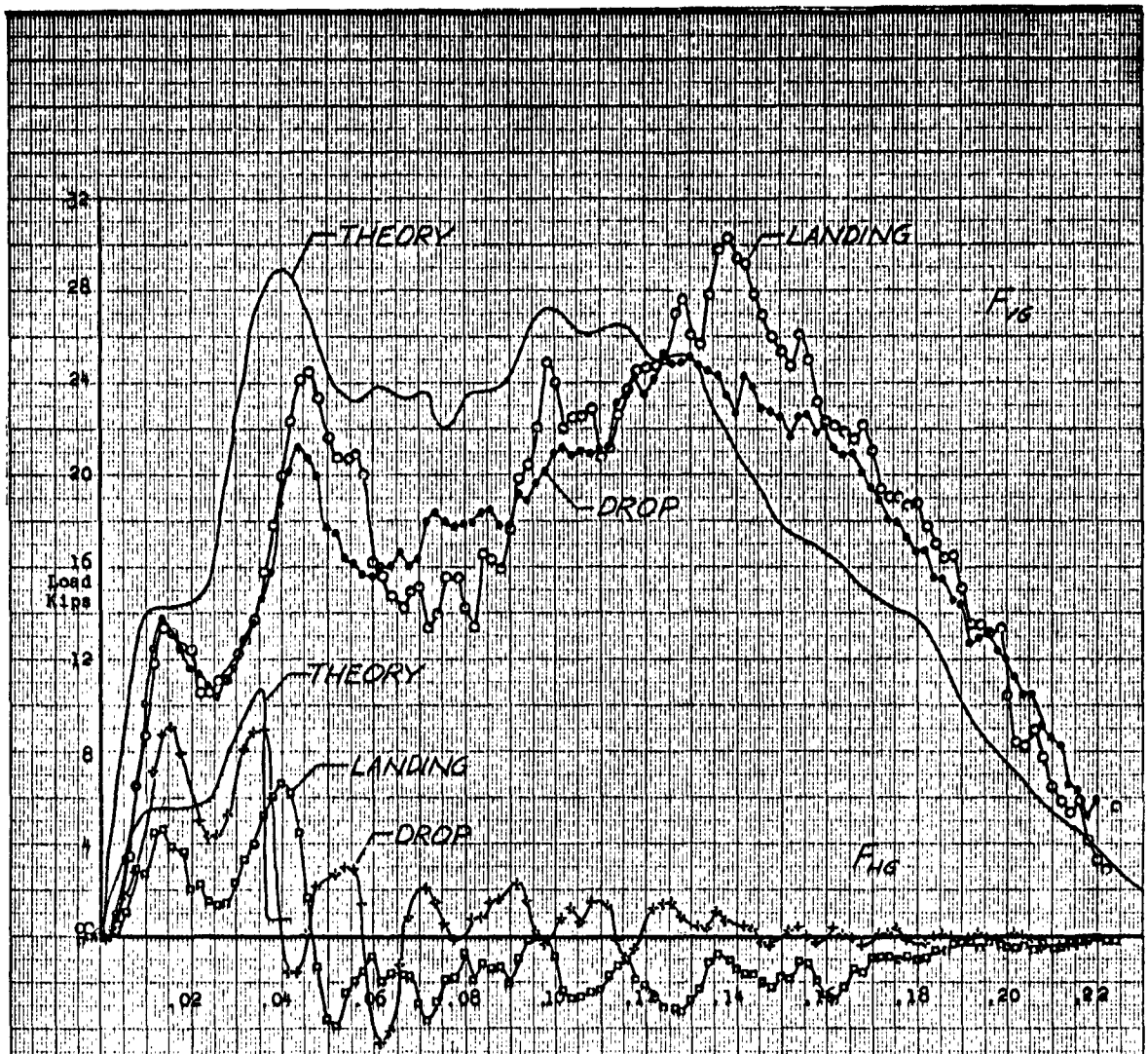

INITIAL CONDITIONS	UNITS	LDG 126	DROP 93	THEORY
SINK SPEED	Ft./Sec.	17.0	16.7	17.0
HORIZ. SPEED	Knots	110.6	"	110.6
GROSS WEIGHT	Lbs.	13,276	13,276	13,276
PITCH ATTITUDE	Deg.	9.3	10.0	9.3
WING LIFT	g's	1.06	1.045	1.06
WHEEL SPEED	R.P.M.	1,933	1,912	"

Figure 18. Vertical and Horizontal Ground Load Comparison

Landing 126 - Right Hand Gear

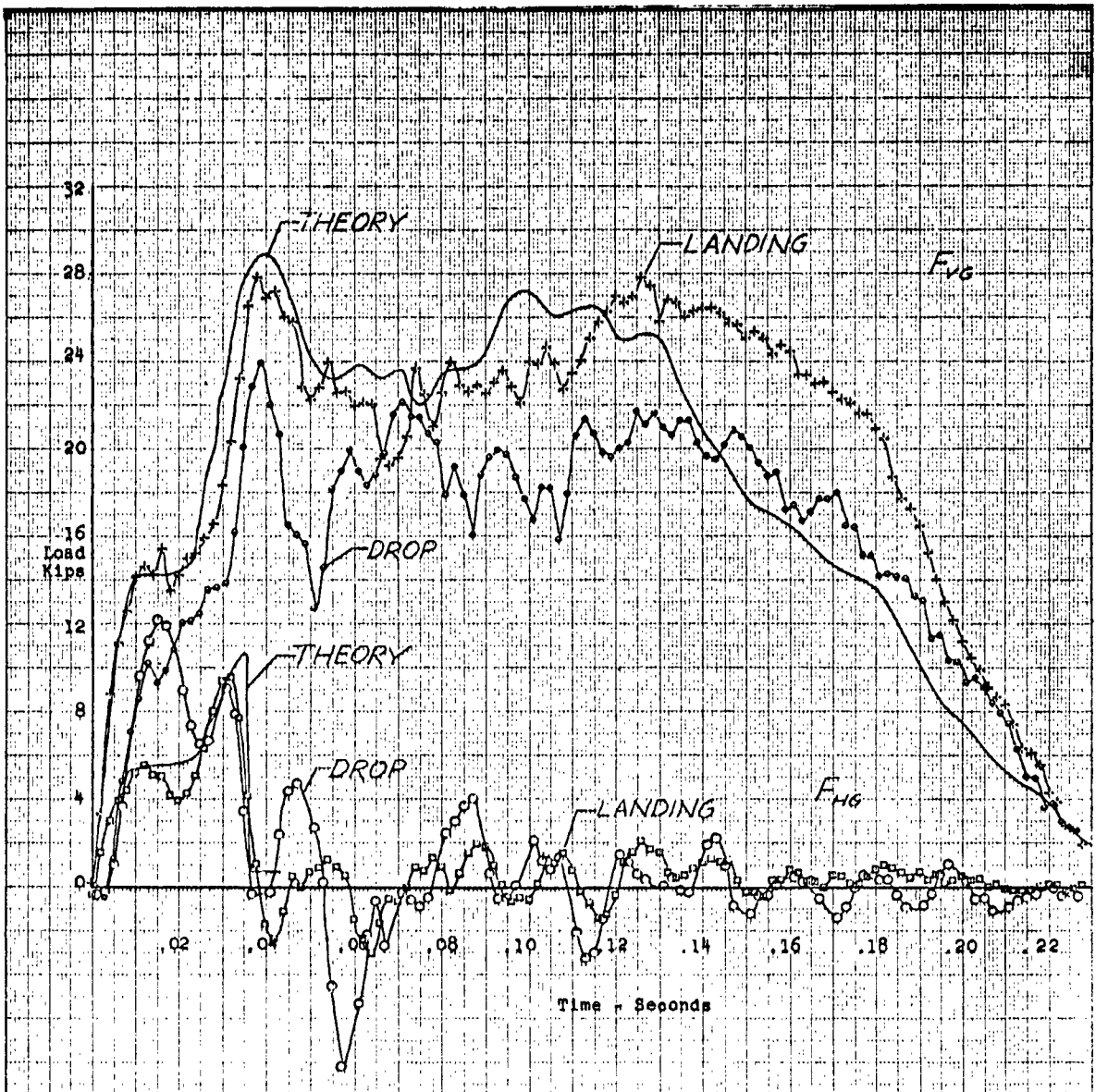

INITIAL CONDITIONS	UNITS	LDG. 126	DROP 93	THEORY
SINK SPEED	Ft./Sec.	17.0	16.7	17.0
HORIZ. SPEED	Knots	110.6	-	110.6
GROSS WEIGHT	Lbs.	13,276	13,276	13,276
PITCH ATTITUDE	Deg.	9.3	10.0	9.3
WING LIFT	g's	1.06	1.045	1.06
WHEEL SPEED	R.P.M.	1,933	1,936	-

Figure 19. Vertical and Horizontal Ground Load Comparison

Landing 126 - Left Hand Gear

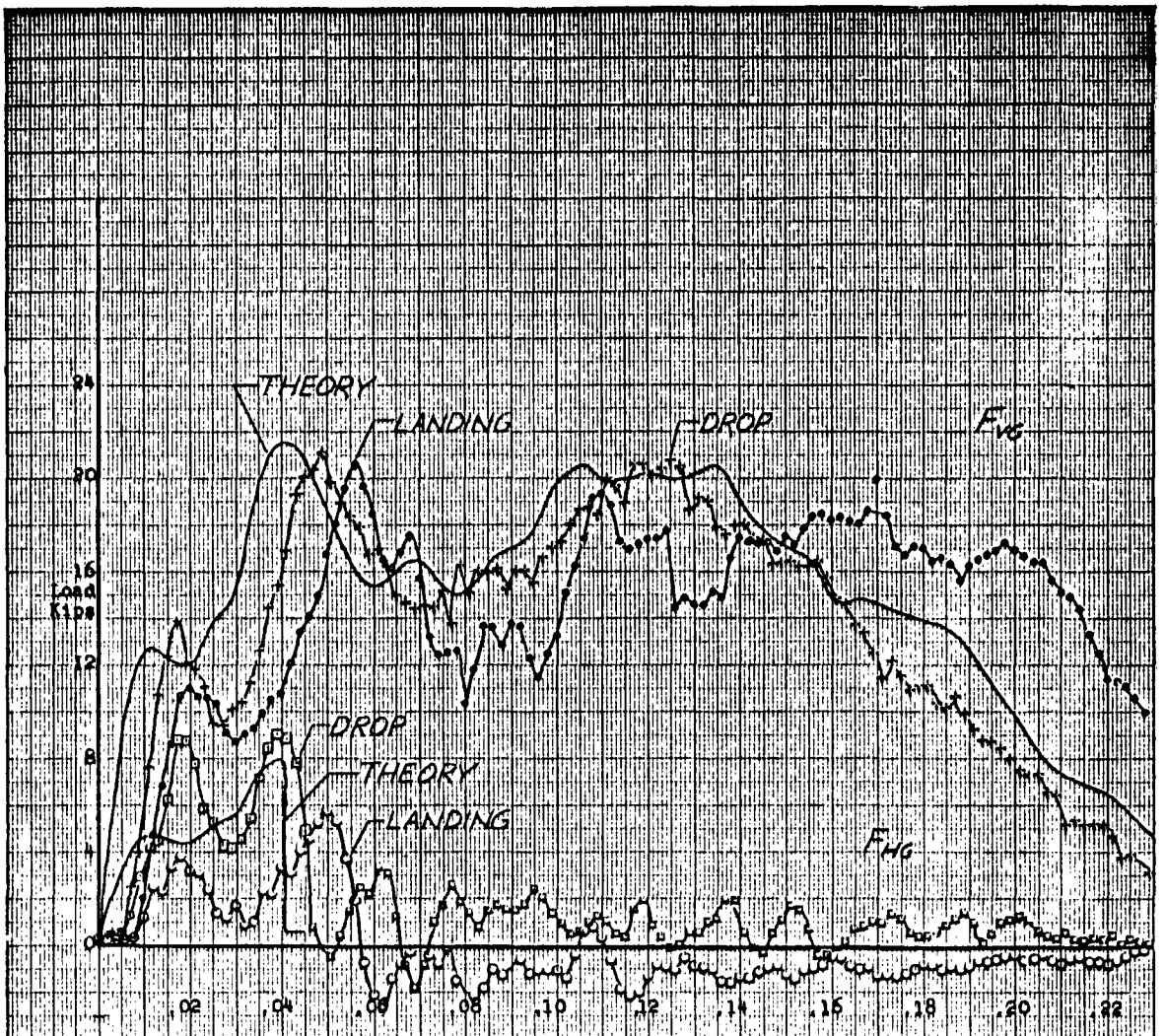

INITIAL CONDITIONS	UNITS	LDG. 128	DROP 82	THEORY
SINK SPEED	Ft./Sec.	14.7	16.2	14.7
HORIZ. SPEED	Knots	109.1	-	109.1
GROSS WEIGHT	Lbs.	12,775	12,876	12,876
PITCH ATTITUDE	Deg.	10.5	6.0	10.5
WING LIFT	G's	1.0	1.05	1.0
WHEEL SPEED	R.P.M.	1,872	2,044	-

Figure 20. Vertical and Horizontal Ground Load Comparison
Landing 128 - Right Hand Gear

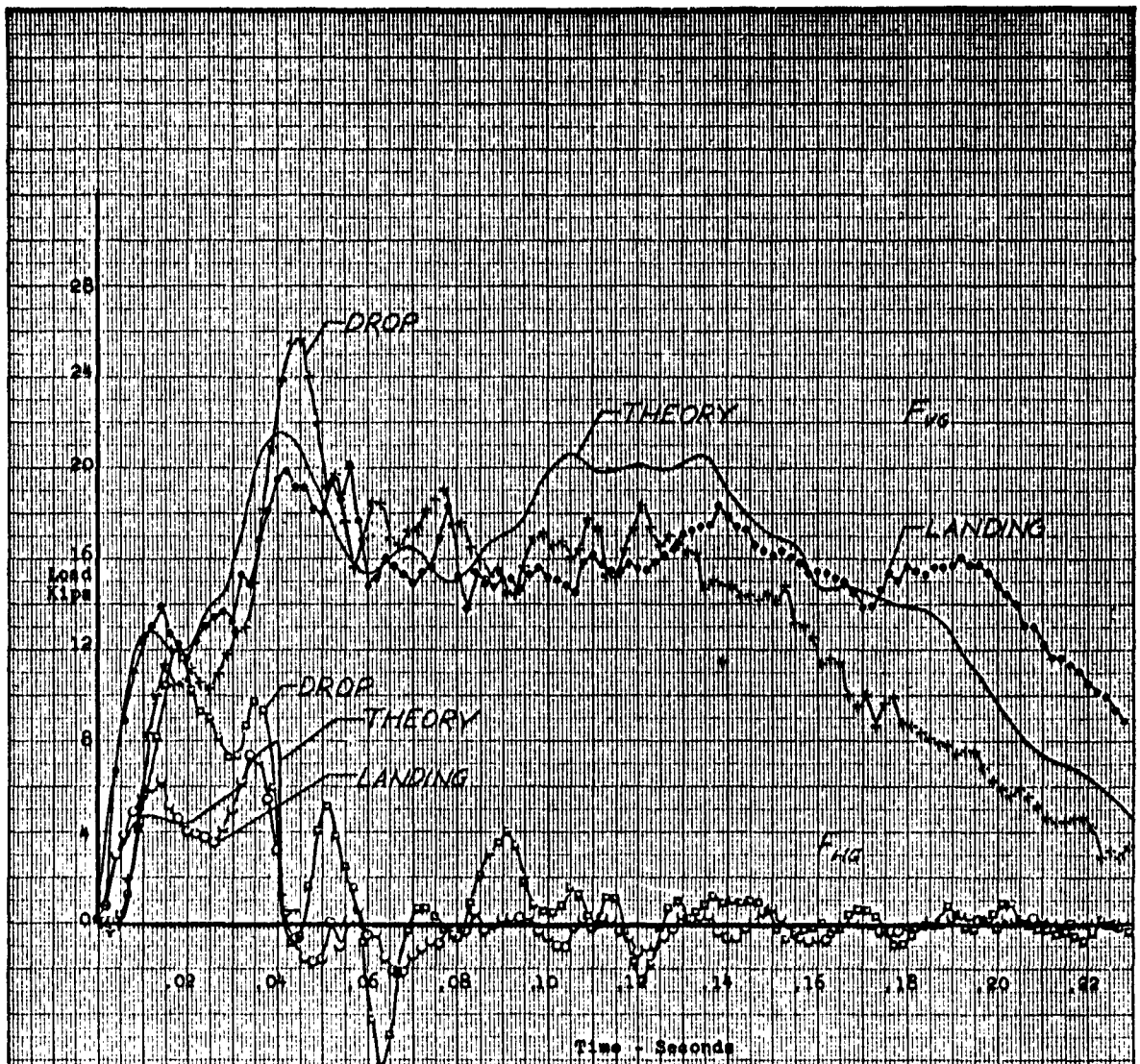

INITIAL CONDITIONS	UNITS	EDO. 128	DROP 82	THEORY
SINK SPEED	Ft./Sec.	14.7	16.9	14.7
HORIZ. SPEED	Knots	109.1	-	109.1
CROSS WEIGHT	Lbs.	12,775	12,875	12,875
PITCH ATTITUDE	Deg.	10.5	6.0	10.5
WING LIFT	G's	1.0	1.05	1.0
WHEEL SPEED	R.P.M.	1,872	2,074	-

Figure 21. Vertical and Horizontal Ground Load Comparison
Landing 128 - Left Hand Gear

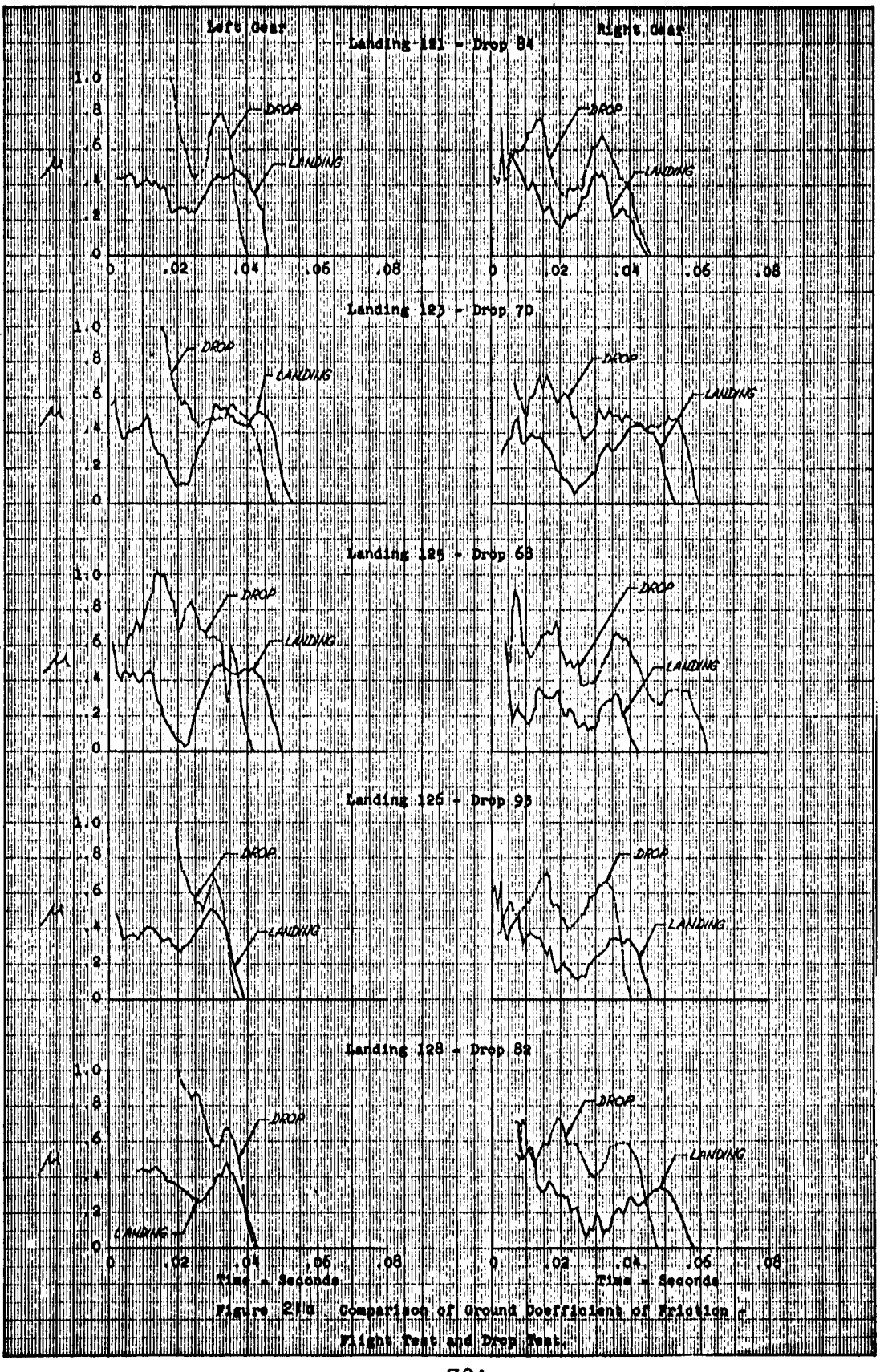

Figure 21a Comparison of Ground Coefficients of Friction - Flight Test and Drop Test.

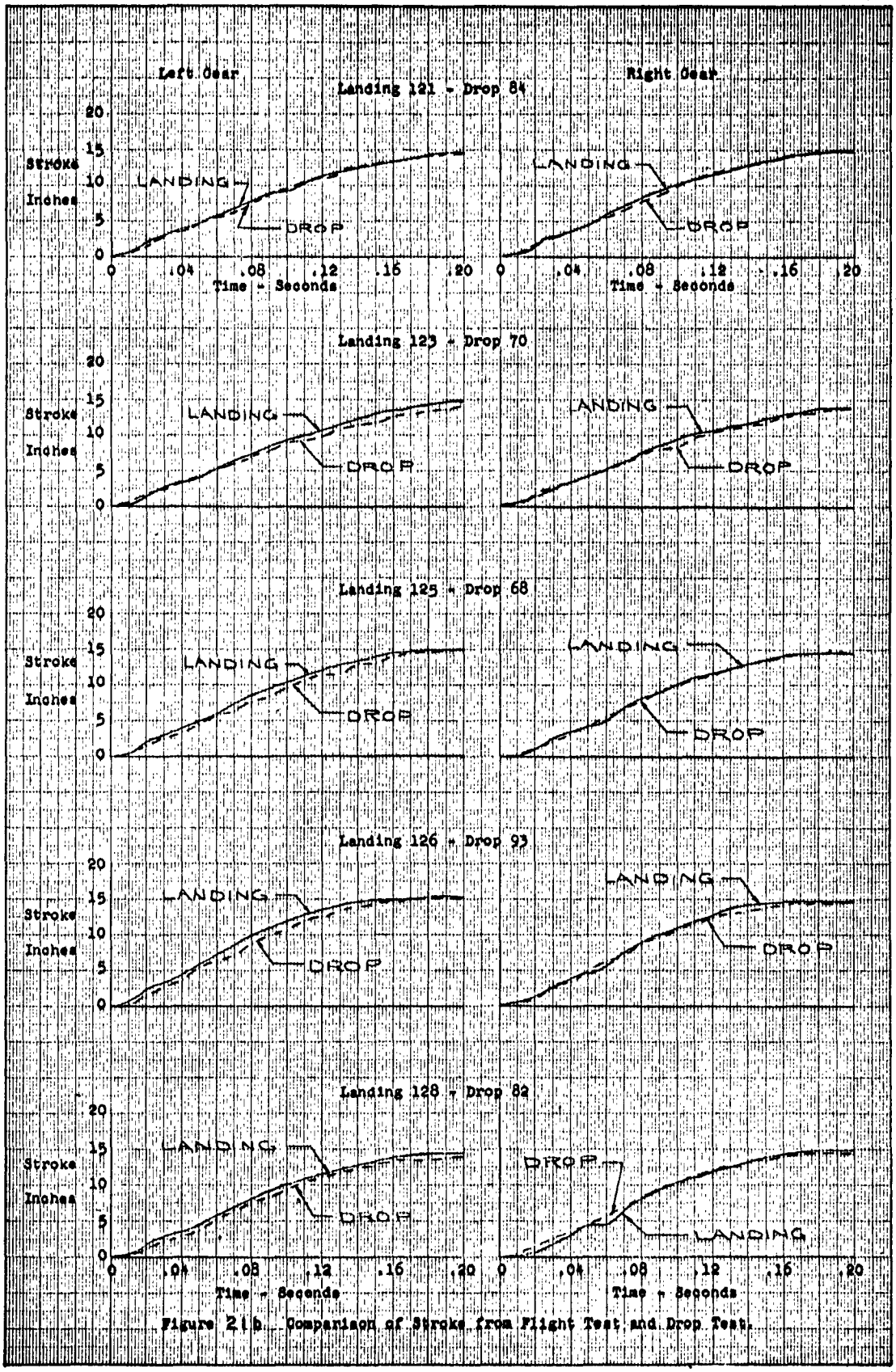

Figure 21b Comparison of Stroke from Flight Test and Drop Test.

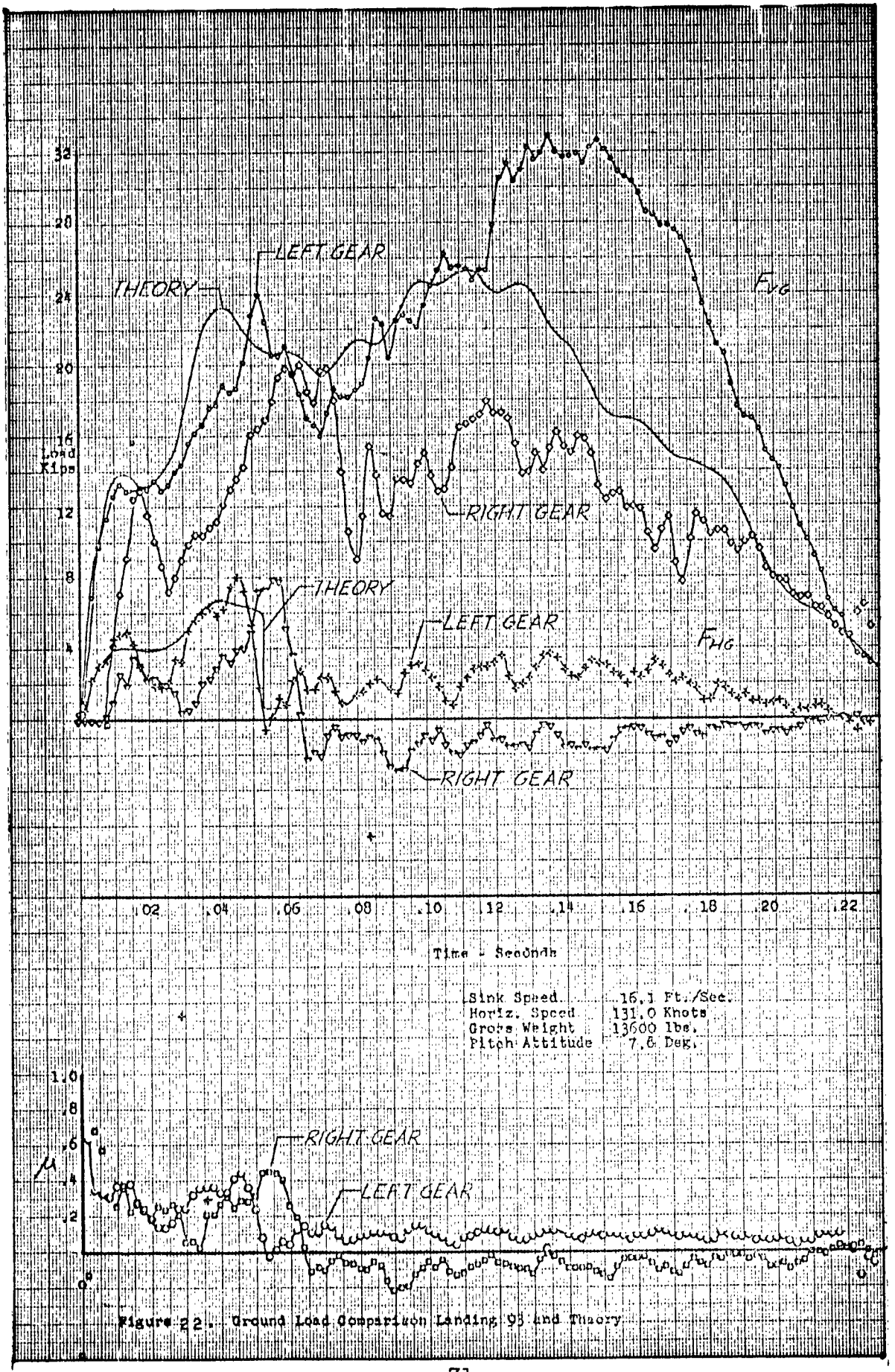

Figure 22. Ground Load Comparison Landing 93 and Theory

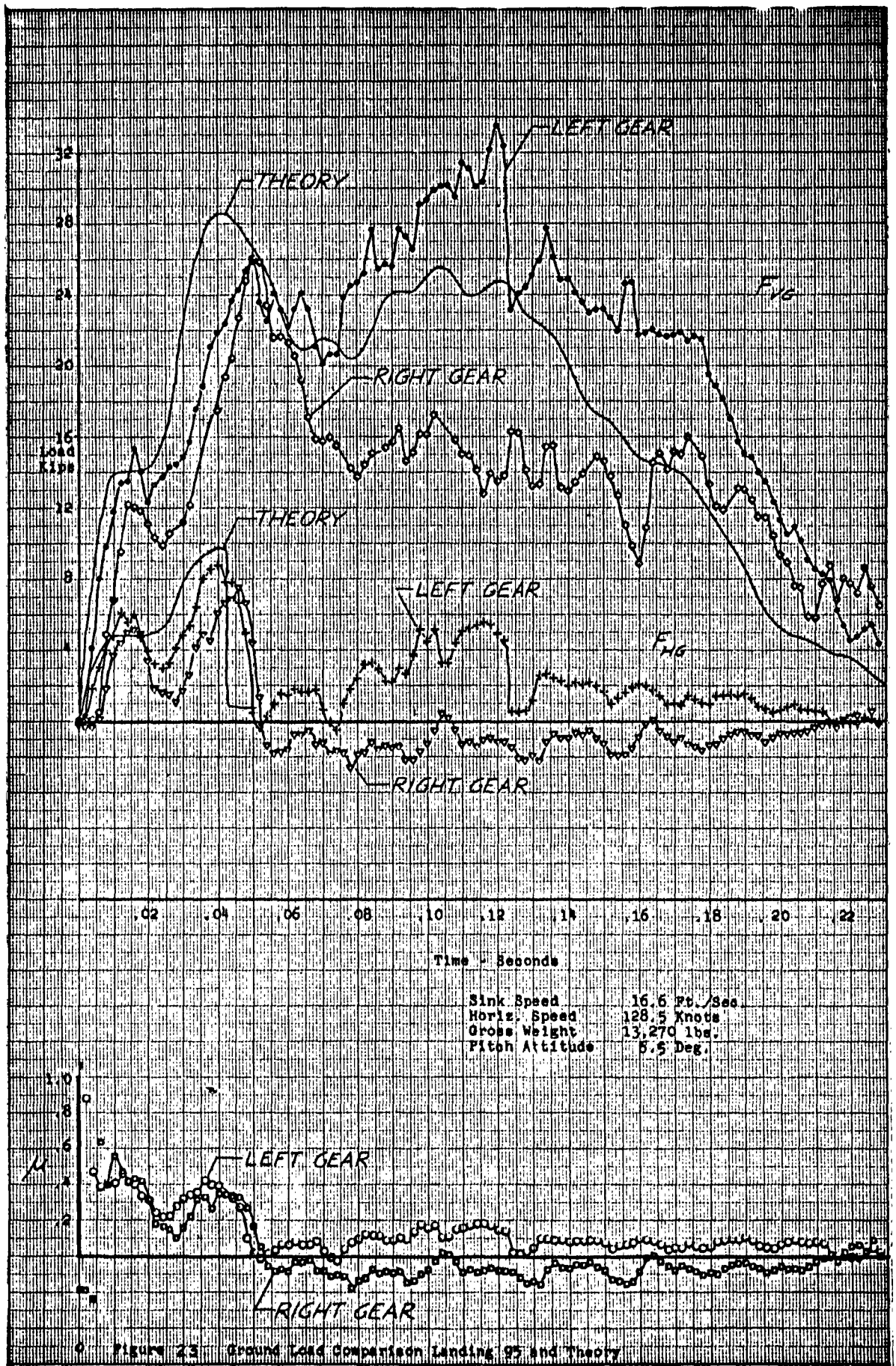

Figure 23 Ground Load Comparison Landing 95 and Theory

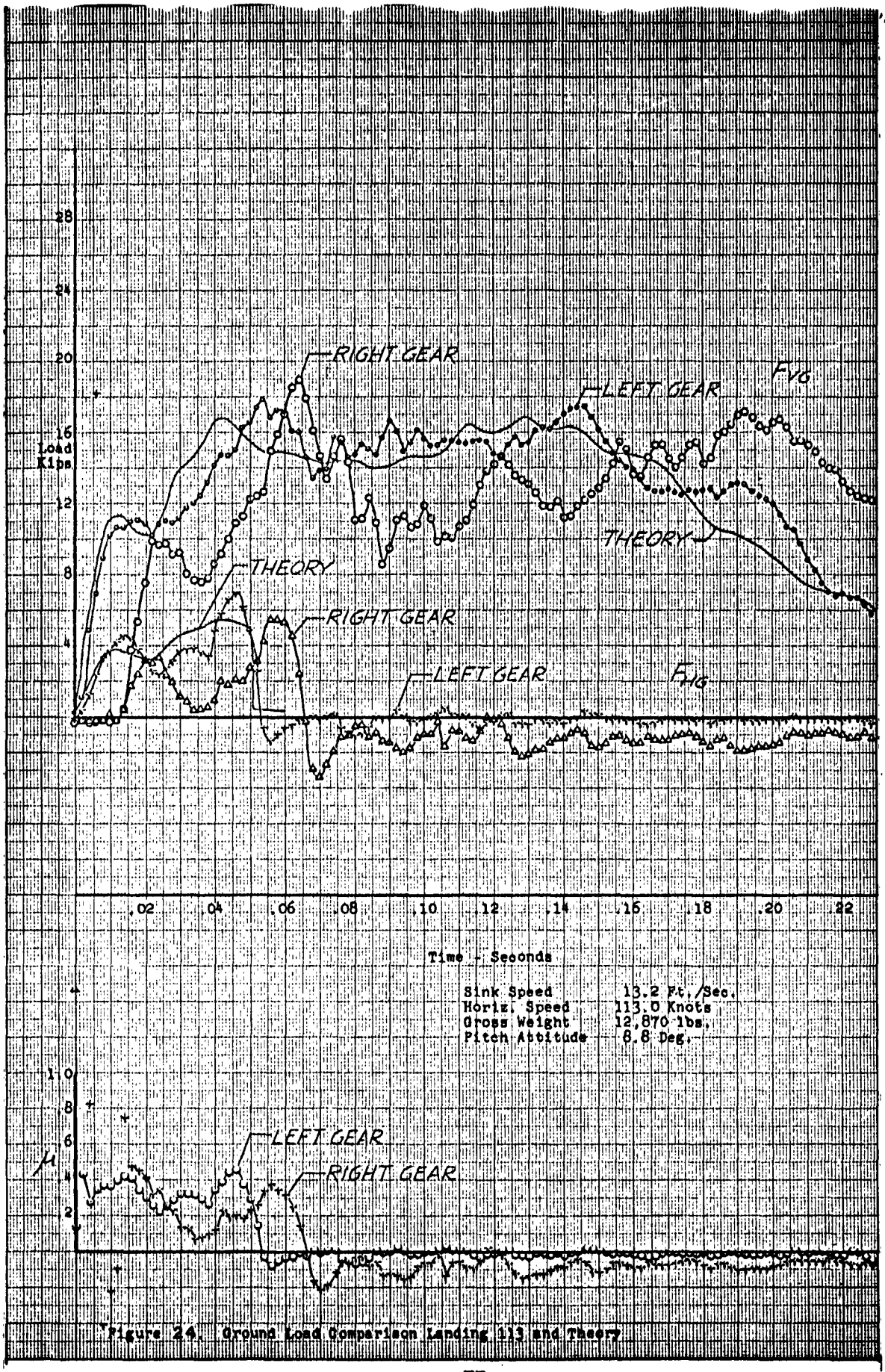

Figure 24. Ground Load Comparison Landing 113 and Theory

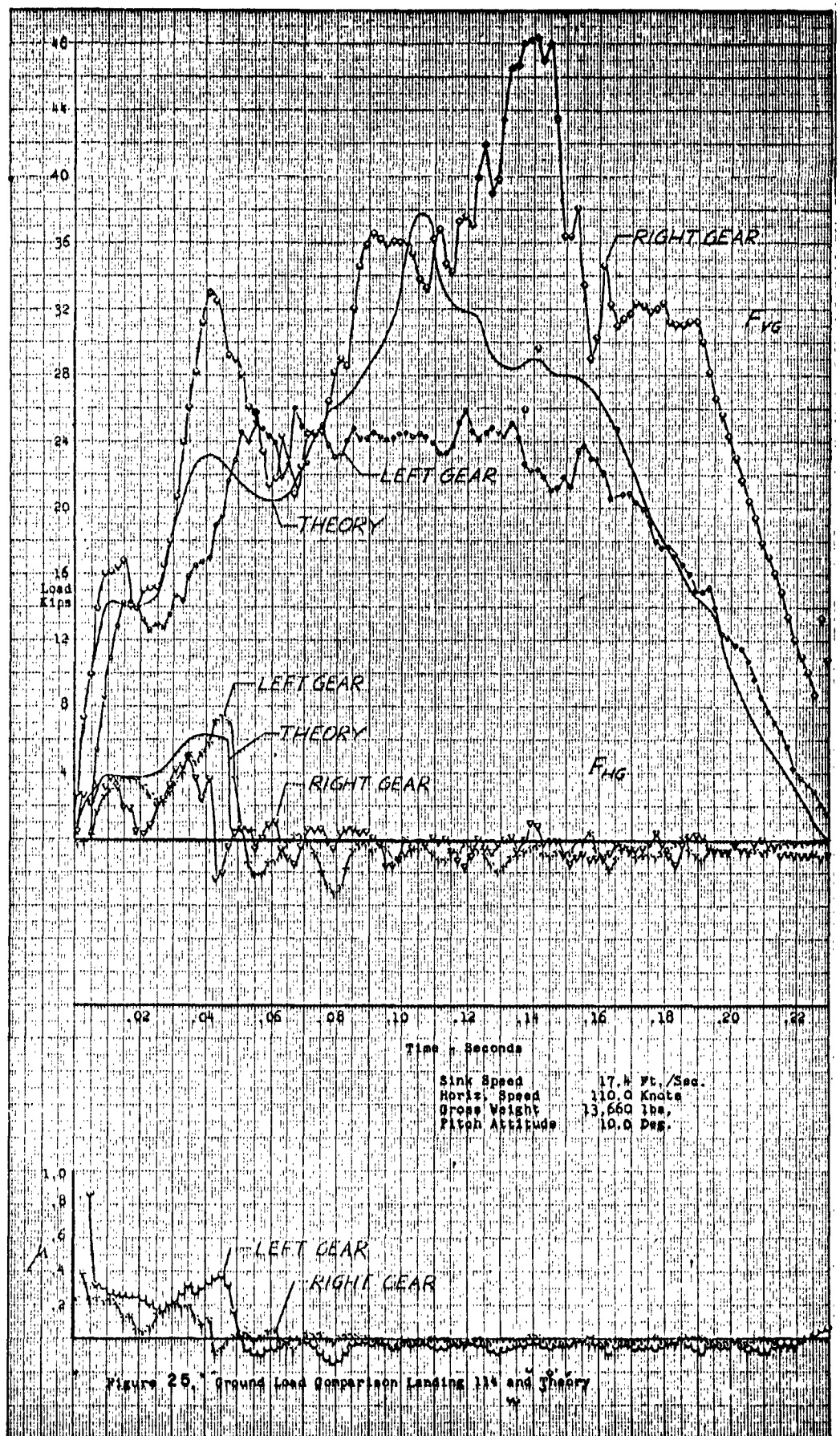

Figure 25. Ground Load Comparison Landing 11% and Theory

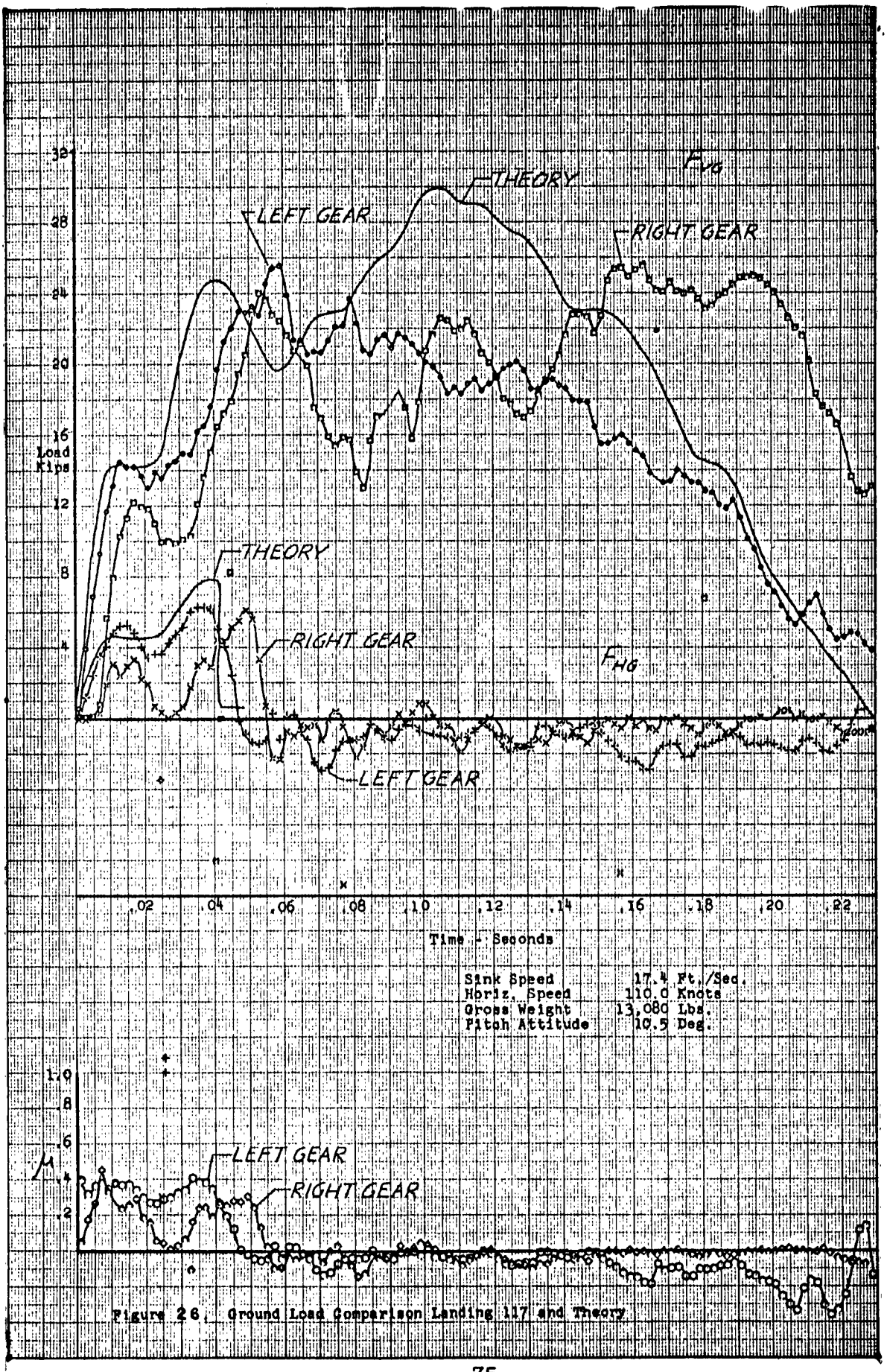

Figure 26. Ground Load Comparison Landing 117 and Theory

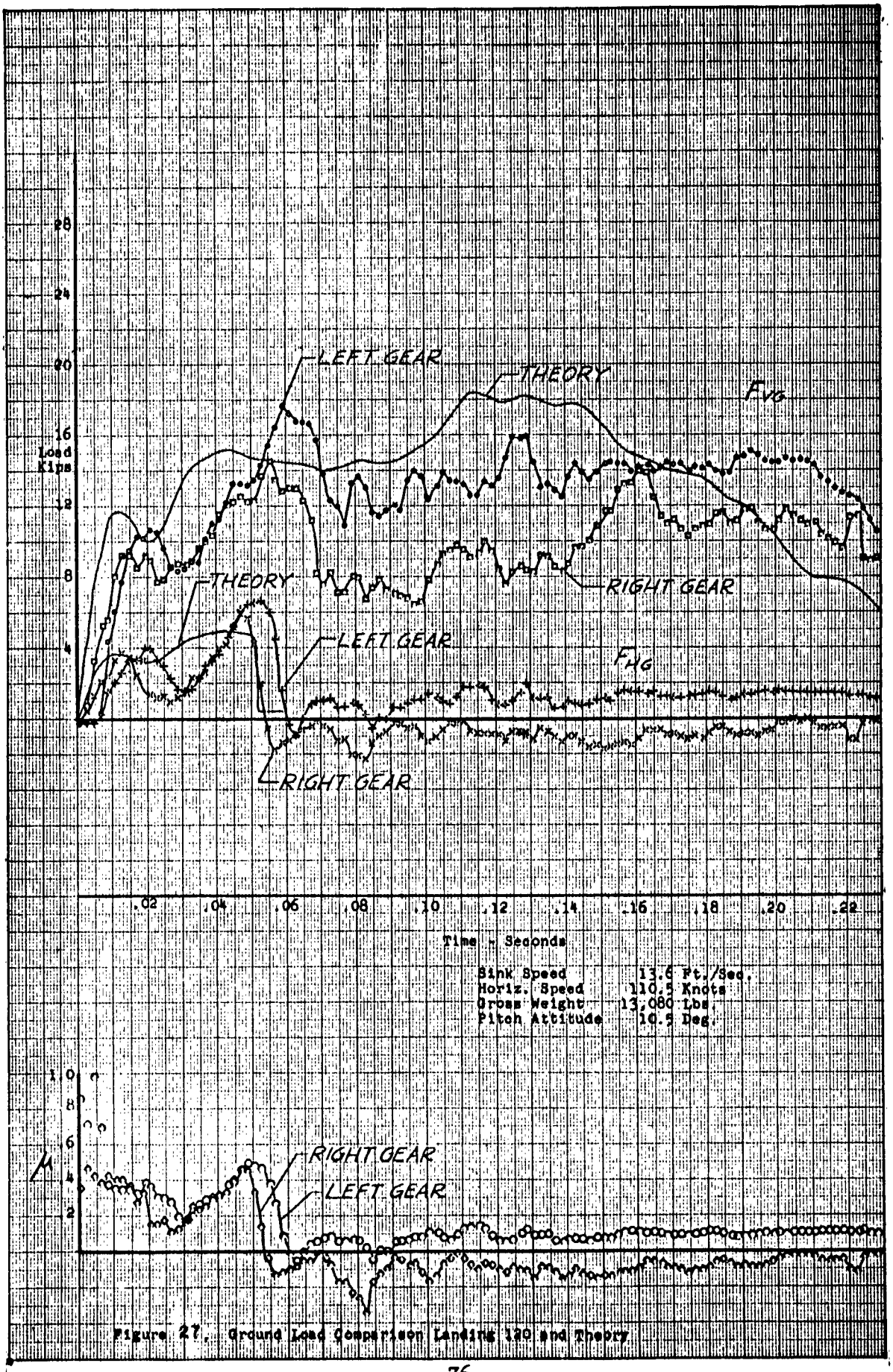

Figure 27. Ground Load Comparison Landing 120 and Theory

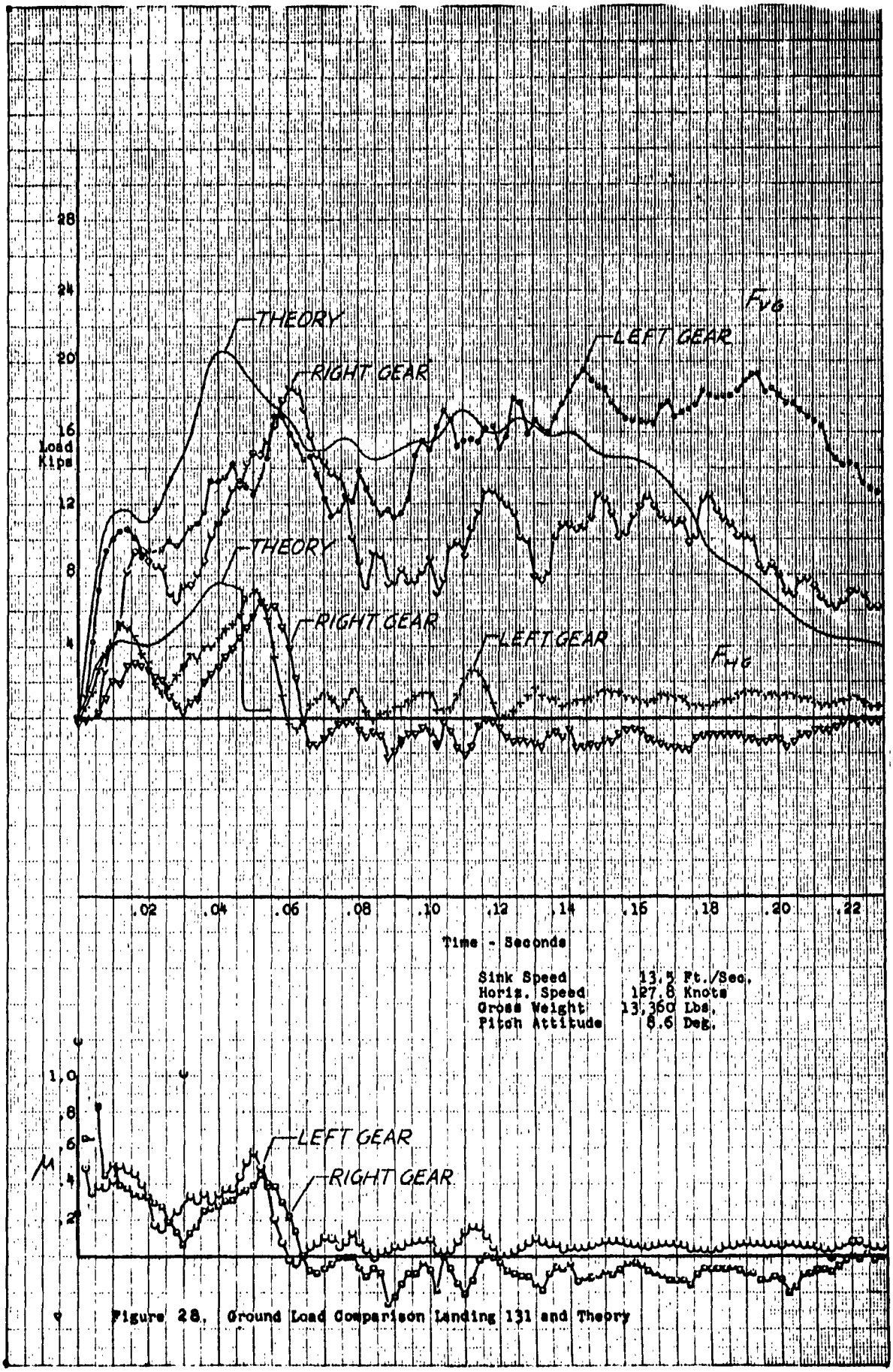

Figure 28. Ground Load Comparison Landing 131 and Theory

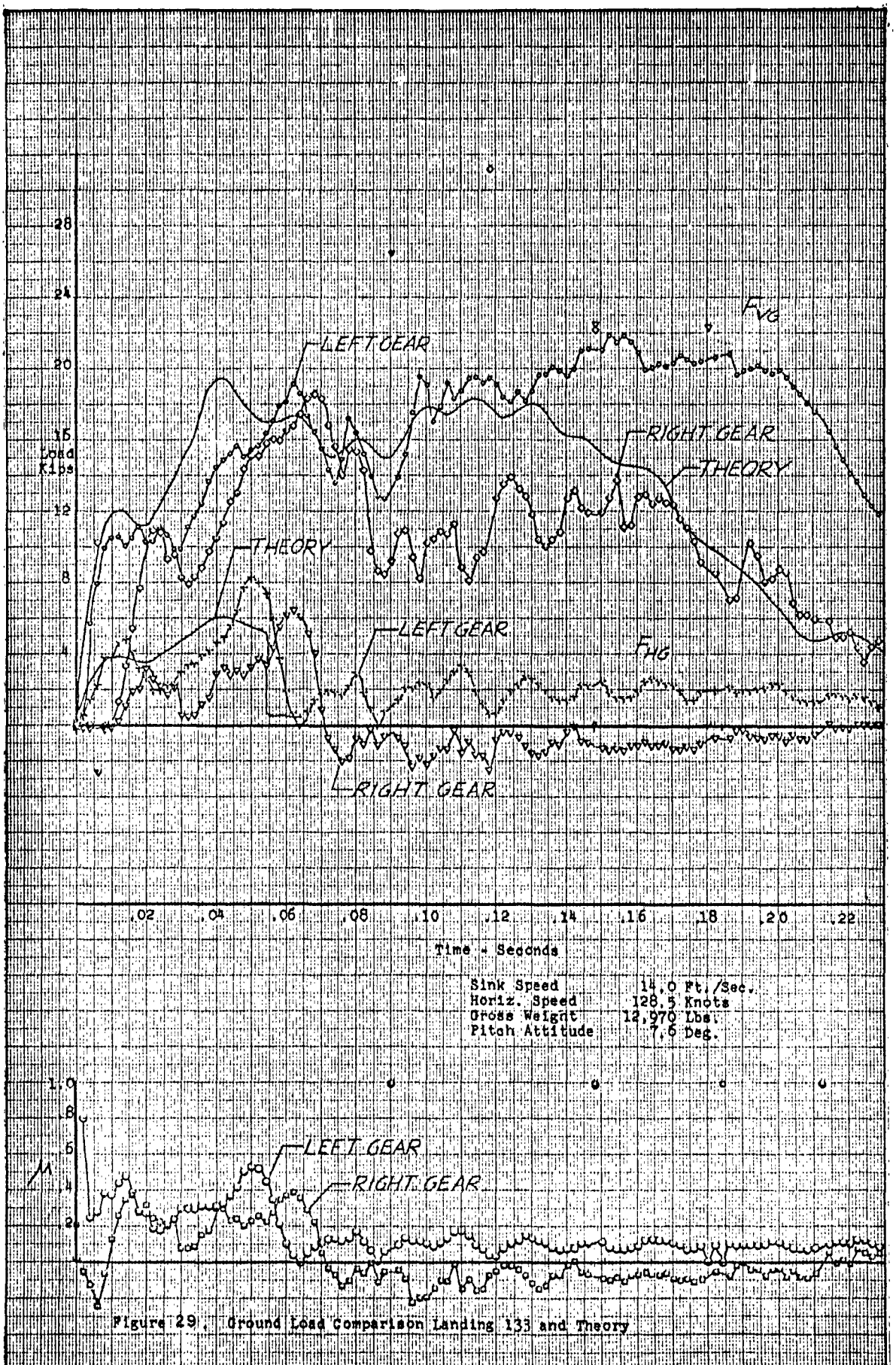

Figure 29. Ground Load Comparison Landing 133 and Theory

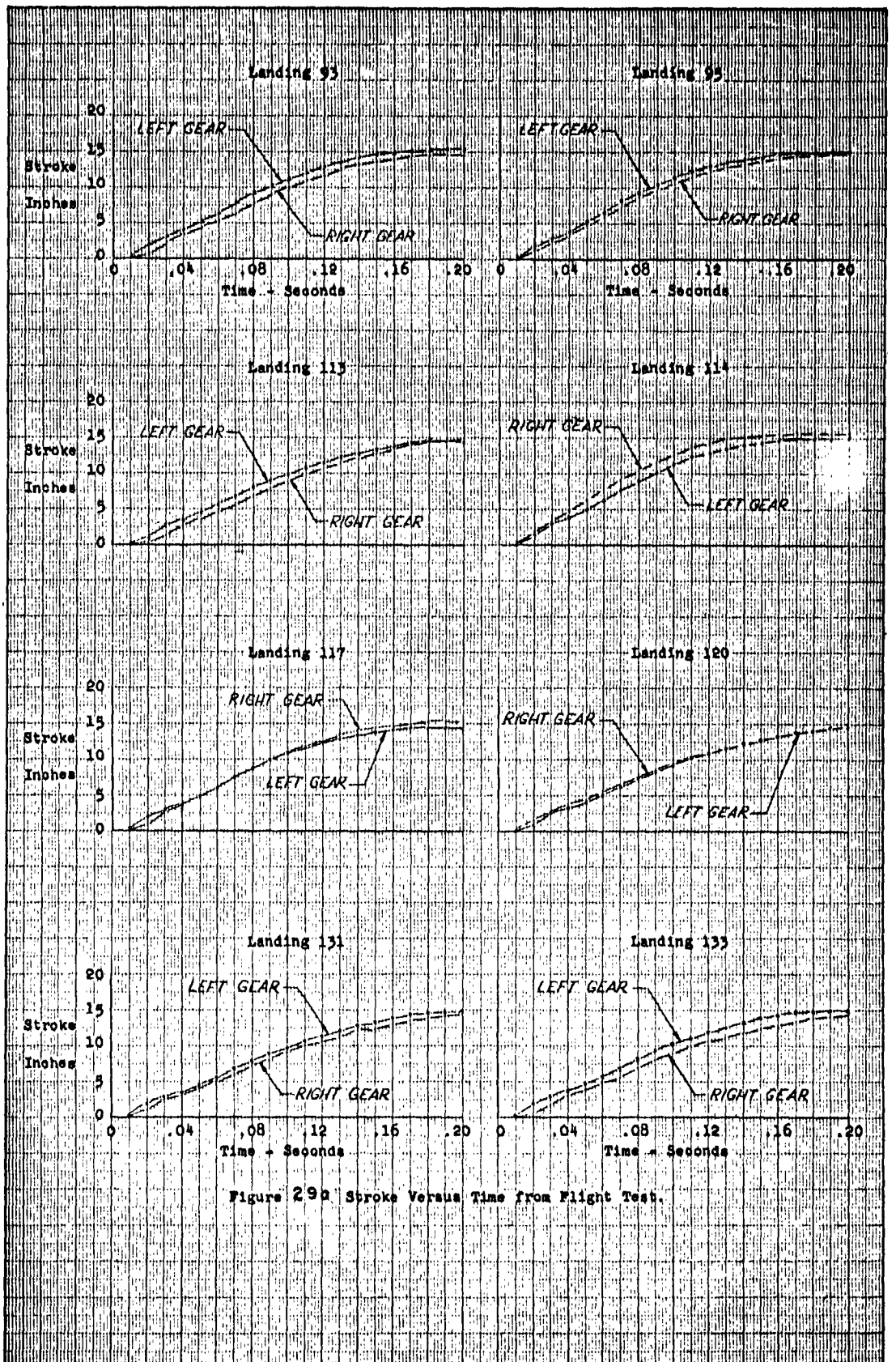

Figure 29a Stroke Versus Time from Flight Test.

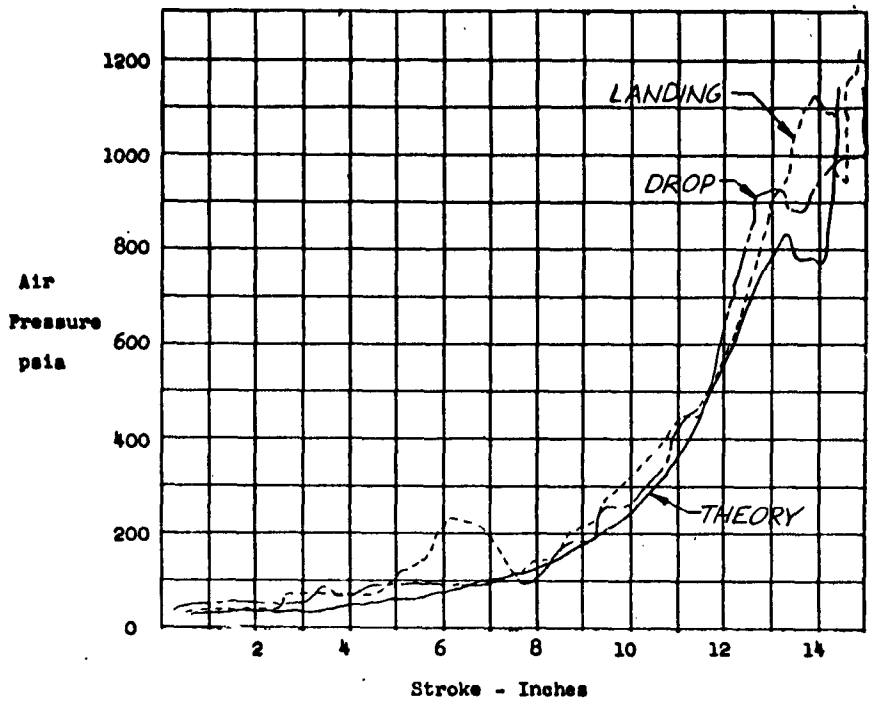

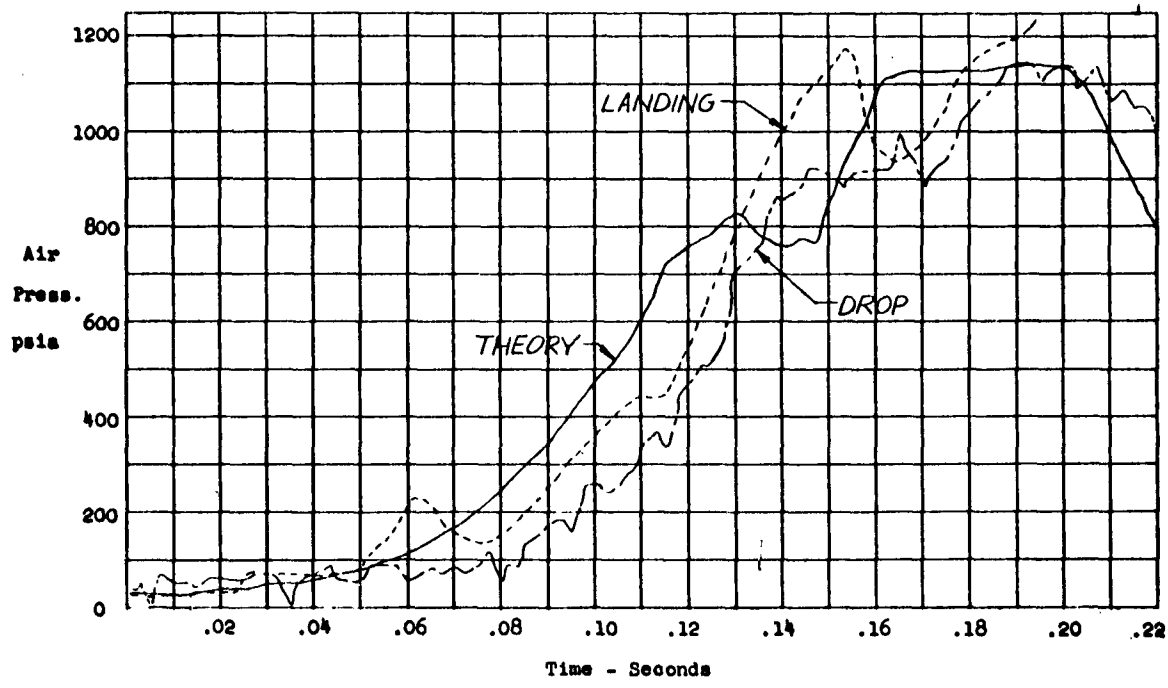

Figure 30. Comparison of Strut Internal Air Pressure Obtained from Landing 125, Drop 68 and Theory.

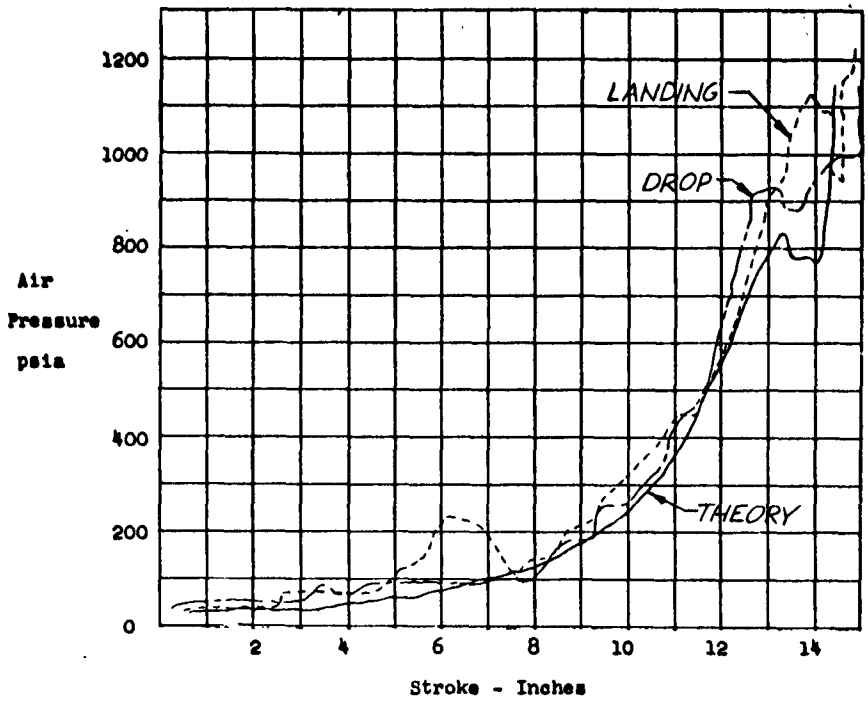

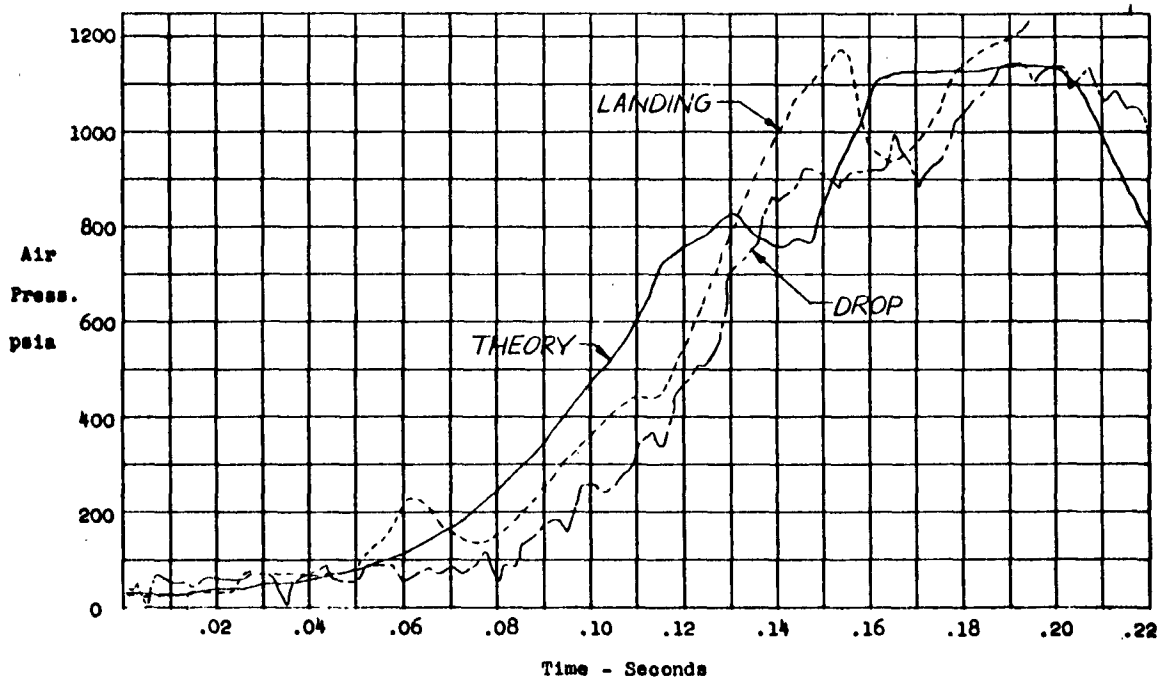

Figure 30. Comparison of Strut Internal Air Pressure Obtained from Landing 125, Drop 68 and Theory.

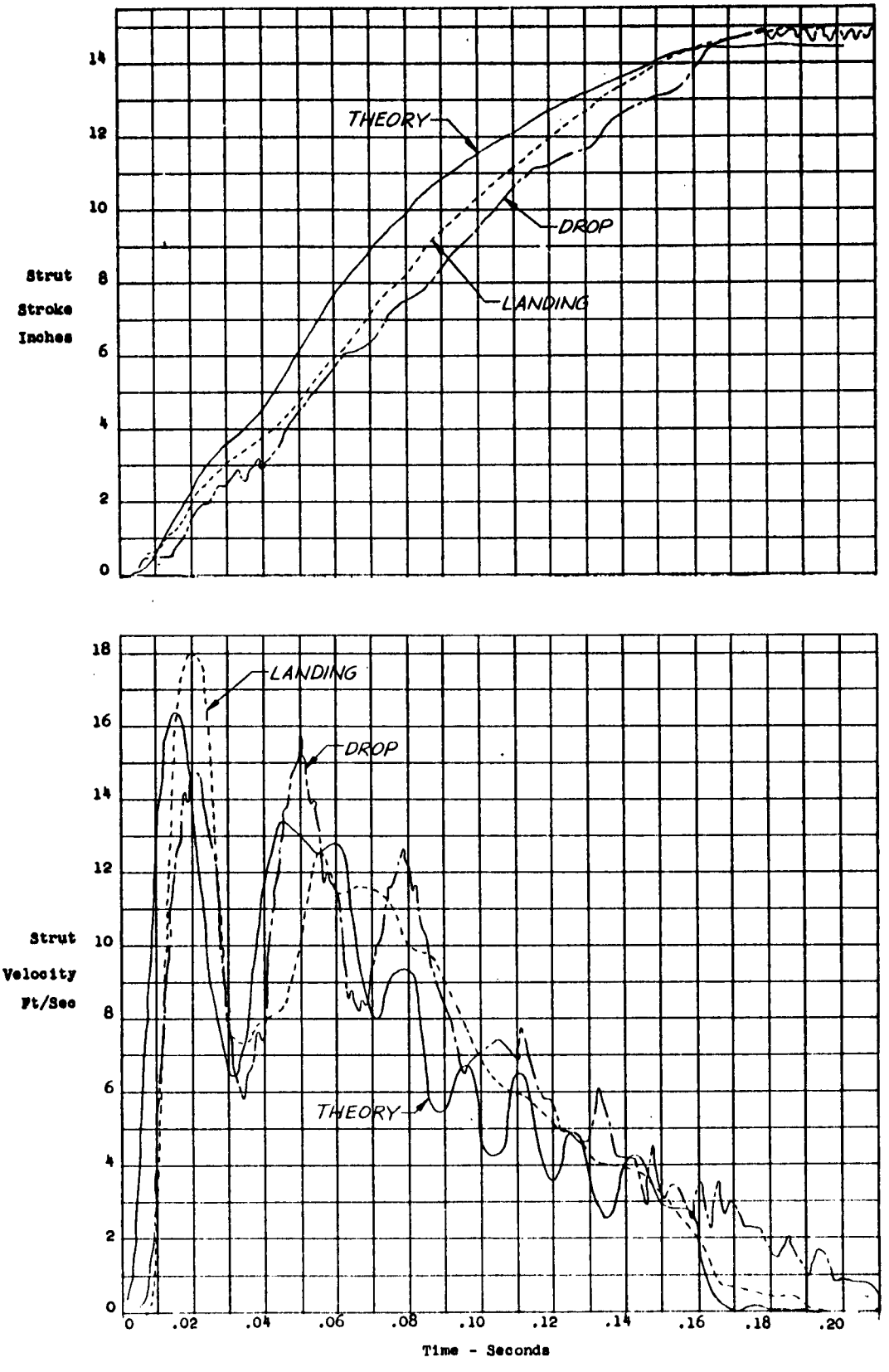

Figure 31. Comparison of Strut Stroke and Velocity for Landing 125, Drop 68 and Theory.

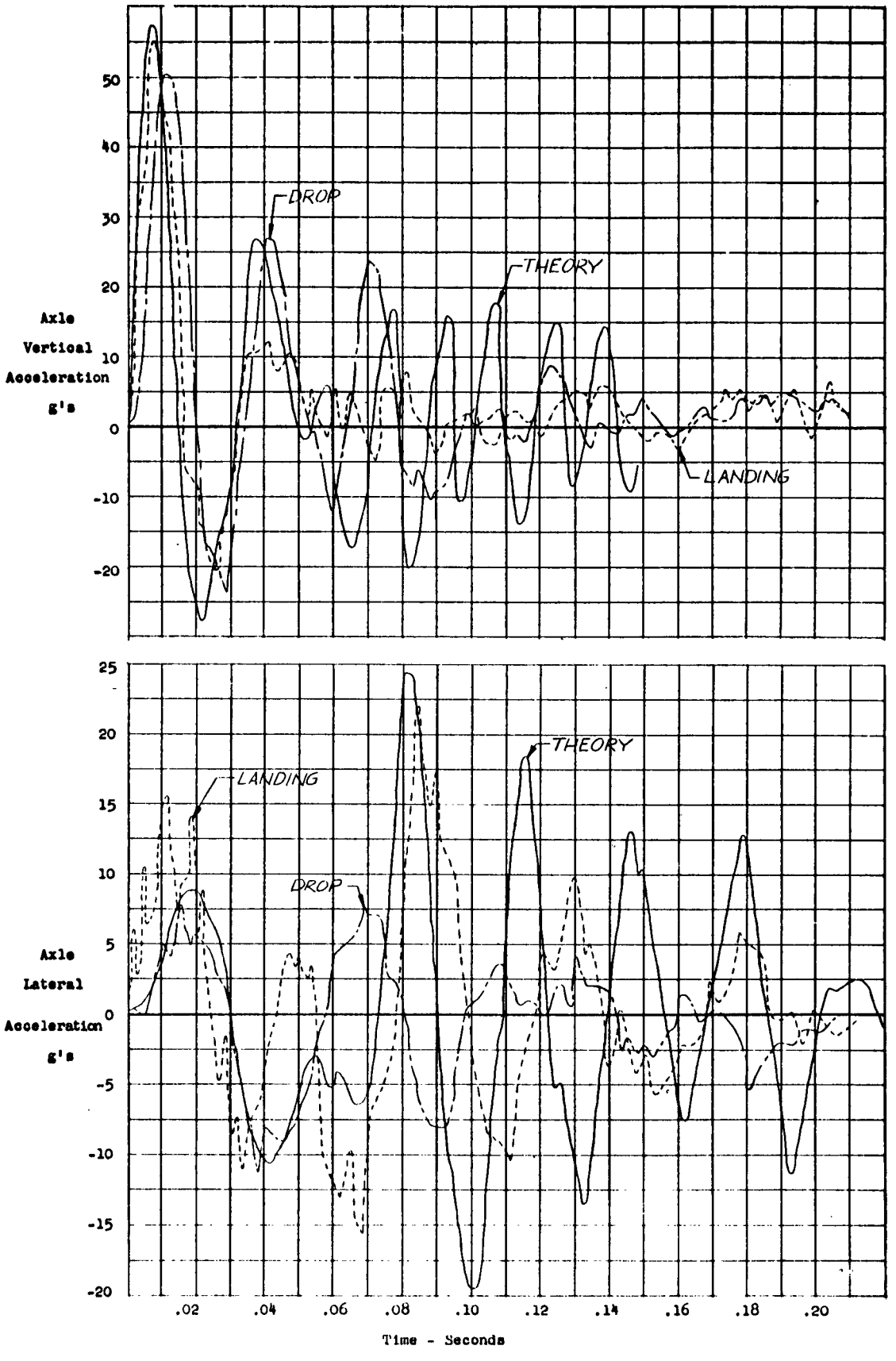

Figure 32. Comparison of Axle Vertical and Lateral Accelerations obtained from Landing 125, Drop 68 and Theory.

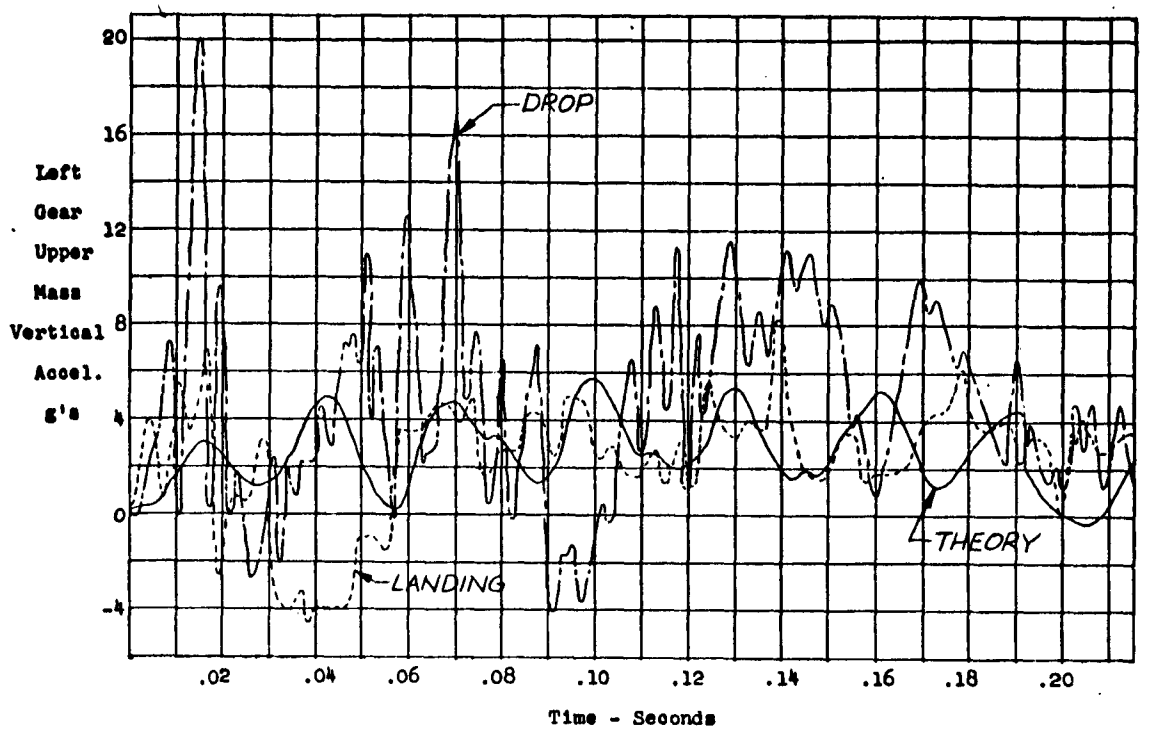

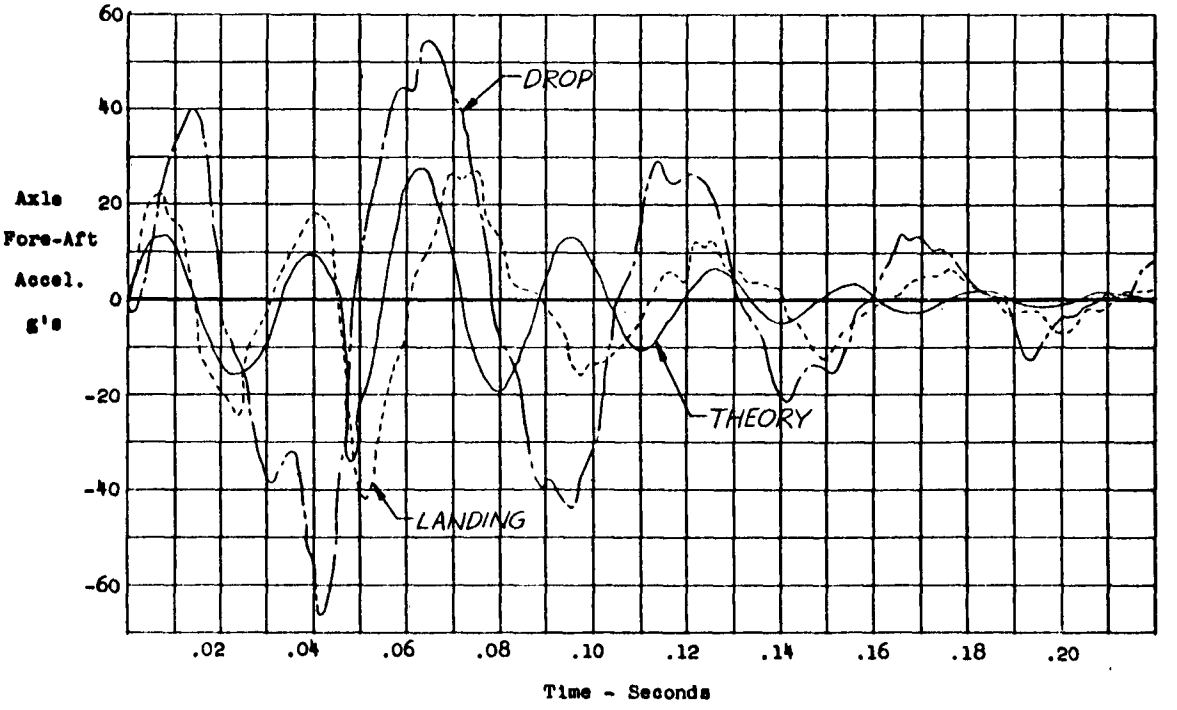

Figure 33. Comparison of Axle Fore-Aft Acceleration and the Acceleration of the Gear Attach Point Obtained from Landing 125, Drop 68 and Theory.

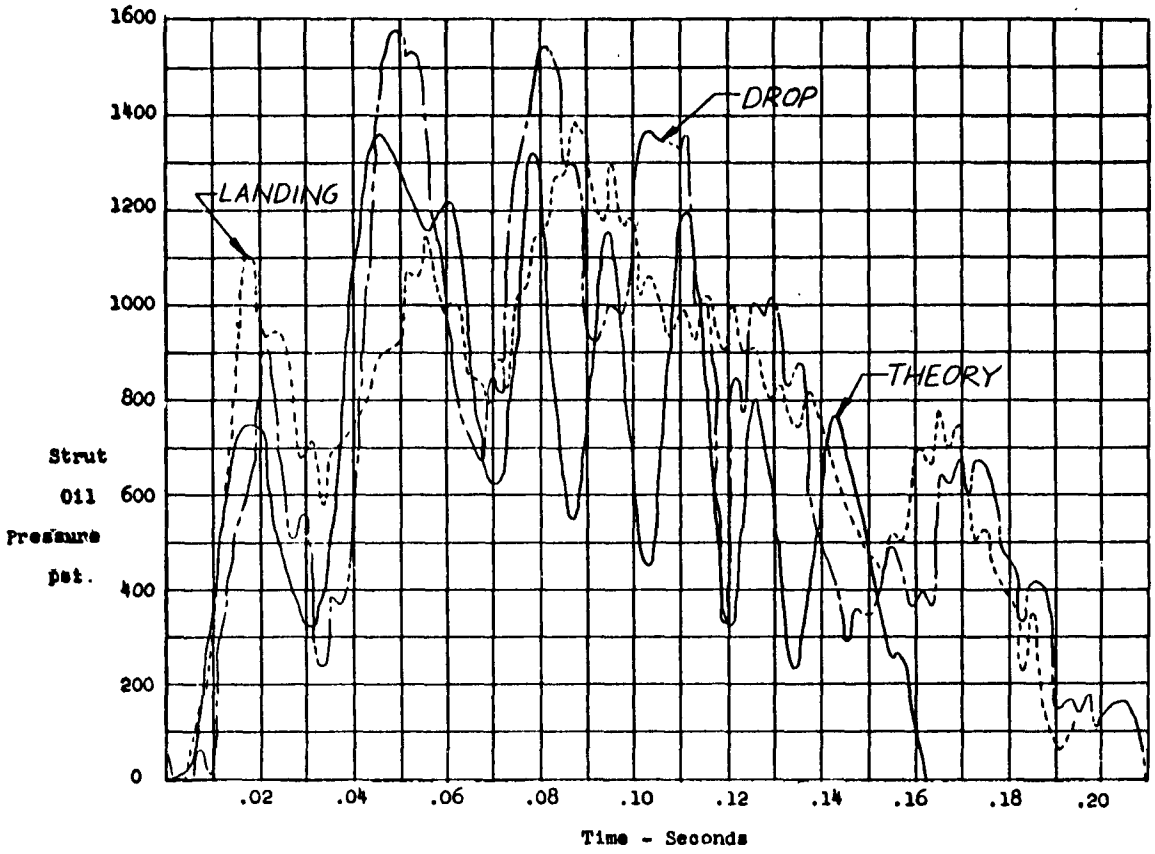

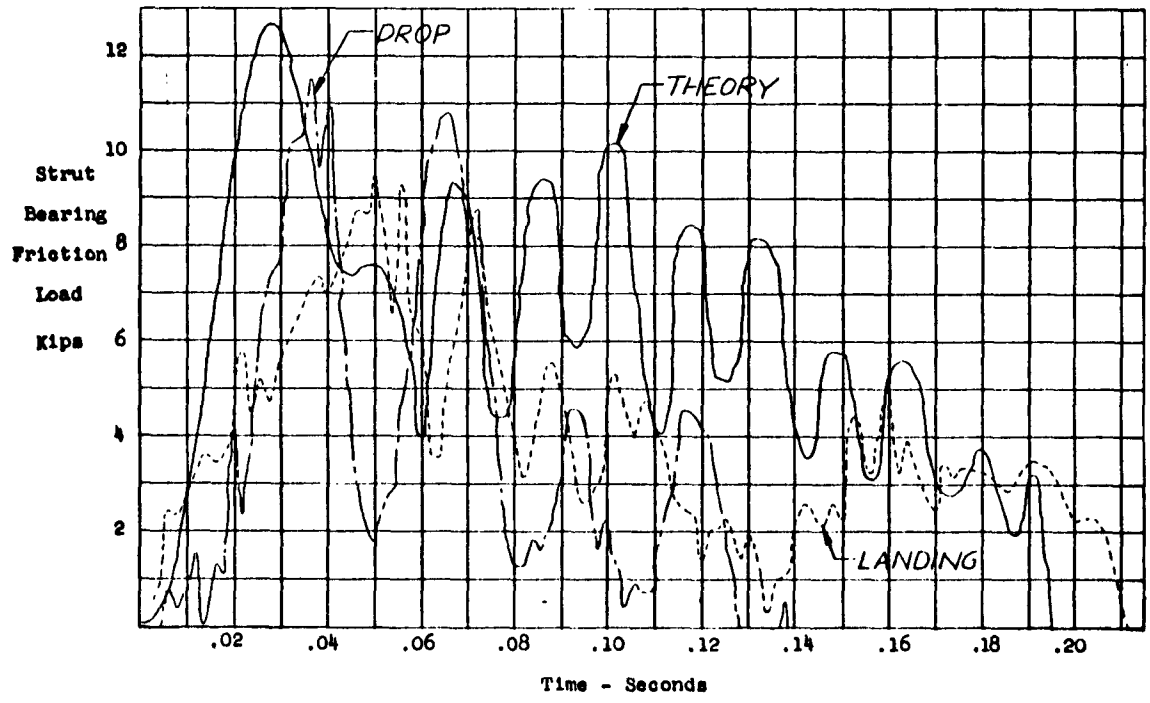

Figure 34. Comparison of Strut Oil and Friction Loads Obtained from Landing 125, Drop 68, Theory.

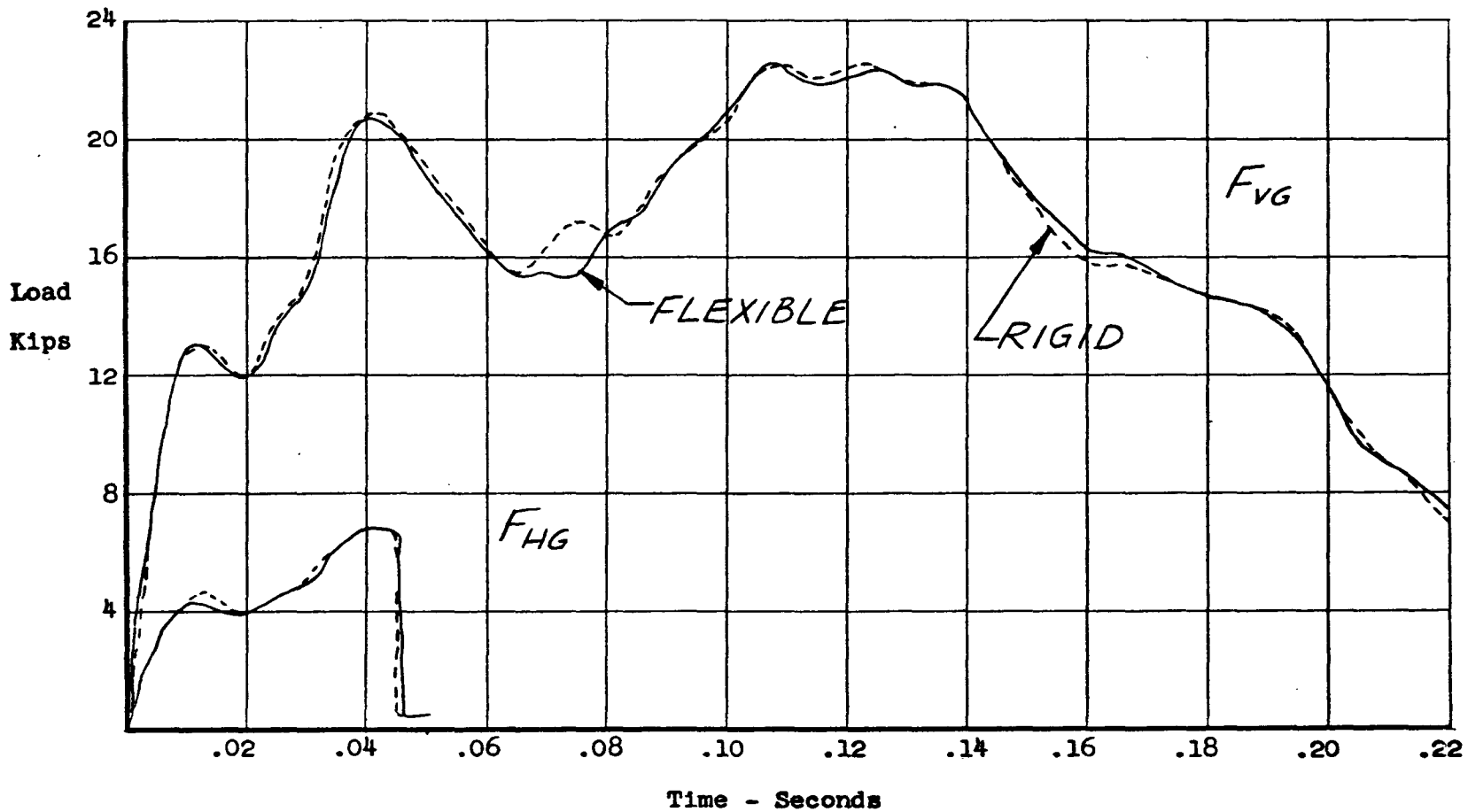

Figure 35. Ground Load Comparison for the Theoretical Analysis of Landing 125 with a Flexible and Rigid Wing.

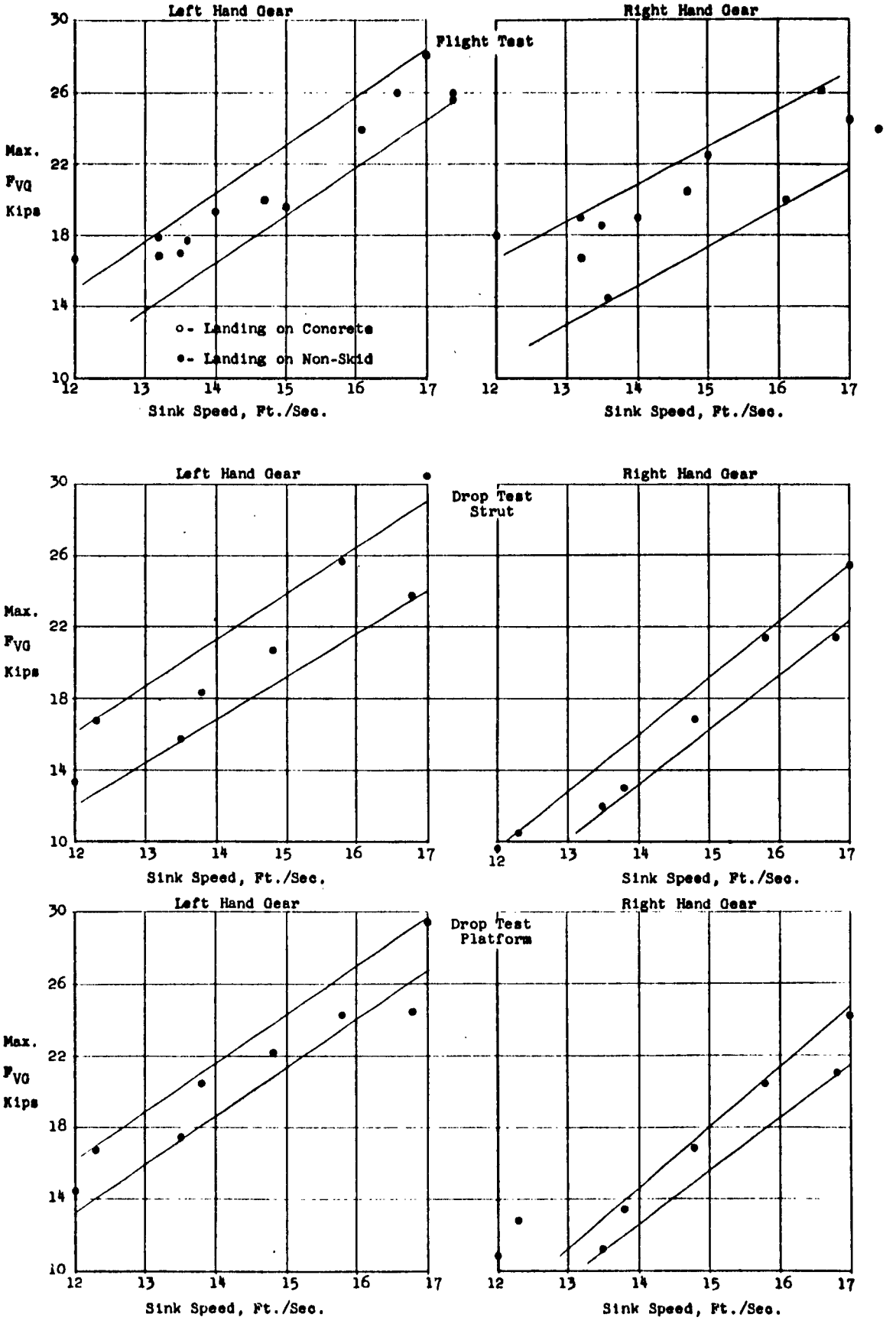

Figure 36. First Peak Maximum Vertical Load Versus Sink Speed.

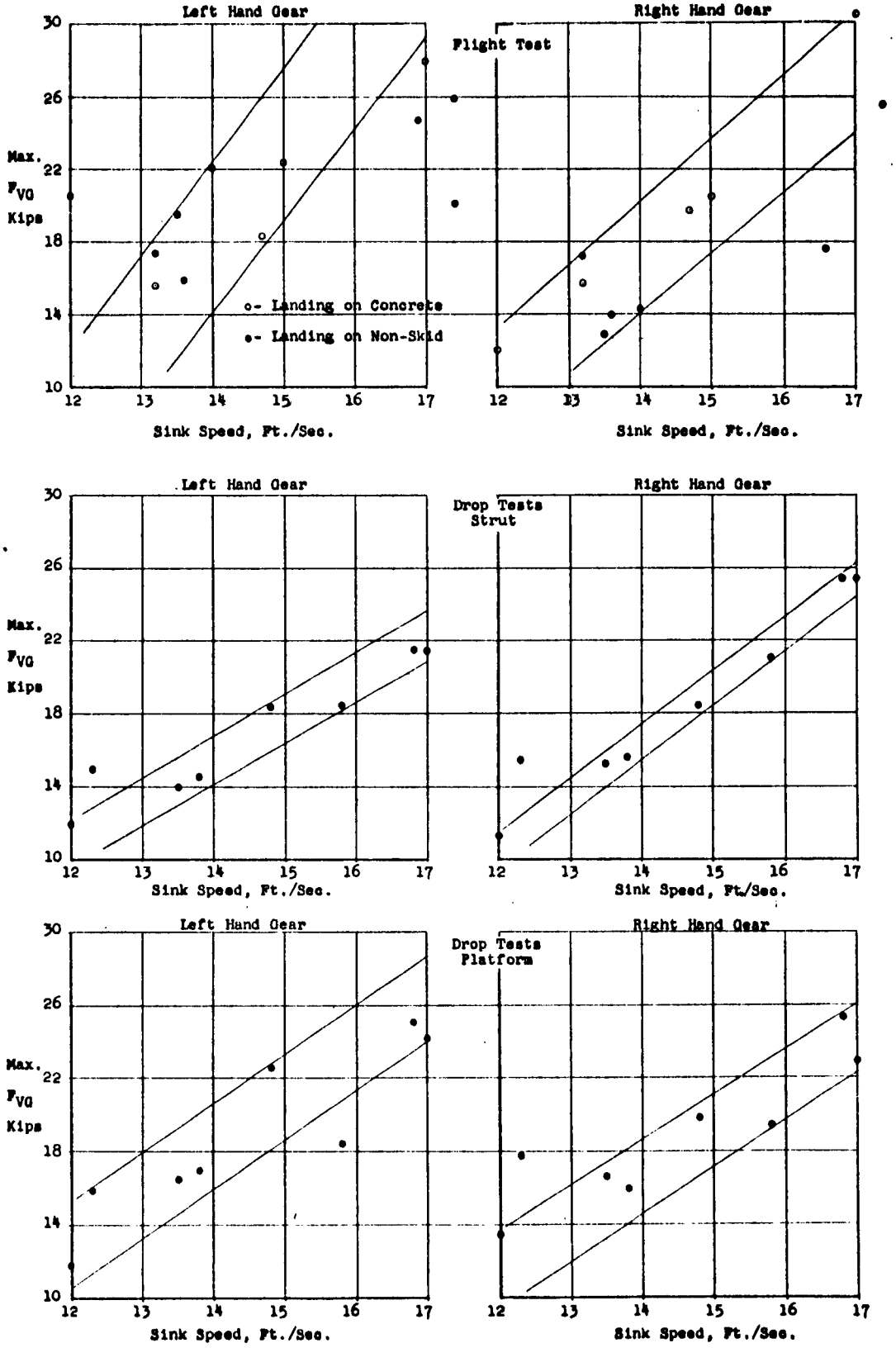

Figure 37. Second Peak Maximum Vertical Load Versus Sink Speed.

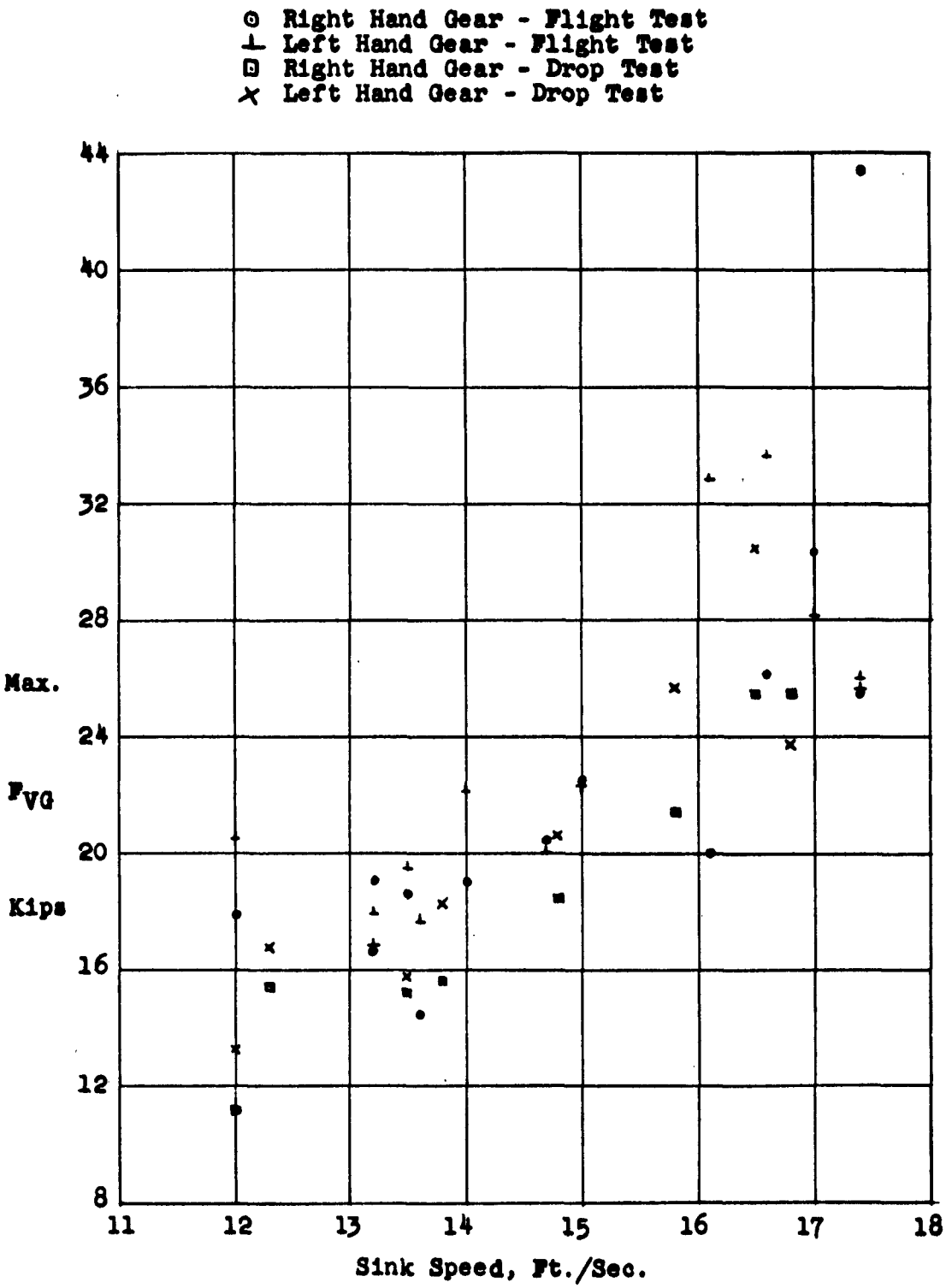

Figure 37a. Maximum Vertical Load Versus Sink Speed from Flight Test and Drop Test.

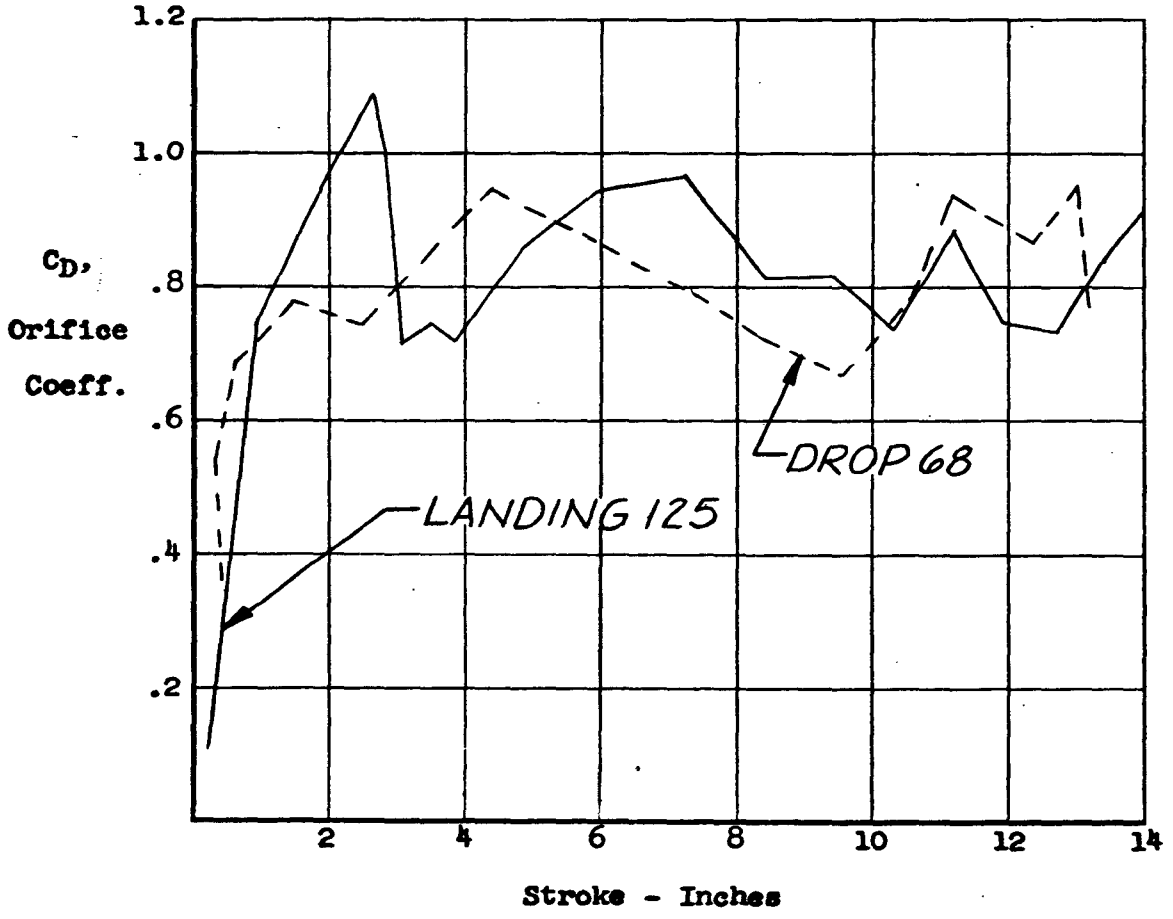

Figure 38. Left Hand Gear Orifice Discharge Coefficient Calculated from Pressures Measured during Landing 125 and Drop 68.

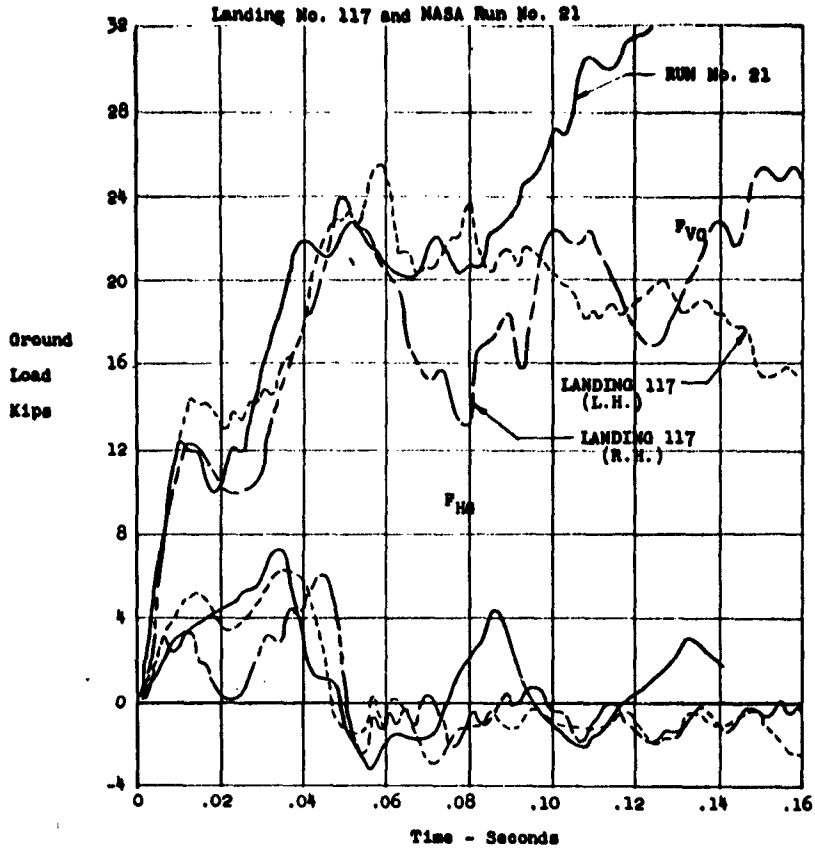

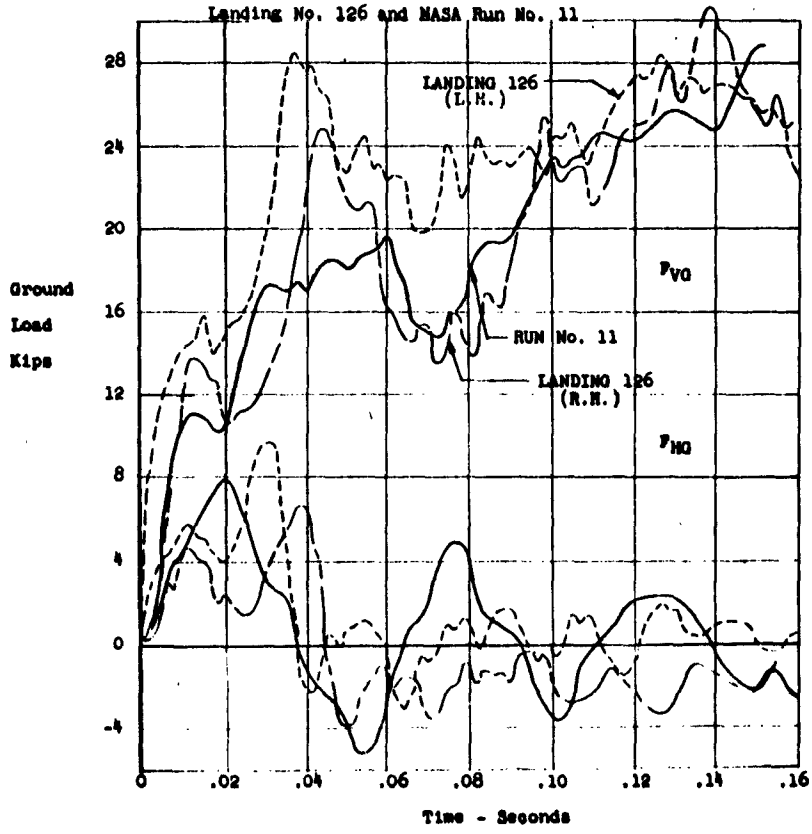

Figure 39. Comparison of Flight Test with NASA Landing-Impact Tests.

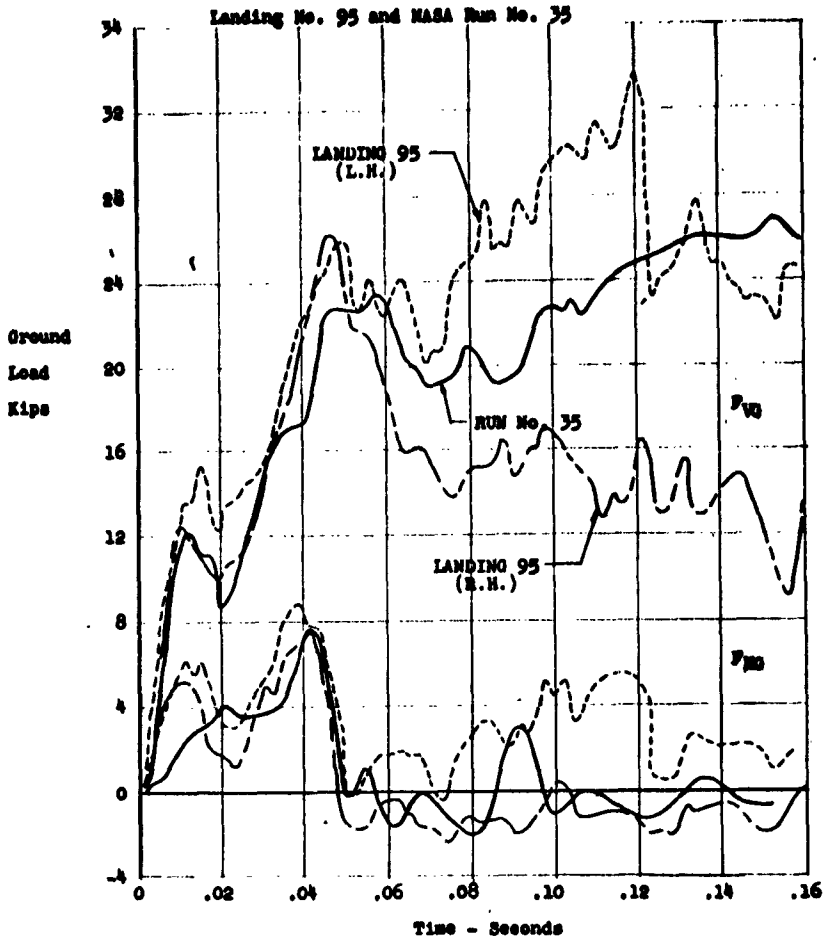

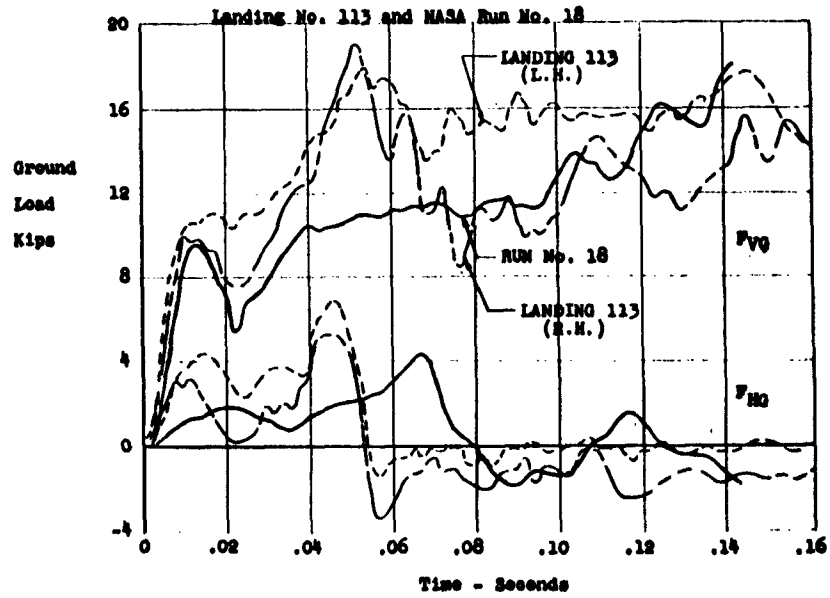

Figure 40. Comparison of Flight Test with NASA Landing-Impact Data.

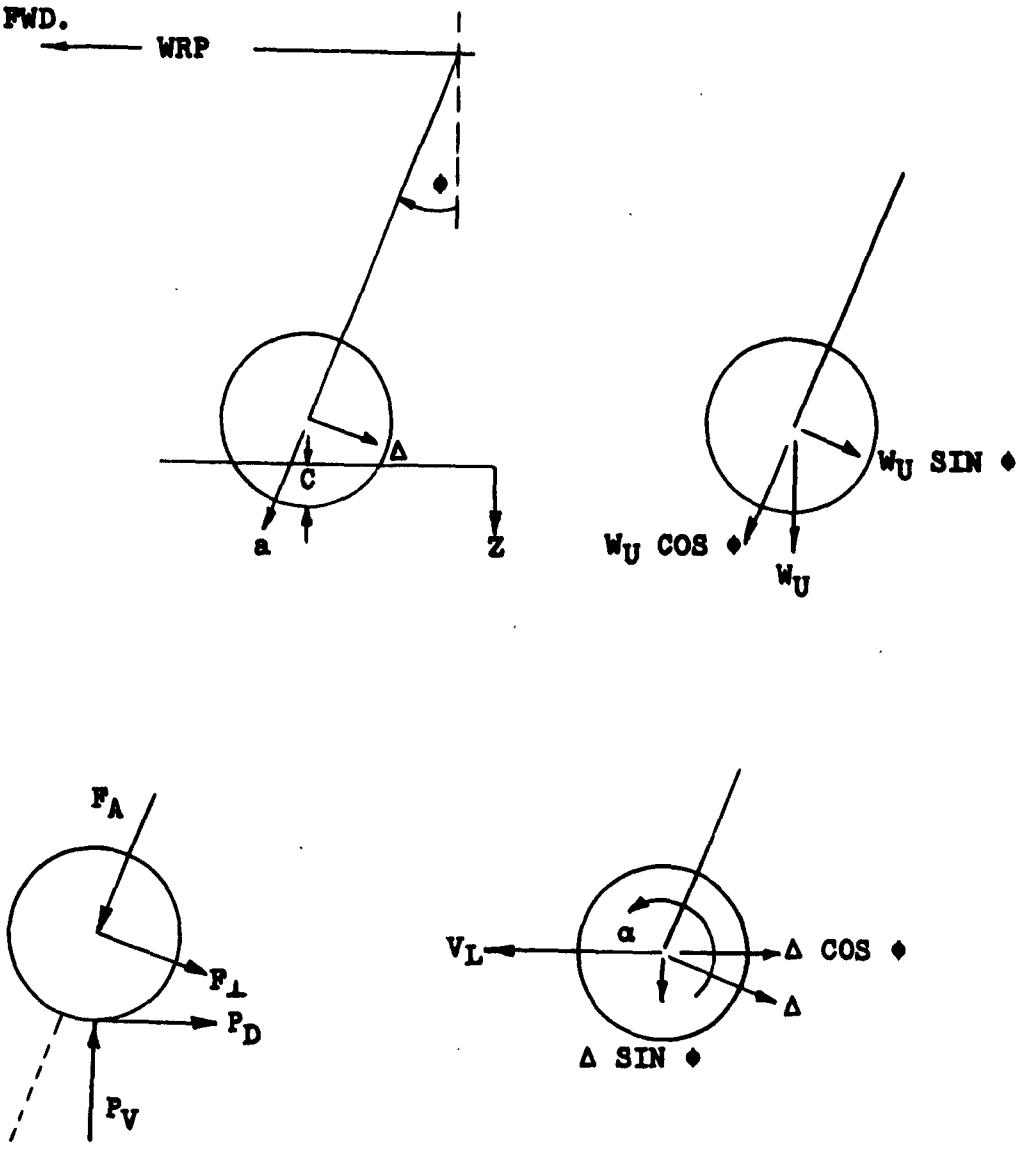

Figure 41. Directions of Positive Displacements and Forces.

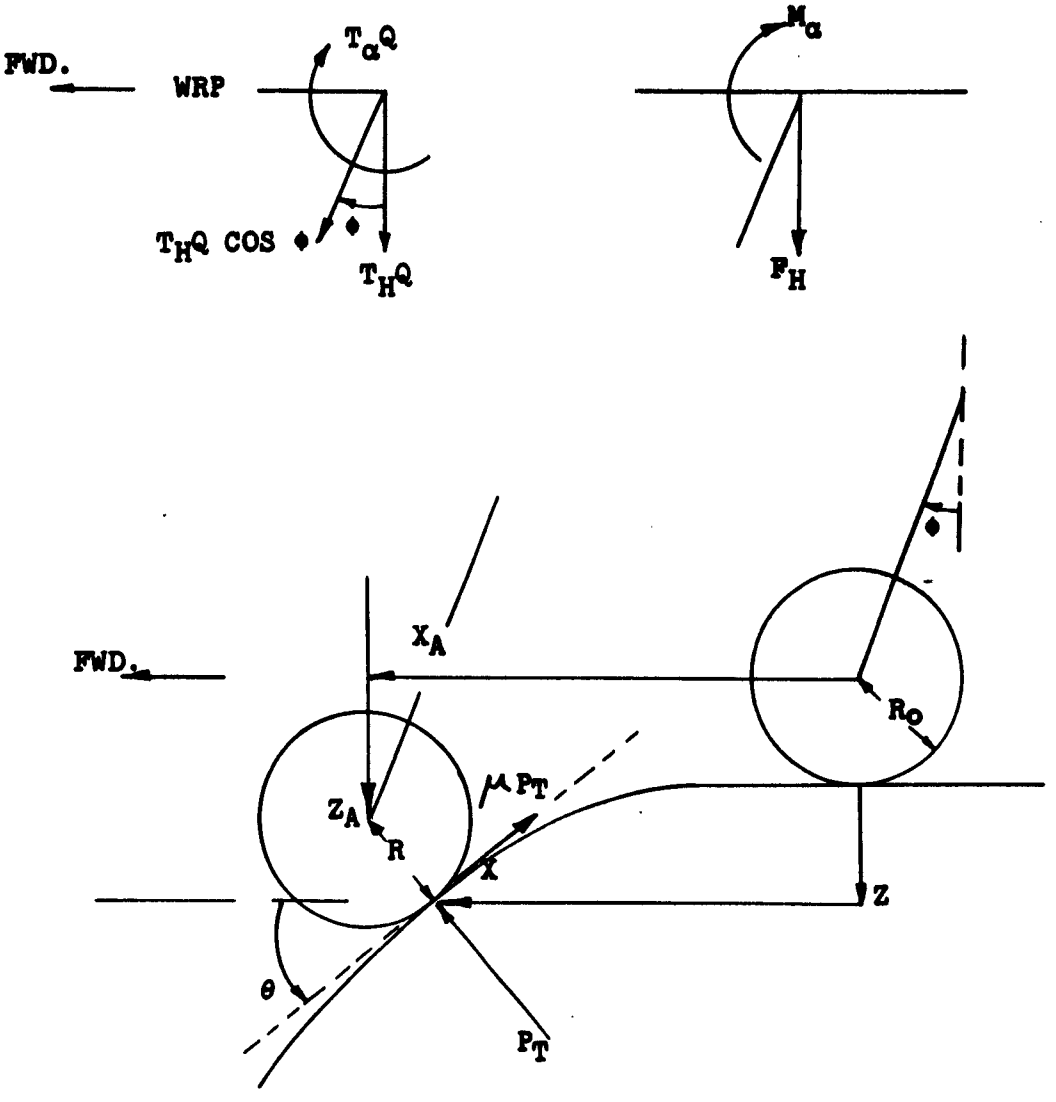

Figure 41. Continued

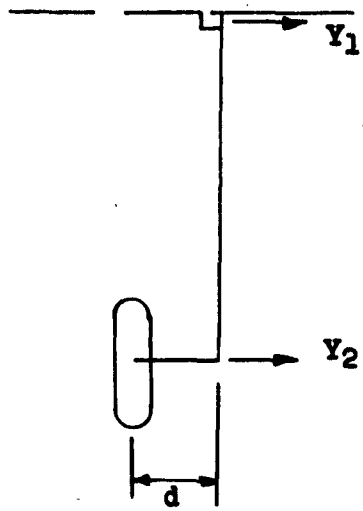

Left Hand Main Gear Looking Forward

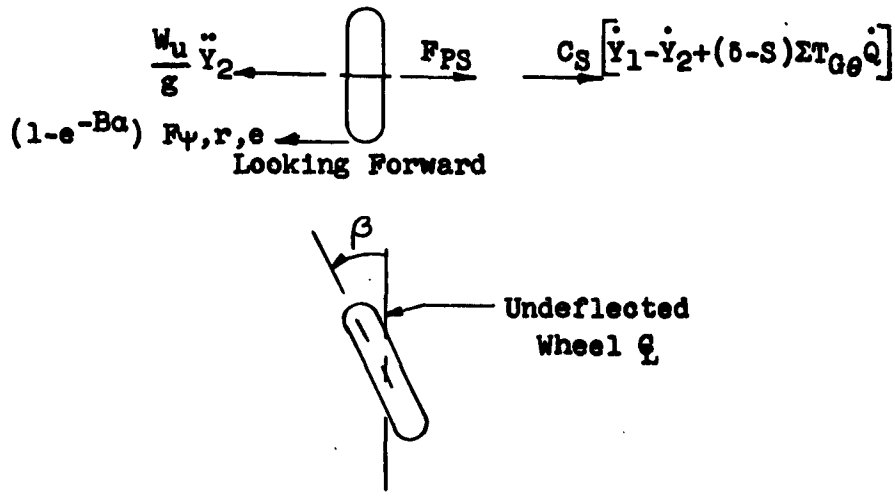

Looking Down

Figure 41. Continued

TABLE 1

INSTRUMENTATION FOR DROP TESTS

Oscillograph 1

	Parameter Measured	Method of Measurement	Transducer Range	Transducer Type
1	L.H. Strut Vertical Load	Strain Gauge Installation on Axle	0-60K	18V 350 Ω
2	*L.H. Strut Drag Load	Strain Gauge Installation on Axle	± 20K	
3	*L.H. Strut Position	Slide Wire Device	0-16 in.	DAC
4	*L.H. Strut Velocity	Velocity Generator	± 30 FPS	Sanborn 10LV 17-n
5	*L.H. Air Chamber Press.	Pressure Transducer	0-5 KSI	DAC
6	*L.H. Metering Chamber Press.	Pressure Transducer	0-5 KSI	DAC
7	*L.H. Lower Mass Vert.Accel.	Miniature Accelerometer in Axle	± 90g's	**A6-100-350
8	*L.H. Lower Mass Long.Accel.	Miniature Accelerometer in Axle	±100g's	A6-100-350
9	*L.H. Lower Mass Side Accel.	Miniature Accelerometer in Axle	±100g's	A6-100-350
10	*L.H. Gear Upper Mass V.Accel.	Accelerometer	± 50g's	A5-50-350
11	*L.H. Gear Upper Mass V.Accel.	Accelerometer	± 50g's	A5-50-350
12	*L.H. Gear Upper Mass D.Accel.	Accelerometer	± 30g's	A5-50-350
13	*L.H. Drag Brace Axial Ld.	Strain Gauges	± 50K	18V 350Ω
14	L.H. Gear Side Bending Mom.	Strain Gauge Installation		18V 350Ω
15	*L.H. Wheel Angular Position	36 Magnets on Wheel - Pick-up on Strut	0-150KC	Electro 3010
16	Nose Gear Strut Position	Slide Wire Device	0-18 in.	DAC
17	Nose Gear Upper Mass V.Accel.	Accelerometer	± 30g's	A5-30-350
18	C.G. Normal Accel.	Accelerometer	± 1g	AJ26-1-350
19	C.G. Normal Accel.	Accelerometer	± 10g's	AJ43-10-350
20	C.G. Long. Accel.	Accelerometer	± 1g	D-06-350
21	Airplane Pitch Attitude	Vertical Gyro Installation	± 80°	P.R. Gyro
22	Airplane Roll Attitude	Vertical Gyro Installation	±160°	P.R. Gyro
23	L.H. Platform Vertical	Reaction Platform	0-60K	DAC
24	L.H. Platform Drag	Reaction Platform	± 15K	DAC

TABLE 1 (Cont.)

INSTRUMENTATION FOR DROP TESTS

Oscillograph 2

	Parameter Measured	Method of Measurement	Transducer Range	Transducer Type
1	*R.H. Strut Vertical Load	Strain Gauge Installation on Axle	0-60K	18V 350 Ω
2	*R.H. Strut Drag Load	Strain Gauge Installation on Axle	± 20K	18V 350 Ω
3	R.H. Strut Side Load	Strain Gauge Installation on Axle	± 8K	18V 350 Ω
4	*R.H. Strut Position	Slide Wire Device	0-16 in.	DAC
5	*R.H. Strut Velocity	Velocity Generator	± 30 FPS	Sanborn 10LV 17-n
6	*R.H. Air Chamber Pressure	Pressure Transducer	0-5 KSI	DAC
7	*R.H. Metering Chamber Press.	Pressure Transducer	0-5 KSI	DAC
8	*R.H. Lower Mass Vert. Accel.	Miniature Accelerometer in Axle	+ 90g's	**A6-100-350
9	*R.H. Lower Mass Long. Accel.	Miniature Accelerometer in Axle	±100g's	A6-100-350
10	*R.H. Lower Mass Side Accel.	Miniature Accelerometer in Axle	±100g's	A6-100-350
11	*R.H. Gr.Upper Mass Vert.Accel.	Accelerometer	± 50g's	A5-50-350
12	*R.H. Gr.Upper Mass Drag Accel.	Accelerometer	± 3g's	A5-50-350
13	*R.H. Drag Brace Axial Load	Strain Gauges	± 50K	18V 350 Ω
14	*R.H. Wheel Angular Position	36 Magnets on Wheel - Pick-up on Strut	0-150KC	Electro 3010
15	L.H. Lift Damper Link	Strain Gauges	0-10K	18V 350 Ω
16	R.H. Lift Damper Link	Strain Gauges	0-10K	18V 350 Ω
17	L.H. Wing Tip Acceleration	Accelerometer	± 50g's	A6-50-35
18	R.H. Wing Tip Acceleration	Accelerometer	± 50g's	A6-50-35
19	*Time	Oscillograph Trace	20-20KC	205AG(H.P.)

* Items Identical on Both Gears

** All Accelerometers by Statham

TABLE 2
ESTIMATED OVERALL RECORDED PARAMETER ACCURACY

PARAMETER	ACCURACY ±%
R.H. Gear Vertical Load	3
R.H. Gear Drag Load	3
L.H. Gear Vertical Load	3
L.H. Gear Drag Load	3
L.H. Gear Lower Mass Vertical Acceleration	2
L.H. Gear Lower Mass Drag Acceleration	2
L.H. Gear Lower Mass Lateral Acceleration	2
R.H. Gear Lower Mass Vertical Acceleration	2
R.H. Gear Lower Mass Drag Acceleration	2
R.H. Gear Lower Mass Lateral Acceleration	2
R.H. Gear Upper Mass Vertical Acceleration	2
R.H. Gear Upper Mass Longitudinal Acceleration	2
L.H. Gear Upper Mass Vertical Acceleration	2
L.H. Gear Upper Mass Longitudinal Acceleration	2
R.H. Gear Strut Position	3
L.H. Gear Strut Position	3
R.H. Gear Strut Velocity	4
L.H. Gear Strut Velocity	4
R.H. Gear Metering Chamber Pressure	3
L.H. Gear Metering Chamber Pressure	3
L.H. Gear Shock Strut Rebound Chamber Pressure	2
R.H. Gear Strut Air Pressure	3
L.H. Gear Strut Air Pressure	3
R.H. Gear Drag Brace Load	2
L.H. Gear Drag Brace Load	2
Nose Gear Strut Position	3
Nose Gear Upper Mass Vertical Acceleration	2
C.G. Normal Acceleration (Low Range)	2
C.G. Normal Acceleration (High Range)	2
C.G. Longitudinal Acceleration	2
Aircraft Pitch Attitude	3
Aircraft Roll Attitude	3
R.H. Wing Tip Vertical Acceleration	2
L.H. Wing Tip Vertical Acceleration	2
R.H. Gear Reaction Platform Vertical Load	2
R.H. Gear Reaction Platform Drag Load	8
L.H. Gear Reaction Platform Vertical Load	2
L.H. Gear Reaction Platform Drag Load	8
Nose Gear Reaction Platform Vertical Load	2
R.H. Wing Lift Link Load	2
L.H. Wing Lift Link Load	2
Timing Clock	0.1

TABLE 3
FREQUENCY RESPONSE CHARACTERISTICS OF RECORDED PARAMETERS

PARAMETER	FLAT RESPONSE-CPS ±2%	±5%
R.H. Gear Vertical Load	115	135
R.H. Gear Drag Load	55	95
R.H. Gear Side Bending Moment	90	180
L.H. Gear Vertical Load	65	195
L.H. Gear Drag Load	50	100
L.H. Gear Side Bending Moment	65	190
L.H. Gear Lower Mass Vertical Acceleration	60	180
L.H. Gear Lower Mass Drag Acceleration	135	150
L.H. Gear Lower Mass Lateral Acceleration	155	175
R.H. Gear Lower Mass Vertical Acceleration	110	130
R.H. Gear Lower Mass Drag Acceleration	45	75
R.H. Gear Lower Mass Lateral Acceleration	40	60
R.H. Gear Upper Mass Vertical Acceleration	50	85
R.H. Gear Upper Mass Longitudinal Acceleration	105	130
L.H. Gear Upper Mass Vertical Acceleration	50	85
L.H. Gear Upper Mass Longitudinal Acceleration	60	90
R.H. Gear Strut Position	65	110
L.H. Gear Strut Position	55	90
R.H. Gear Strut Velocity	45	70
L.H. Gear Strut Velocity	50	90
R.H. Gear Metering Chamber Pressure	70	180
L.H. Gear Metering Chamber Pressure	60	185
L.H. Gear Strut Rebound Chamber Pressure	55	185
R.H. Gear Strut Air Pressure	15	40
L.H. Gear Strut Air Pressure	15	40
R.H. Gear Drag Brace Load	60	100
L.H. Gear Drag Brace Load	50	80
Nose Gear Strut Position	80	135
Nose Gear Upper Mass Vertical Acceleration	120	145
C.G. Normal Acceleration (Low Range)	25	40
C.G. Normal Acceleration (High Range)	40	55
C.G. Longitudinal Acceleration	20	35
Aircraft Pitch Attitude	30	35
Aircraft Roll Attitude	20	35
R.H. Wing Tip Vertical Acceleration	65	160
L.H. Wing Tip Vertical Acceleration	50	80
R.H. Wing Lift Link Load	55	170
L.H. Wing Lift Link Load	125	145

TABLE 4

INPUT CONSTANTS FROM GEAR GEOMETRY

$\bar{a}$	= 20.2 in.	r	= 2.0615 in.
A_o	= .5391 in.^{2}	R_o	= 12.0 in.
A_1	= 8.71 in.^{2}	S_C	= 16.0 in.
A_{POD}	= 11.04 in.^{2}	V_E	= 173.5 in.^{3}
A_R	= 2.36 in.^{2}	W_U	= 149 lbs.
A_{SPL}	= 13.4 in.^{2}	$\mu_{1,3,5}$	= .65
$\bar{b}$	= 9.7 in.	$\mu_{2,4}$	= .20
δ	= 53.435 in.	μ_6	= .25
$\bar{e}$	= 0	$\bar{C}$	= 20.82 lb.-sec./in.
d	= 6.75 in.	C_S	= 26.0 lb.-sec./in.
I_R	= 11.25 lb.-in.-sec.^{2}	C_β	= 1000 in.-lb.-sec./Rad.
I_V	= 20.0 lb.-in.-sec.^{2}		
K_{32}	= 5500 lb./in.		
K_4	= .0000485 in./lb.		
K_β	= 782000 in.-lb./Rad.		
n	= 1.35		

TABLE 5

GENERALIZED MASS MATRIX, M *(lb-Sec^2 inch per 1/2 Airplane)

MODE NO.	(2)	(3)	(4)	(5)	(1)	(6)
MODE (CPS)	13.6	16.3	29.8	33.6	0(BOBBING)	0**(PITCHING)
13.6	.3304	-.0421	.0001	-.0153	-.0070	7.43
16.3	-.0421	.3985	-.0148	.0131	-.1592	11.96
29.8	.0001	-.0148	.1717	-.0072	-.0764	-15.07
33.6	-.0153	.0131	-.0072	.1780	.0804	-15.05
0(BOBBING)	-.0070	-.1592	-.0764	.0804	16.708	-31.16
0**(PITCHING)	7.43	11.96	-15.07	-15.05	-31.16	137850.

* M is generalized from the Modal amplitudes and local mass data given in Reference 9. The elements have the stated dimensions when the plotted amplitude of each mode is represented by a reference co-ordinate of one-inch translation.

** Pitching is about x = 235; z = 0

TABLE 6

FLEXIBLE WING DATA

Vertical deflection of the gear attach point.

Mode	Mode f cps	M $\frac{\text{Lb-Sec}^2\text{-In}}{\text{Mode}}$	h (at Sta. 40)	α	h' (at Sta. 40)	α'
1	0	16.708	-	-	-	-
2	13.6	.3304	-.02	-.0004	-.0018	-.000018
3	16.3	.3985	-.05	+.001	+.0016	+.000045
4	29.8	.1717	-.04	+.0002	0	+.000028
5	33.6	.1780	-.10	+.0002	-.0029	0
6	0	137,850.	25.125	1.0	-	-

Mode	m_i	T_{H_i}	T_{α_i}	$T_{G\theta_i}$
1	1.3923	.083333	0	0
2	.02753	-.003015	-.0004	-.00227
3	.03321	-.000797	.001	.00277
4	.01431	-.002659	.0002	.001
5	.01483	-.007659	.0002	-.00303
6	11,480	2.09375	1.0	0

Mode	B_{ij}	C_i	D_i	F_i
1	0	.05985	0	0
2	-7302	-.10952	-.01453	-.08246
3	-10490	-.024	.03011	.08341
4	-35059	-.18581	.01398	.06988
5	-44570	-.51645	.01349	-.20432
6	0	.000182	.0000871	0

See following page for definition of symbols and equations pertaining to this table.

TABLE 6 (Cont'd.)

INPUT DATA

FORMULAS FOR FLEXIBLE WING

$m_i = M_i/12$

$T_{H_i} = (h_i + 40.443\ \alpha_i)/12$

$T_{\alpha i} = \alpha_i$

$T_{G\theta_i} = h_i' + 40.443\ \alpha_i' - .65455\ \alpha_i$

h_i' is the slope of the h_i curve at the gear attach point (Sta. 40)

α_i' is the slope of the α_i curve at the gear attach point

$B_{ij} = -(2\pi f_i)^2$

$C_i = T_{H_i}/m_i$

$D_i = T_{\alpha_i}/m_i$

$F_i = T_{G\theta_i}/m_i$

E_i is calculated by the program

TABLE 7

INITIAL CONDITIONS

AIRPLANE DROPS AND CORRESPONDING FLIGHT TEST LANDINGS

Landing No.	Drop No.	Gross Weight Lbs.	FRL Angle Degrees	Horiz. C.G. Position	Wing Lift ÷ Weight	Sink Speed fps	Horizontal Speed Wheel RPM	Horizontal Speed Knots
121		12,876	13.0	232.9	1.10	13.2	1793	106.1
	84	12,876	13.4	232.9	1.055	13.9	1811(L) 1794(R)	
123		13,735	8.5	235.2	1.10	12.0	1930	113.9
	70	13,516	9.5	234.5	1.03	12.2	2097(L) 2089(R)	
125		13,446	9.5	234.3	1.07	15.0	1933	112.9
	68	13,446	8.8	234.3	1.07	15.0	1925(L) 1918(R)	
126		13,276	9.3	233.9	1.06	17.0	1933	110.6
	93	13,276	10.0	233.9	1.045	16.7	1936(L) 1912(R)	
128		12,775	10.5	232.7	1.00	14.7	1872	109.1
	82	12,876	6.0	232.9	1.05	16.2	2074(L) 2044(R)	

TABLE 8

INITIAL CONDITIONS

FLIGHT TEST LANDINGS ON NON-SKID

Landing No.	Gross Weight Lbs.	FRL Angle Degrees	Horiz. C.G. Position	Wing Lift ÷ Weight	Sink Speed fps	Horiz. Speed Knots
93	13,600	7.6	235.1	1.14	16.1	131.0
95	13,270	6.5	234.3	1.04	16.6	128.5
113	12,870	8.8	233.3	.97	13.2	113.0
114	13,660	10.0	235.2	1.04	17.4	110.0
117	13,080	10.5	233.9	1.14	17.4	110.0
120	13,080	10.5	233.9	1.08	13.6	110.5
131	13,360	8.6	234.6	1.06	13.5	127.8
133	12,970	7.6	233.6	1.06	14.0	128.5

TABLE 9

START TIME INPUT DATA

Landing No.	$\dot{Q}_1$	$\ddot{Q}_1$	θ	$\dot{a}$	$\ddot{a}$	Δ	$\dot{\Delta}$	$\ddot{\Delta}$	Y_2	β	V_L	z_o	C_1	μ_s
93	193.2	-54.05	1.6	193.12	-54.03	.00086	5.390	-1.508	.00824	.000041	2655.6	-12.000024	.05677	.29
95	199.2	-15.44	.5	199.20	-15.44	.00025	1.733	-0.134	.00752	.000012	2606.4	-12.000002	.05818	.34
113	158.4	11.58	2.8	158.21	11.57	.00128	7.730	0.565	.00700	.000061	2292.0	-12.000063	.05999	.33
114	208.8	-15.44	6.0	208.30	-15.40	.00197	14.570	-1.078	.00750	.000093	2234.3	-12.000137	.05652	.27
117	208.8	-54.05	4.5	208.20	-53.88	.00243	16.390	-4.243	.00821	.000115	2230.8	-12.000191	.05903	.32
120	163.2	-30.89	4.5	162.69	-30.79	.00230	12.810	-2.425	.00778	.000109	2242.8	-12.000181	.05903	.32
131	162.0	-23.17	2.6	161.84	-23.15	.00131	7.355	-1.052	.00765	.000062	2590.8	-12.000059	.05779	.37
133	168.0	-23.17	1.6	167.93	-23.16	.00080	4.687	-0.646	.00766	.000038	2602.8	-12.000022	.05953	.32
121	158.4	-38.61	7.0	157.23	-38.32	.00364	19.310	-4.707	.00789	.000173	2150.4	-12.000443	.06387	.36
123	144.0	-38.61	2.5	143.90	-38.58	.00109	5.276	-1.414	.00794	.000052	2307.0	-12.000040	.05621	.36
125	180.0	-27.03	3.5	179.66	-26.98	.00177	10.990	-1.650	.00772	.000084	2288.2	-12.000056	.05742	.33
126	204.0	-23.17	3.3	203.65	-23.13	.00166	11.750	-1.335	.00765	.000079	2241.6	-12.000095	.05815	.39
128	176.4	0	4.5	175.95	0	.00194	12.610	0	.00721	.000092	2210.0	-12.000139	.06044	.37

See following page for symbols and equations pertaining to this table.

TABLE 9 (Cont'd.)

FORMULAS FOR START-TIME INPUTS

$\dot{Q}_1$	=	Sink Speed	(in./sec.)
$\ddot{Q}_1$	=	(1.0 - WL) 386	(in./sec.^{2})
$\dot{a}$	=	$\dot{Q}_1 \cos \phi$	(in./sec.)
$\ddot{a}$	=	$\ddot{Q}_1 \cos \phi$	(in./sec.^{2})
Δ	=	$\left(\frac{1}{K_{32}} W_U \right) (WL) \sin \phi$	(in.)
$\dot{\Delta}$	=	$\dot{Q}_1 \sin \phi$	(in./sec.)
$\ddot{\Delta}$	=	$\ddot{Q}_1 \sin \phi$	(in./sec.^{2})
Y_2	=	$K_4(W_U)(WL) \cos \phi$	(in.)
β	=	$(W_U)(WL) \frac{d}{K_\beta} \sin \phi$	(rad./sec.)
Z_o	=	$-(12 + (\Delta) \sin \phi)$	(in.)
C_1	=	T_{H_1}/m_1	(1/lb.sec.^{2})
μ_s	=	Average Ground Coefficient of Friction at Time of Spin-up, from Flight Test Data Pages 61 to 78.	
ϕ	=	Pitch Attitude -6°	

TABLE 10

COMPARISON OF MAXIMUM VERTICAL LOADS

Landings				Drop Tests				Theory
Max.Vert.Load				Max.Vert.Load				Max.Vert.Load
No.	Left	Right	Ave.	No.	Left	Right	Ave.	
121	16900	16700	16800	84	18300	15700	17000	16300
123	20500	17900	19200	70	13300	11300	12300	16000
125	22300	22600	22450	68	20700	18500	19600	22600
126	28200	30400	29300	93	23800	25500	24650	28900
128	20000	20500	20250	82	25700	21500	23600	21500
93	32800	20000	26400					25300
95	33600	26200	29900					28600
113	17900	19000	18450					16900
114	26000	43400	34700					37800
117	25600	25500	25550					29900
120	17700	14500	16100					18400
131	29500	18600	19050					20600
133	22100	19000	20550					19500

COMPARISON OF AVERAGE (LEFT AND RIGHT) MAXIMUM VERTICAL LOADS

(A) Landings			(B) Drop Test			(C) Theory	Ratios	
No.	V_V	Ave.Max. Load	No.	V_V	Ave.Max. Load	Max.Load	(B)/(A)	(C)/(A)
121	13.2	16800	84	13.9	17000	16300	1.01	.97
123	12.0	19200	70	12.2	12300	16000	.64	.83
125	15.0	22450	68	15.0	19600	22600	.87	1.005
126	17.0	29300	93	16.7	24650	28900	.84	.99
128	14.7	20250	82	16.2	23600	21500	1.16	1.06
93	16.1	26400				25300		.96
95	16.6	29900				28600		.96
113	13.2	18450				16900		.92
114	17.4	34700				37800		1.09
117	17.4	25550				29900		1.17
120	13.6	16100				18400		1.14
131	13.5	19050				20600		1.08
133	14.0	20550				19500		.95

TABLE 11

COMPARISON OF MAXIMUM DRAG LOADS

Landings				Drop Tests				Theory
	Max. Drag Load				Max. Drag Load			Max. Drag Load
No.	Left	Right	Ave.	No.	Left	Right	Ave.	
121	6000	5440	5720	84	9930	7030	8480	5200
123	6870	6360	6615	70	8510	6730	7620	5700
125	7040	6630	6835	68	9940	8350	9145	6800
126	9680	6880	8280	93	12410	9480	10945	10700
128	7300	5530	6415	82	11880	9190	10535	8000
93	8080	8090	8085					6800
95	8820	7660	8240					9700
113	7040	5660	6350					5500
114	7940	4990	6465					6300
117	6420	6080	6250					7800
120	6880	6130	6505					5000
131	7320	6580	6950					7600
133	8330	6580	7455					6000

COMPARISON OF AVERAGE (LEFT AND RIGHT) MAXIMUM DRAG LOADS

(A) Landings			(B) Drop Test			(C) Theory	Ratios	
No.	V_V	Ave.Max. Load	No.	V_V	Ave.Max. Load	Max. Load	(B)/(A)	(C)/(A)
121	13.2	5720	84	13.9	8480	5200	1.47	.91
123	12.0	6614	70	12.2	7620	5700	1.15	.86
125	15.0	6835	68	15.0	9145	6800	1.34	.995
126	17.0	8280	93	16.7	10945	10700	1.32	1.29
128	14.7	6415	82	16.2	10535	8000	1.64	1.25
93	16.1	8085				6800		.77
95	16.6	8240				9700		1.18
113	13.2	6350				5500		.87
114	17.4	6465				6300		.97
117	17.4	6250				7800		1.25
120	13.6	6505				5000		.77
131	13.5	6950				7600		1.09
133	14.0	7455				6000		.80

TABLE 12

DATA COMPARING CONCRETE
AND NON-SKID LANDING SURFACES

Ldg. No.	Spin-Up Time		Average		Maximum Drag Load		Max. Wheel Speed Measured		$\frac{\Sigma F_{HG}(R_o-C)\Delta t^{**}}{I_R}$		$\dot{\alpha}$ (Theory)
	SEC		-		LBS		RPM		RPM		RPM
	LH	RH	LH	RH	LH	RH	LH	RH	LH	RH	
121*	.046	.045	.36	.35	5995	5438	1700	1786	1520	1205	1800
123*	.052	.052	.36	.29	6868	6356	1859	1748	1725	1585	1960
125*	.049	.049	.33	.28	7043	6629	1824	1795	1722	1421	1970
126*	.038	.044	.39	.28	9678	6876	1929	1719	1710	1430	1995
128*	.042	.050	.37	.27	7295	5530	1795	1776	1645	1212	1920
93	.053	.057	.29	.31	8084	8092	2187	2120	2005	1680	2305
95	.050	.047	.34	.31	8819	7655	1757	2130	2195	1660	2320
113	.053	.053	.33	.26	7040	5657	1881	1881	1840	945	1950
114	.048	.043	.27	.18	7942	5102	1851	1860	1630	970	1940
117	.047	.050	.32	.20	6421	6082	1832	1860	1760	1179	1960
120	.054	.054	.34	.32	6876	6130	1853	1853	1780	1389	1890
131	.059	.060	.37	.31	7323	6577	2120	2120	2040	1619	2225
133	.064	.061	.31	.24	8330	6583	2210	2210	2220	1600	2230

* Concrete Average = .328
Non-Skid Average = .294

** Wheel RPM Computed from Measured Drag and Tire Radius

TABLE 13

INITIAL CONDITIONS

FLIGHT TEST AND NASA LANDING IMPACT TESTS

	Fig.	Sink Speed Ft./Sec.	Horiz Speed Knots	Runway Surface	ϕ Deg.	Wing Lift ÷Weight	Weight/ Gear Lbs.
Landing 117	39	17.4	110.0	Non-Skid	4.5	1.14	6540
NASA Run 21	39	17.3	103.4	Non-Skid	2.5	1.0	6630
Landing 126	39	17.0	110.6	Concrete	3.3	1.06	6638
NASA Run 11	39	16.4	76.0	Concrete	2.5	1.0	6630
Landing 95	40	16.6	128.5	Non-Skid	- .5	1.04	6635
NASA Run 35	40	16.4	95.3	Non-Skid	-5.1	1.0	6630
Landing 113	40	13.2	113.0	Non-Skid	2.8	.97	6435
NASA Run 18	40	12.4	92.6	Non-Skid	2.5	1.0	6630

TABLE 14

ENERGY COMPARISON

(1)		(2) E_{Final}	(3) $E_{Initial}$	(4) Ratio,(2)/(3)
Landing 121		33,736	33,116	1.02
Drop 84	Gear	32,682	37,705	.87
	Platform	35,327		.94
Theory		32,698	33,226	.98
Landing 123		32,315	28,878	1.12
Drop 70	Gear	25,137	30,727	.82
	Platform	27,347		.89
Theory		29,784	29,130	1.02
Landing 125		42,163	45,694	.92
Drop 68	Gear	40,666	45,687	.89
	Platform	43,577		.95
Theory		46,997	45,698	1.03
Landing 126		55,880	58,443	.96
Drop 93	Gear	51,116	56,678	.90
	Platform	53,451		.94
Theory		60,187	58,494	1.03
Landing 128		40,980	42,866	.96
Drop 82	Gear	40,675	51,676	.79
	Platform	41,256		.80
Theory		44,072	42,863	1.03

Average Ratios, (2)/(3)

Landings		1.00	(.96)*
Drops	Gear	.85	
	Platform	.90	
Theory		1.02	

* Eliminating Ldg. 123

E_{Final} = Area of load versus stroke plus tire deflection curve + energy in airplane pitch

$E_{Initial} = \frac{1}{2} MV_v^2$ - (Lift-Weight) x Stroke

Douglas Aircraft Co., Aircraft Div., Long Beach, Calif. Report No. LB-31038. Prepared for Bureau of Naval Weapons, Wash. D. C. AN INVESTIGATION OF THE LANDING LOADS EXPERIENCED BY THE A4D-2 AIRPLANE DURING FLIGHT TESTS AND DROP TESTS AND A COMPARISON WITH THEORY, Oct. 1962. Final Report 118 p. inc illus., tables, refs.

Unclassified Report

This report presents the results of an investigation conducted for the purpose of evaluating the adequacy of simulating landing loads by airplane laboratory drop tests and for the purpose of determining the accuracy with which these loads may be calculated by means of a dynamic analysis. Curves are presented which compare ground loads obtained from airplane landings, airplane drops, and theoretical analyses. The computing program for the theoretical analysis and its required input data are described.

1. Landing Loads
2. Loads, Aircraft
3. Dynamic Analysis
4. Drop Tests
5. Flight Landings
I. Contract NOa(s) 59-6226c
II. Douglas Aircraft Co., Inc.
III. F. C. Allen
L. B. Mosby
IV. Aval fr Naval BuWeps

Douglas Aircraft Co., Aircraft Div., Long Beach, Calif. Report No. LB-31038. Prepared for Bureau of Naval Weapons, Wash. D. C. AN INVESTIGATION OF THE LANDING LOADS EXPERIENCED BY THE A4D-2 AIRPLANE DURING FLIGHT TESTS AND DROP TESTS AND A COMPARISON WITH THEORY, Oct. 1962. Final Report 118 p. inc illus., tables, refs.

Unclassified Report

This report presents the results of an investigation conducted for the purpose of evaluating the adequacy of simulating landing loads by airplane laboratory drop tests and for the purpose of determining the accuracy with which these loads may be calculated by means of a dynamic analysis. Curves are presented which compare ground loads obtained from airplane landings, airplane drops, and theoretical analyses. The computing program for the theoretical analysis and its required input data are described.

1. Landing Loads
2. Loads, Aircraft
3. Dynamic Analysis
4. Drop Tests
5. Flight Landings
I. Contract NOa(s) 59-6226c
II. Douglas Aircraft Co., Inc.
III. F. C. Allen
L. B. Mosby
IV. Aval fr Naval BuWeps